

WASHINGTON MONUMENT Seismic Assessment

National Mall, Washington DC



Final Report
August 29, 2012



Prepared for:
National Park Service, Denver Service Center

WASHINGTON MONUMENT Seismic Assessment

National Mall, Washington DC

Prepared by:

Wiss, Janney, Elstner Associates, Inc.

2000 Powell Street, Suite 1650
Emeryville, California 94608
510.428.2907 tel | 510.428.0456 fax

Tipping Mar

1906 Shattuck Avenue
Berkeley, California
510.549.1906 tel | 510.549.1912 fax

TABLE OF CONTENTS

Executive Summary	1
Findings	2
Recommendations	3
Background	4
Relevant Monument Terminology	4
Abbreviated Construction History	6
Description of Monument	7
Pyramidion Structure	10
Seismic Assessment	16
Conceptual Seismic Behavior and Evaluation	18
Benchmark Ground Motion	19
MCE Ground Motion	24
Washington Monument Analytical Modeling	26
Overview	26
Model Development	26
Soils and Monument Foundation	27
Shaft	29
Shaft from 0 feet to 150 feet	30
Shaft from 150 feet to 470 feet	30
Shaft from 470 ft to 500 ft	32
Pyramidion Rib Stones	33
Pyramidion Panels	40
Analyses	46
Modal Analysis	46
Nonlinear Modal Time History	52
Analysis Results General	53
Analysis Results Soils and Monument Foundation	55
Analysis Results Shaft	57
Analysis Results Pyramidion	65
Supplemental Analysis Confirmation	76
Conclusions and Recommendations	77
Upper Shaft	79
Ribs	79
Teeth	80
Panels	82
Cruciform	82
Tie Beams	83
References	84

Appendix A: Ground Motion Hazard and Geotechnical Evaluation

Appendix B: Analysis Confirmation

WASHINGTON MONUMENT Seismic Assessment

National Mall, Washington DC

EXECUTIVE SUMMARY

On August 23, 2011, the Washington Monument (Monument) was subjected to ground shaking from the Magnitude 5.8 Mineral, Virginia earthquake (Mineral event), whose epicenter was roughly 82 miles (132 kilometers) from the National Mall. Swaying of the Monument in response to the shaking resulted in damage, primarily to the pyramidion. The Monument has been closed to the public since the earthquake event. A post-earthquake damage assessment project catalogued the damage to the Monument and that information was used to develop specifications and drawings for repair of the earthquake damage.

The Mineral event and the damage to the Monument that ensued raised questions about the seismic vulnerability of the Monument should stronger ground shaking occur in the future. The earthquake also raised questions about seismic strengthening measures that might be considered, if necessary, in order to protect the Monument during future earthquakes from damage more consequential than that which occurred on August 23. The purpose of this assessment is to address those questions, particularly as they pertain to an earthquake with a 2,475-year return period, which is commonly relied on as a basis for seismic assessments of existing structures and seismic design of new structures throughout the United States. In engineering parlance, a 2,475-year return period earthquake is called the Maximum Considered Earthquake (MCE). It is the maximum event required to be used by the building codes and other standards for seismic design of new structures and for seismic assessment of existing ones.

The seismic assessment of the vulnerability of the Monument to future earthquakes addressed the entire Monument but focused on three distinct components; the pyramidion, the shaft, and the foundation. The assessment involved multiple studies, including; studies of the type and distribution of physical damage documented subsequent to the August 23 Mineral event; conceptual studies of the general behavior of the Monument when subjected to lateral forces; and seismological studies that were used to develop a science-based understanding of the shaking intensity at the National Mall that actually occurred during the August 23 Mineral event and of the shaking that might someday occur during future 2,475-year earthquakes from various other sources. These latter studies produced synthetic mathematical representations of the shaking of the ground during the Mineral event as well as during postulated future earthquake events.

Earthquake engineering analysis studies of the Monument responding to the mathematical characterizations of ground shaking developed by the seismologists were also conducted. These analyses employed detailed computer models of the Monument that were developed as part of the assessment. The models were designed to capture the most important structural characteristics of the 555-foot tall unreinforced masonry tower, the soil beneath its base, as well as the intricacies of the pyramidion construction. In the analyses, simulations of the Monument responding to the Mineral event were run by subjecting the models to the synthetic representations of shaking during the Mineral event. The models were then validated by comparing damage predictions from the simulations with the physical damage that actually occurred during the August 23 earthquake. With the validated models, the effects of future potentially more damaging 2,475-year earthquake events were then determined by subjecting the models to mathematical representations of those earthquakes, and the significance of the predicted damage was evaluated and compared to what occurred on August 23. This general analytical approach was followed

by Wiss, Janney, Elstner Associates, Inc. (WJE), who conducted the primary detailed analyses and by Tipping Mar (TM) who conducted supplemental validation analyses using different analytical models and different analysis software. Although the analyses by WJE and TM were independent, the results revealed wide-ranging agreement between the two disparate modeling approaches. AMEC Environment and Infrastructure Inc. (AMEC) conducted the geotechnical and seismological studies utilized by the structural analyses. This report summarizes the results of these studies.

Findings

The items described below summarize the primary milestones and findings of the seismic assessment.

- When the Monument is subjected to ground shaking during an earthquake, like all other structures, it responds by swaying. That swaying causes deformation of the pyramidion, the shaft and/or the soils beneath the foundation to occur to varying degrees, depending on certain subtle characteristics of the shaking during different earthquake events. In other words, some earthquake events from some sources may excite the pyramidion relatively more than the shaft and base of the Monument, but other events may excite the shaft and base more than the pyramidion.
- The ground shaking at the National Mall during the August 23 Mineral event caused a substantial amount of deformation to the pyramidion and to the top of the shaft just below the pyramidion, but relatively little deformation to the lower portions of the shaft and to the soils beneath the foundation. The dynamic characteristics of the Mineral event caused the deformations to be concentrated in the pyramidion, which is what caused the damage to the Monument to be concentrated in the pyramidion.
- The type of damage experienced by the pyramidion and the top of the shaft during the August 23 Mineral event can be predicted reasonably well using the now understood characteristics of the shaking on the Mall on August 23 and the models developed during this seismic assessment.
- The pyramidion was found to be the most vulnerable portion of the Monument, in part because the particular motion to which it responds the most is amplified by the soil layers beneath the Monument. In engineering terms, the period of vibration of the pyramidion is very similar to the period of vibration of the soils supporting the Monument.
- The occurrence of another earthquake capable of causing more damage to the pyramidion than occurred on August 23 is judged to be extremely unlikely. This finding is based on the unusually high energy content of this earthquake in the period range of the supporting soils and the pyramidion. With respect to the particular shaking characteristics to which the pyramidion is most vulnerable, the shaking on the National Mall during the Mineral event was roughly 10 to 20% stronger than the predicted median 2,475-year event. To say it another way, a future 2,475-year event is more likely to have similar or less damage potential with respect to the pyramidion than the Mineral event. The pyramidion therefore appears to have just experienced its 2,475-year event, or similar.
- Damage to the pyramidion similar to that which occurred during the Mineral event should be expected during some 2,475-year events. That damage did not present a concern for collapse but did introduce some concern of potential falling hazards. Because of inherent randomness in earthquake generated shaking, the expected damage patterns will not be precisely the same as they were on August 23 and certain stone masonry units and joints in the pyramidion that were not damaged during the August 23 event are likely to be damaged in a future event. The severity of damage in a future 2,475-year event, however, is not predicted to be worse than what occurred during the Mineral event.
- Ground shaking from a 2,475-year earthquake that is likely to excite the shaft and base of the Monument more than the pyramidion -- and to cause substantially more deformation of the shaft and supporting soils than occurred on August 23 -- is likely to have a more distant source than the Central Virginia region that was the source of the Mineral event. A Magnitude 7.5 earthquake from the

Charleston, South Carolina source occurred in 1886. That earthquake is believed to have generated shaking intensity at the National Mall that is consistent with or exceeds the 2,475-year hazard. Charleston, South Carolina is a likely source of a future 2,475-year earthquake.

- The simulations run with the computer models being subjected to 2,475-year earthquake motions from a more distant source demonstrate that the shaft of the Monument and the soils that support are adequate to withstand a 2,475-year earthquake, with some cracking of mortar joints and perhaps minor spreading of some masonry but essentially without damage to competent stone masonry units. It should be noted, however, that a number of stone masonry units in the shaft have deteriorated over the years since construction, and some have failing repairs. These locations are likely to be detrimentally affected by a future 2,475-year event.
- The finding that the structure of the shaft and soils supporting the base of the Monument are adequate to withstand a distant 2,475-year event is supported by the historical record; construction of the Monument was completed in 1884 and historical records accessed during this project do not mention that any damage occurred to the Monument during the 1886 Charleston earthquake.

Recommendations

- The pyramidion is potentially subject to being damaged again during a future 2,475-year event; careful consideration was therefore given to whether remediation of the potential for damage was necessary in order to achieve conformance with commonly invoked seismic safety expectations. These expectations, briefly described, are that the primary goal of seismic resistant design is to protect life safety that the occurrence of structural and nonstructural damage during a major earthquake is acceptable, and that such damage may or may not be repairable. While the pyramidion may well experience some damage in a future 2,475-year earthquake, the re-occurrence of damage even of the severity of what occurred during the August 23 Mineral event, with an estimated return period between 2,000 and 3,000 years, is relatively remote. Moreover, seismic safety standards employed nationally for new construction require structures to satisfy life safety criteria for a so-called “design earthquake” which is equivalent to only two-thirds of the predicted 2,475-year event. A “design earthquake” in accordance with this industry standard definition would cause substantially less damage to the pyramidion than what occurred on August 23. Seismic improvements to the pyramidion are therefore not needed to conform to the seismic safety standards that are applicable to other public and privately owned properties in the United States. However, the existing panel-to-rib connections that were not damaged during the August 23 Mineral event and will therefore not be positively attached with steel brackets during the upcoming repair phase are at some risk during future very strong but rare events and the possibility of some of these panels becoming dislodged cannot be discounted entirely. The degree of risk is difficult to characterize in part because different earthquakes have the potential to damage different panel-to-rib connections. Especially because repair work in the pyramidion is being scheduled, it would not be unreasonable to at the same time install additional earthquake-resistant panel-to-rib connections to the more vulnerable of the currently undamaged locations. The panel-to-rib connections at which two panels are supported were found to be more vulnerable, and exhibited a far greater damage rate after the Mineral event, than the panel-to-rib connections at which only a single panel is supported. In addition, the panel-to-rib connections in the course just below the tie-beams are considered to be more vulnerable. This assessment recommends that if improvements to the panel-to-rib connections are considered, these two categories of connections be considered. There are approximately 14 connections that fall into these categories.
- The shaft and the soils supporting the Monument are not vulnerable to safety-compromising damage from a 2,475-year event; seismic strengthening measures are therefore not needed to conform to the seismic safety standards that are applicable to other public and privately owned properties in the

United States. This assessment also finds that neither the shaft nor the soils is expected to experience permanent deformations more severe than minor cracking of mortar joints and minor but localized spreading of the masonry. We do, however, recommend that the deteriorated stone masonry units and damage documented on the exterior of the Monument be stabilized to limit the potential for falling hazards during a strong earthquake.

BACKGROUND

This seismic assessment of the Washington Monument, located in the National Mall in Washington DC was conducted at the request of the National Park Service (NPS) Denver Service Center. The assessment was prompted by the occurrence of the Mineral, Virginia earthquake of August 23, 2011, and by the damage to the Monument, especially to the pyramidion and the top of the shaft. Due to the visible earthquake-related damage and to protect the safety of visitors, NPS restricted public access to the Monument immediately after the earthquake. Shortly thereafter, an engineering team comprised of Wiss, Janney, Elstner Associates, Inc. (WJE), Tipping Mar (TM) and engineers from the National Park Service - Denver Service Center, arrived on site to perform an initial post-earthquake safety assessment. A close-range on-site survey of the damage was subsequently conducted by WJE between September 25 and October 5, 2011 using a trained "Difficult Access Ropes Team" and, shortly thereafter, WJE was requested to develop designs and construction documents for repair of the earthquake damage. During the course of post-earthquake on-site damage documentation surveys to catalogue the extent and severity of the damage requiring repair, WJE and TM were requested to study the adequacy of the Monument to resist future large earthquakes.

The scope of the seismic assessment of the Monument consisted of three distinct but inter-related components of study.

1. WJE developed the analysis approach and primary computer models of the Monument, and conducted the primary analysis effort used for the assessment. WJE closely coordinated efforts with AMEC and with TM.
2. AMEC, as a geotechnical subcontractor to WJE, developed the geotechnical data used to model the soil supporting the Monument foundation and synthesized the seismological data describing the shaking to which the Monument was subjected during the August 23 Mineral event, as well as synthesized the seismological data used to the study the seismic adequacy of the Monument to resist future 2,475-year events. AMEC describes their work and findings in a report that is attached as Appendix A to this report.
3. TM developed an independent computer model that was used to provide supplemental validation of the results of the WJE's assessment and analyses. Despite TM's employment of independently developed models and different analysis software, their results revealed wide-ranging agreement with WJE's results. A brief discussion of the TM models and results are provided in the "Supplemental Analysis Confirmation" section in the body of this report. TM describes their work in greater detail in a report that is attached as Appendix B.

Relevant Monument Terminology

In order to describe the monument's construction, the observed earthquake damage, and the specifics of the structural analyses conducted during the course of this assessment, the following terms are defined:

Pyramidion - The pyramidal construction comprising the upper 55 feet of the monument.

Courses - A “course” is a horizontal level of stone masonry. Courses within the shaft of the monument are typically 2 feet in height. Courses within the pyramidion exterior are typically 4 feet in height.

Wythe - A “wythe” is a continuous vertical segment of masonry, one unit in thickness. A wythe can be independent of or interlocked with adjacent wythes.

Bed Joint - Horizontally-oriented mortar joints between courses of stone units.

Panels - The “panels” are the exterior 7-inch thick facing stones that enclose the pyramidion structure. They have been referred to as roof panels at times in historic documents.

Facets - The four triangular faces of the pyramidion.

Ribs - The “ribs” are the 12 structural elements that serve to support the exterior stone facing of the pyramidion. Each rib is a stack of large blocks of stone (rib stones), with a mortis and tenon joint at the bed joints. There are three ribs on each face of the pyramidion with the center rib extending higher up the pyramidion than the ribs nearer the pyramidion corners. The ribs begin at the 470-foot level and are integrated into the shaft walls at every other course. They become free standing above the 500-foot level and work together above that level to function as arched-frames when subjected to lateral forces, providing lateral stiffness to support the pyramidion walls out-of-plane. The rib stone courses above the 500-foot level are numbered alphabetically beginning with ‘A’ at the 504-foot course, continuing up through K and skipping the letter J. These alphabetic descriptors were used by the engineer, Lieutenant Colonel Casey, responsible for the original design and construction of the Monument above the 160-foot elevation.

Cruciform - This is a cross-shaped keystone that occurs at course ‘H’ of the pyramidion structure and bridges between the four central ribs. It is engraved on the underside with the year 1884, the year in which construction of the Monument was completed.

Lug - The “lugs” are the thickened faceted portions of stone that project from the lower interior portion of the pyramidion’s panels. The lugs provide a bearing area that projects from the plane of the panels and allows for gravity support of the panels on the rib stones. This has been referred to as a bracket at times in historic documents.

Tooth - The “teeth” are the “saw-tooth” shaped projections of the pyramidion’s rib stones used to engage and support the panels. This projection provides a bearing surface for support of the panel course above. Because the mating surfaces of the “teeth” and “lugs” are sloped rather than horizontal, and because the “teeth” are let into the panels, the teeth integrate the behavior of the panels and rib stones in both out-of-plane and in-plane action. The “teeth” have been referred to as rib projections or as shoulders in historic documents. They are also referred to as “rib tips” in the earthquake repair documents.

Corner stones - The “corner stones” are large blocks that cap the two side ribs that intersect at each corner of the pyramidion at course ‘F.’ There are four corner stones, located at the interior corners of course G (at the 525-foot elevation) within the pyramidion structure.

Tie Beam - The “tie beams” are the eight horizontally-oriented structural elements at course ‘F’ --- the elevation where the shorter corner ribs terminate --- which interconnect all the ribs to one another.

Abbreviated Construction History

The following is a brief construction history, for the purposes of providing historic context for the understanding of the seismic assessment and recommendations set forth herein. The primary source for this abbreviated history is the 2004 Historic Structure Report (HSR) on the Washington Monument and Associated Structures.¹

The Washington National Monument Society was established in 1833 to spearhead the planning and financing of a memorial to George Washington in Washington D.C. The society raised funds and held a competition for the design of the monument in 1836, but a design was not selected from those submitted. In 1845, after additional fund-raising, the society selected a design by Robert Mills. Mills' monument design consisted of a 600-foot tall obelisk surrounded by a 250-foot diameter, 100-foot tall pantheon, with an estimated cost of \$200,000. Construction commenced in 1848, but was halted in 1854 when the Monument was approximately 156-feet in height due to lack of funds.

The Monument remained in a partially complete, unfinished state until after the Civil War. Approaching the nation's centennial, renewed interest in the completion of the Monument took shape and ownership was transferred to the federal government in 1876. The Army Corps of Engineers was commissioned to study the integrity of the foundations. Their studies led to structural modifications, which began in 1878 under the direction of Lieutenant Colonel Thomas Lincoln Casey, Chief Engineer of the Monument construction project. The foundation-strengthening work, which increased the footprint of the foundation, was completed in 1880, and construction resumed on the superstructure of the Monument that year. Six feet of previous construction from the top of the existing walls was found to be inadequate and was removed prior to work commencing on the shaft from the 150-foot level. Casey developed an internal iron structure for the Monument to support work platforms and a steam-powered hoist. He redesigned the Monument somewhat by adjusting the proportions of the pyramidion to conform to those of known ancient Egyptian obelisks, a design strategy which also influenced the design of the final height of the structure. The final design of the obelisk consisted of a 500-foot shaft, topped by a steeply-sloped pyramidion 55-feet in height (Figure 1).

When the Monument was dedicated in 1885 it was the tallest man-made structure in the world, a title it held for four years until the completion of the Eiffel Tower. Today, the Monument is one of the most recognizable and symbolic structures in the nation. Generations of Americans have enjoyed visiting the Monument and repair campaigns have been executed periodically in an effort to maintain it.

¹ John Milner Associates, Historic Structure Report Washington Monument and Associated Structures, (National Park Service, 2004).



Figure 1. Pyramidion and upper portion of the shaft of the Monument

Description of Monument

The Monument stands 555 feet $5\frac{1}{8}$ inches tall with a base 55 feet $1\frac{1}{2}$ inches wide on each side.² The exterior of the Monument shaft tapers approximately $\frac{1}{4}$ -inch per foot from the base, up to the 500-foot level, which marks the end of the shaft and the beginning of the pyramidion (Figures 1 and 2). The Monument is 34-feet $5\frac{3}{8}$ inches wide at the 500-foot level. A small inscribed cast-aluminum tip, an extraordinarily rare product for its time, is featured at the top of the 55 feet $5\frac{5}{8}$ inches tall pyramidion.

² Ibid.

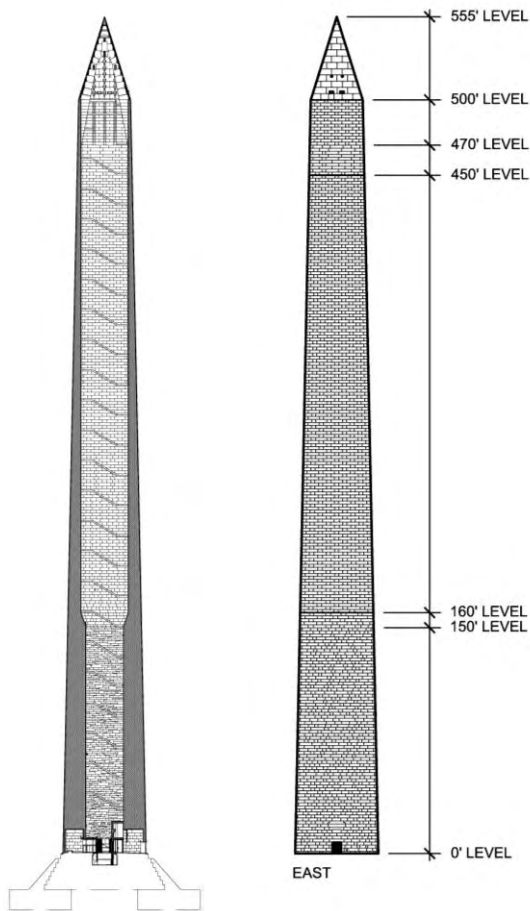


Figure 2. Cross-section and elevation of the Monument

Structurally, the Monument is a stone-masonry bearing wall structure consisting of four exterior walls. It is largely a hollow shaft, with archaic iron interior framing that supports the elevator structure and the interior stair structure. The foundation of the Monument was originally constructed from stone masonry, with plan dimensions of 80 feet by 80 feet. Significant underpinning and widening of the foundation with concrete, as well as integrating of the widened footprint into the existing construction with concrete buttressing, was performed by the Army Corps of Engineers prior to re-initiating construction to complete the shaft. The widened footprint of the foundation is roughly 126 feet by 126 feet. A photograph of the in-progress concrete foundation work is shown in Figure 3 with completed buttressing shown in Figure 4.

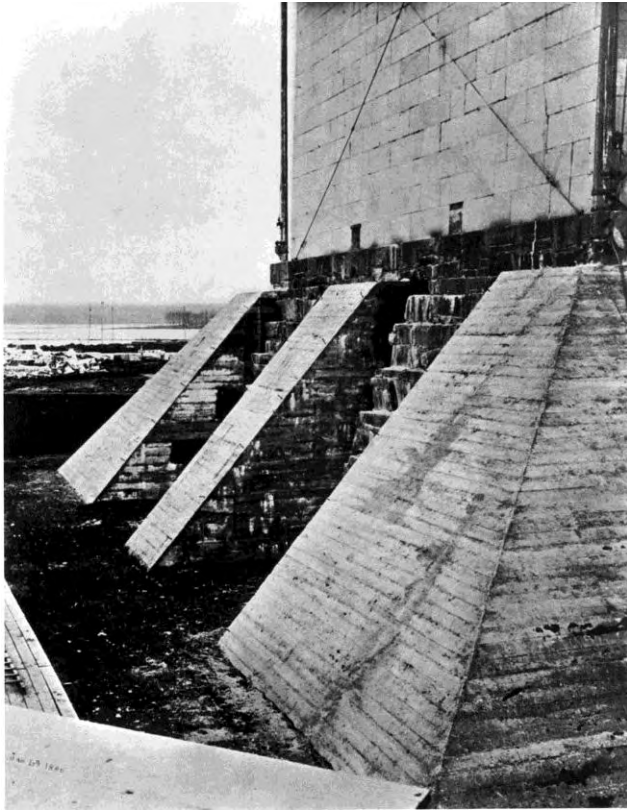


Figure 3. In-progress concrete buttressing, circa 1880

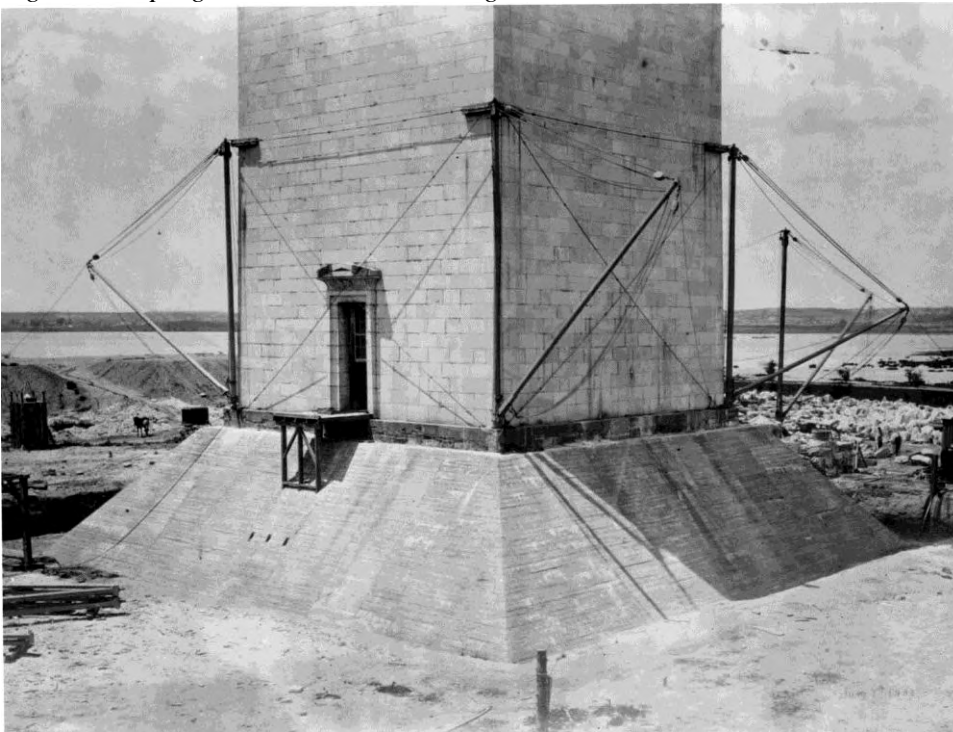


Figure 4. Washington Monument foundation after underpinning and buttressing, prior to backfilling, circa 1880

The tapered obelisk shape of the Monument and the relatively constant interior dimensions of the interior of the shaft lead to a gently tapering wall thickness along the height of the shaft, with one exception. The structural stone masonry of the Monument also changes with height and employs a variety of types of stone and masonry types. At a transition in the method of masonry construction at 150 feet, the wall thickness changes relatively abruptly. A description of the various types of construction is given below.

The lowest portion of the Monument shaft (from grade to 150 feet) consists of two finish face wythes of stone block masonry with a rubble infill between and was constructed in 1848-1858. The stone block wythes are constructed of gneiss on the interior and Texas marble from Texas, Maryland on the exterior of the shaft. The space between the interior and exterior stone wythes is filled with rubble stone masonry consisting of “large undressed pieces of blue gneiss, spalls and mortar”, but the extent of any voids and the type of stone within the rubble masonry is unclear (John Milner Associates 2004). The masonry mortar in this part of the Monument was made with natural cement (Cummings 1898). The shaft wall thickness at the base is in excess of 15 feet and the shaft tapers to 11 feet 8 inches at the 150-foot level.

The section of the shaft between approximately 150 to 160-feet is transitional. Above the 150-foot level, the shaft walls are constructed entirely of stone block masonry, without any rubble masonry in their interior. In this transitional zone, the wall thickness changes dramatically, from 11 feet 8 inches to 8 feet 7 inches. This thickness transition is visible as an abrupt taper of the interior walls of the shaft that widens the dimensions of the hollow interior space.

Above 150 feet, the Monument construction was supervised by the Army Corps of Engineers. From the transition to 500 feet, the interior walls of the shaft are constructed of blue gneiss and granite stone masonry units, transitioning entirely to marble at the 452-foot level. The exterior stone masonry units are two types of marble; four courses of Lee marble from Lee, Massachusetts and the balance of Cockeysville marble from Cockeysville, Maryland. The multiple wythes of stone block in this portion of the Monument are set with a Portland cement mortar. The shaft wall thickness at the 160-foot level is 8 feet 7 inches, gradually tapering to 1-foot 6 1/2 inches at the 500-foot level. At elevation 260-feet and above, the stone units that form the header course of the exterior marble, extend the full thickness of the shaft wall and can be observed from the interior of the shaft. At elevation 452-feet and above, the stone masonry shaft wall is a single wythe of marble. The single wythe construction of the shaft above 452 feet includes bent iron cramps in the mortared bed joint connecting adjacent stone units; some historical documents identify these as 3/4 bent galvanized iron bars (Brewer, unknown). Based on WJE’s non-destructive testing and the finding that cramps are located about six-inches from the interior face of masonry, there is a reasonable possibility that a double line of cramps exists in each course. At elevation 470-feet and above, the shaft wall contains iron cramps and mortise and tenon joints in the bed courses (John Milner Associates, Inc. 2004). The lower extensions of the pyramidion ribs, which are integrated into the shaft masonry between 470 feet and the top of the shaft, are also presumably connected with iron cramps. Both the mortise and tenon joints and the iron cramps are likely intended to control lengthening of the walls in the upper regions associated with spreading of adjacent stone units relative to each other.

Pyramidion Structure

The elegantly simple exterior of the pyramidion, comprised of twelve courses of large marble panels in four facets, belies the extremely complex nature of the masonry structure behind the panels. Although from the exterior, the panels appear to be stacked in the same manner as the shaft below, the panels are largely supported, both for gravity and out-of-plane, by a system of interior 1-foot wide ribs --- stone

arched-frames that begin at the 470-foot level. There are 12 ribs in total, three associated with each face of the Monument. The lower portions of the ribs between 470 and 500 feet are integrated into and dovetailed with the shaft masonry by alternating courses of rib stones that extend the full thickness of the shaft walls to the exterior (Figure 5). These penetrating rib stones appear on the exterior of the Monument as 2 feet square blocks which align vertically in alternate courses, in three vertical bands on each elevation from the 470- to 500-foot level. Between the 470 and 500 foot elevations, the projections of the rib stones towards the interior taper with each successive course. At 470-feet, the rib stones project only six-inches beyond the interior face of the shaft walls into the interior. At 500 feet, the middle ribs of each elevation project into the shaft approximately 6 feet, while the shallower side ribs project into the shaft approximately 4 feet 6 inches.

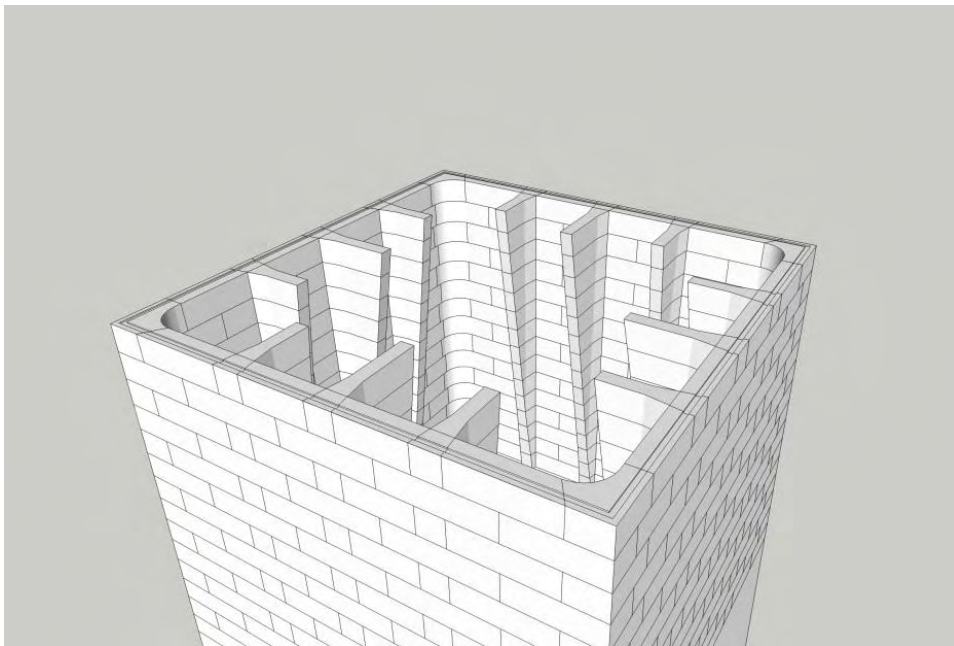


Figure 5. Rendering of rib structure cut at the 500-foot level of the shaft with the pyramidion above not shown for clarity

Above the 500-foot level the exterior panel and rib courses are approximately 4 feet 4 inches in height versus the 2 foot height of the courses of the shaft. Above this level, the ribs take on an arched profile, arching towards the interior (Figure 6). While the bed joints for the rib stones are horizontal between the 470 and 500-foot levels, these bed joints above 500-feet through course “H” are sloped downward towards the interior.

As shown in Figure 6, the corner ribs do not reach the full height of the pyramidion, but truncate in course “F”. Adjacent corner ribs join together in a complex mitered joint condition that stretches from the upper portion of course “E” through course “F”. This joint also includes mitered joinery with the haunched tie beams that extend around the interior perimeter of the pyramidion. These corner joints are each capped by a two-piece corner stone, both being 2 feet 8 inches square in plan, and a combined 5 feet 8 inches in approximate height. Of note, in plan, the tie beams do not exactly parallel the pyramidion wall planes. The tie beams are instead canted in plan such that an apex is formed at the common center rib stones to which the smaller ends opposing tie beams are joined with a mortise and tenon joints, thus providing additional out-of-plane support for the pyramidion wall panels (Figure 7).

Also as shown in Figure 6, at course “H”, the relatively small plan dimensions of the pyramidion cause opposing center ribs to approach closely enough to permit the cruciform stone to span the gaps between opposing ribs. The center rib stones at course “H” are joined to the cruciform and to course “G” below with mortise and tenon joints. The cruciform acts as the keystone for the intersecting arch-frames of the center ribs and has sloped joint surfaces typical of masonry keystones. While the cruciform acts as a keystone, it is not the highest point of the rib structure. Courses “I” and “K” of the center ribs continue up and terminate at course “K” with a single cross-lintel stone that runs east to west. The north and south center ribs key into this cross lintel stone with a vertical mortise and tenon joint.

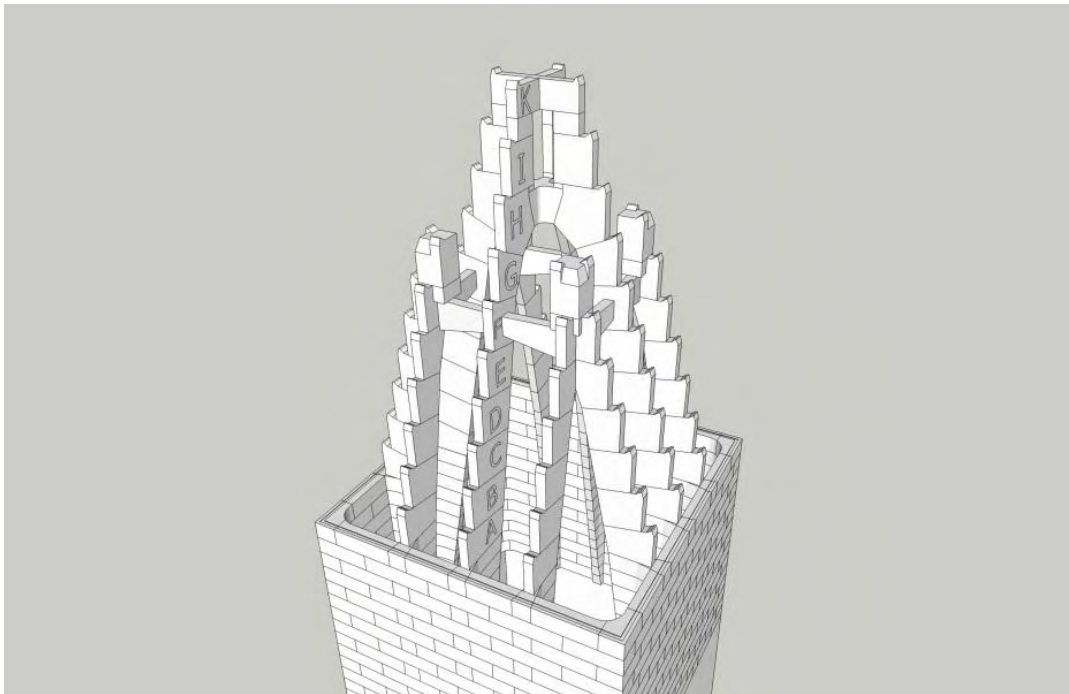


Figure 6. Rendering of the upper portion of the rib structure with the exterior panels not shown for clarity

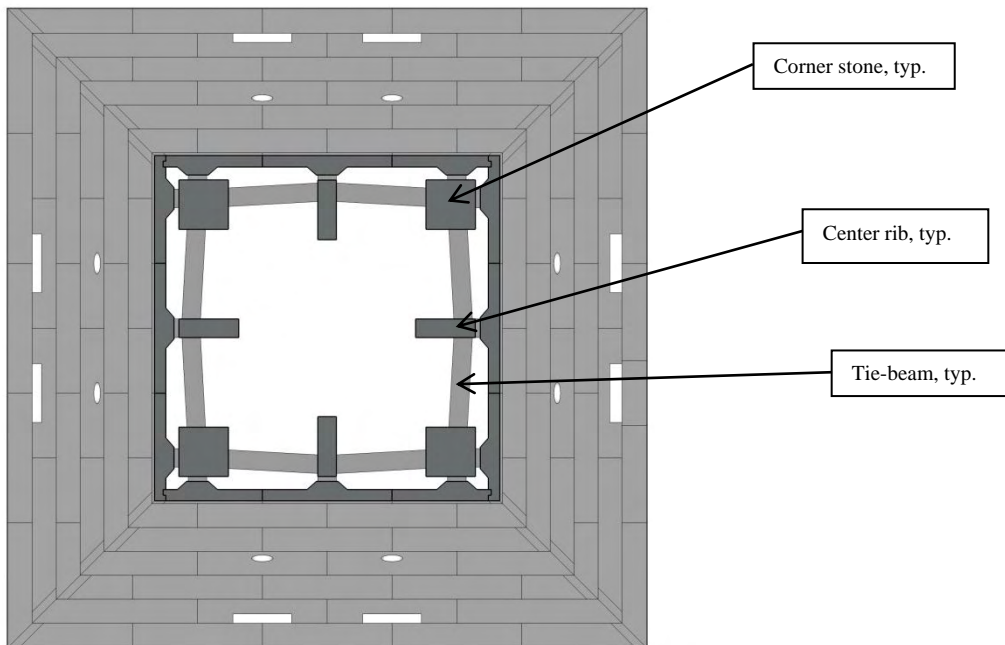


Figure 7. Plan section of pyramidion at tie beam elevation showing cant and apex at center ribs

The typical seven-inch thick exterior panels of the pyramidion appear to be “stacked” but are not self-supporting; except for the corner panels and other isolated locations, they are supported on the rib structure described above. The connections between the panels and the ribs are made at a sloped bearing “lug” that projects from the panels toward the interior at the base of each panel. The lugs bear on opposing sloped bearing surfaces, the “teeth”, which project from their associated rib stones. Thin sheets of lead shims with a thickness of about 3/32-inch are located at each of these bearing locations. The shims provide a more uniform bearing condition than can normally be achieved with stone-on-stone bearing. The lugs occur either at the center of the panels or at the ends of the panels, depending on the location of the rib stones with respect to the panels. The bearing surfaces of the lugs and rib stones mate such that the shiplap horizontal joints between panel courses maintain a 1/8 inch opening between courses, i.e. these joints are not mortared. The shiplap “step” is approximately 2 inches tall and occurs at the midpoint of the panel thickness. Treated oakum was packed into the joints to seal them, as is sheet metal flashing located below vertical joints. The side-to-side vertical panel joints have offset slots fitted with Z-shaped sheet metal and oakum. The typical horizontal joint is capped with the horizontal elements of the lightning protection system. The discussion above regarding typical panels notwithstanding, a few of the panels at the corners and at course 550 are not supported by lugs and presumably rest on the course below. The panel joints at the corners are interlocked in a manner similar to a squared-off dove-tail joint. Also, panel course “A” bears directly on the 500-foot level of the shaft and is connected with a continuous rabbet joint.

As described, each rib stone has a projecting angled bearing surface that carries the panel of the course above (Figure 6). We refer to this extension as a tooth. The bearing surface on the lug is also angled such that the tooth is positioned within a shallow recess in the lug. The term tooth is used in part because of the saw-toothed appearance of the projections in profile. The teeth provide far more structural integration between the panels and the rib stones than would a simple bearing. In addition to gravity support, the

teeth provide interlocking action, both in-plane and out-of-plane, between the rib stones and the panels. Very substantial in-plane interlocking is the result of the letting of the tooth on each rib into a chase cut into the adjacent panel or panels. The chase locks the rib stone into the panel relative to the in-plane direction of the exterior wall, particularly where the chase is cut into a single panel. Where vertical panel joints line up at ribs, the sides of the chase still interlock with the ribs, but only in one-direction. To make the connection tight, the small gaps between the sides of the chases and the rib stones necessary for fitting the stones together were filled with molten lead --- identified as “type metal” on the drawings --- after the placement of the panels (Figure 8). Out-of-plane support is provided by interlocking of the teeth that project upward and into the lugs and resist outward movement of the panels relative to the rib stones, as well as by the lap joint with the panel above (Figure 9).

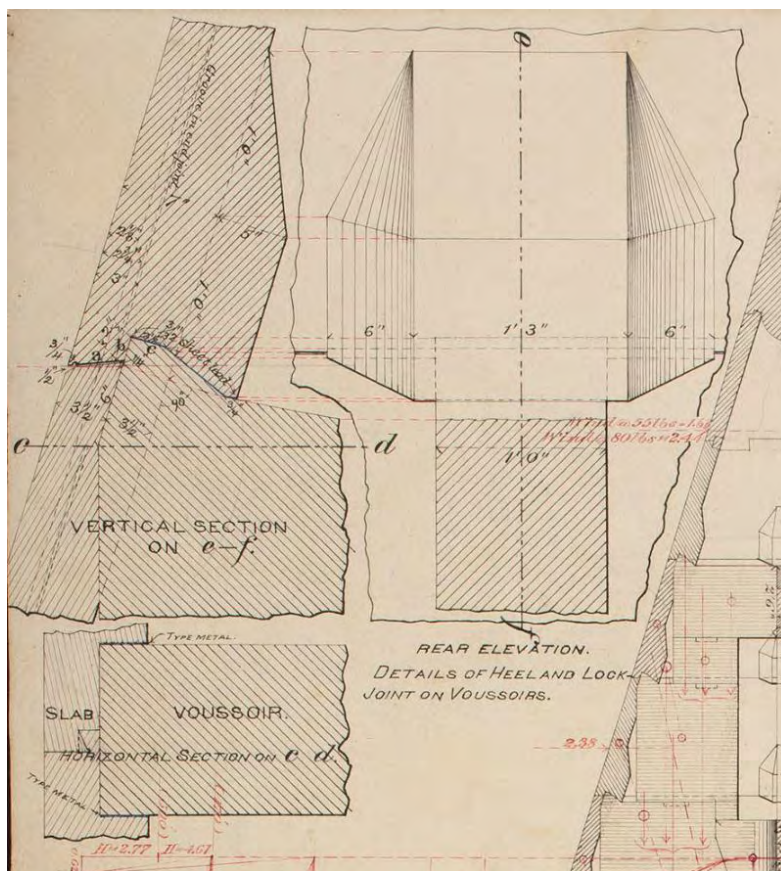


Figure 8. Army Corps of Engineers sketch circa 1880 of rib-stone-to-panel connection, from National Archives

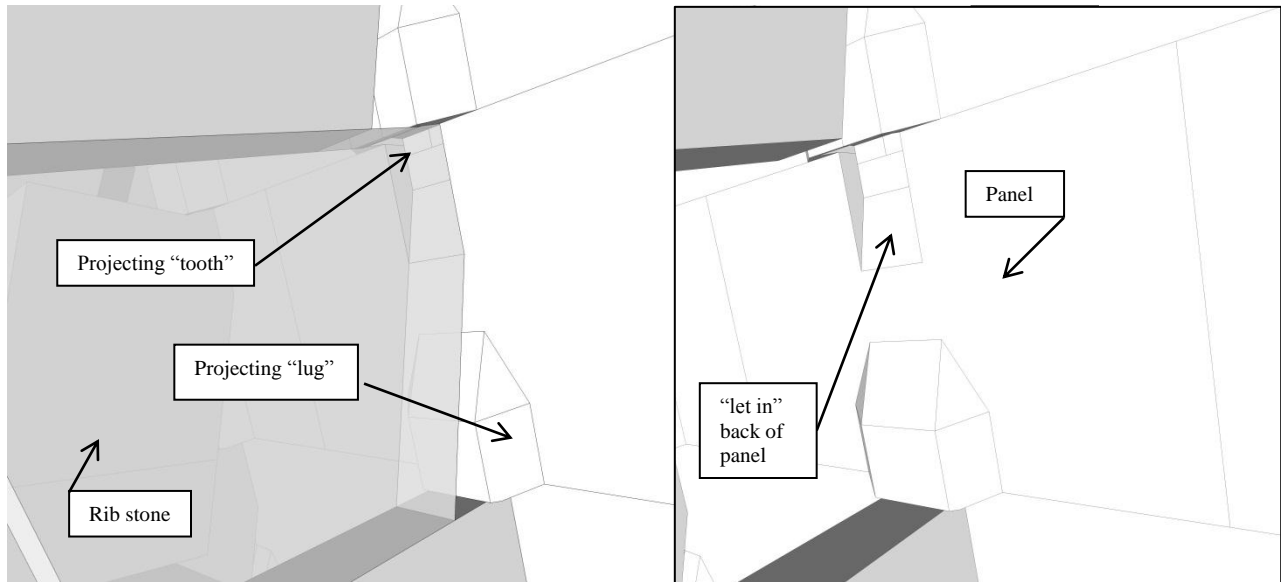


Figure 9. Images of projecting panel "lug" and projecting rib "tooth" at panel-to-rib bearing connections (Left with rib stone, Right without rib stone for clarity)

The panels of the course at the 546-foot elevation rest on top of the cross lintel of course "K" of the rib structure, this is the last exterior panel course that is supported by the rib structure. Course 550 rests directly on Course 546 and has an approximately 1 foot 7 inches wide by 2 feet 4 inches tall opening in the southern panel for access to the exterior of the Monument. The lower interior edges of courses 546 and 550 have a thickened edge similar to a lug, although this thickened condition runs the entire width of the bottom of each panel, and is mitered on either end. The final stone course, 555 is a solid block with a projection on the underside. This 3,300 pound stone is penetrated through the center by the lightning protection system and is capped by an engraved piece of solid aluminum approximately 9 inches tall. Figure 10 shows two cutaway renderings of the relative positioning of the ribs and the panels, as well as the layout of the lugs.

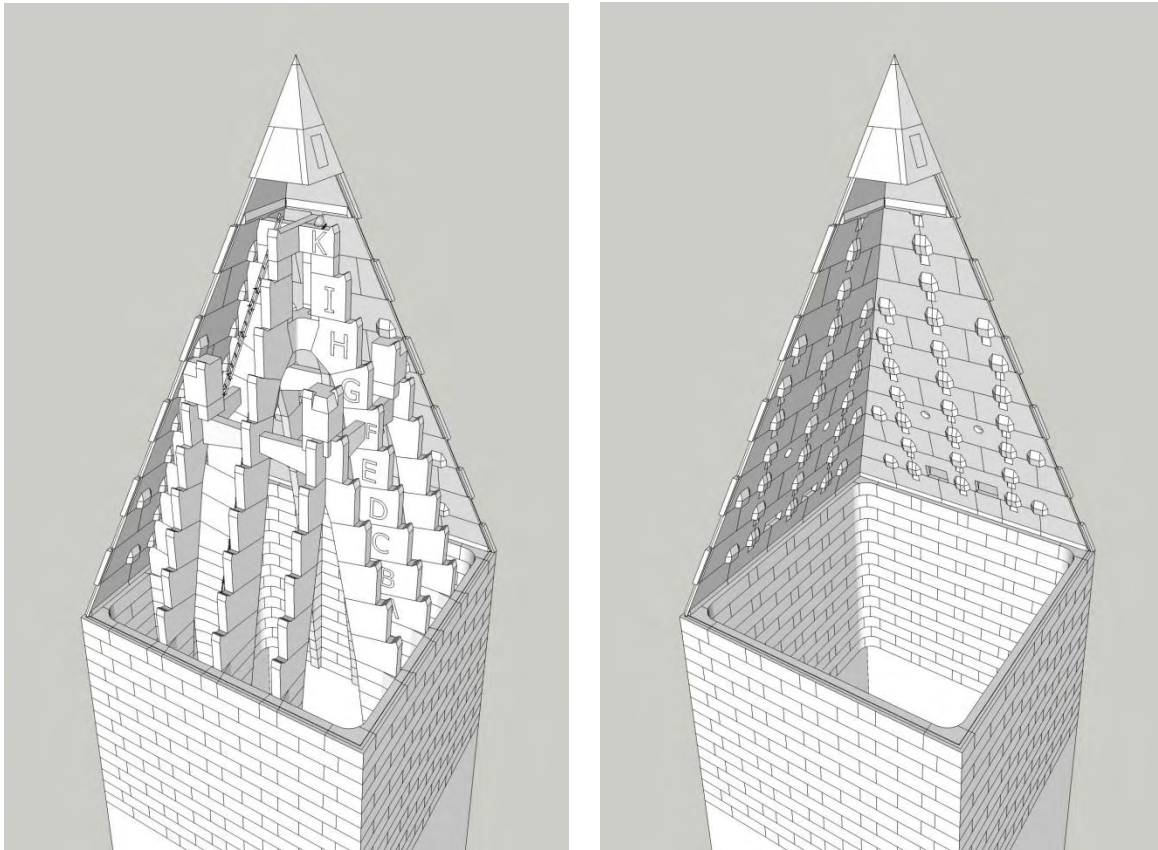


Figure 10. Left: Rendering of the pyramidion masonry with two exterior faces not shown for clarity. Right: Rendering of the interior face of the pyramidion panels showing the layout of lugs

SEISMIC ASSESSMENT

The seismic assessment of the Monument was essentially an assessment of its vulnerability to future strong earthquakes. It was intended to develop a characterization and quantification of the direct physical effects of future earthquake ground shaking on the structure for the purpose of determining if the extent and severity of damage that the Monument would experience would either prevent it from adequately protecting life safety and/or would substantially exceed that damage which resulted from the Mineral event. The occurrence of damage in a structure responding to earthquake ground shaking is a complex function of a multitude of factors, but fundamentally, prediction of damage to a structure caused by an earthquake requires a determination of how far the structure is pushed, in whole or in part, beyond its damage-free limit, otherwise known as its elastic limit. Seismic assessments therefore normally entail developing a physical and mathematic understanding of the manner in which the structure and its various components sway and deform in response to the ground shaking, estimating the amount of swaying and deformation that the structure and its various component parts can sustain prior to the onset of damage, and estimating how far beyond that point or points the structure and its component parts will get pushed by the specific earthquake of interest. With the level of deformation at the onset of damage being known as the structure's elastic limit, and the behavior of the structure up to that point being called "linear", evaluation of the amount of damage that a structure will sustain when it is pushed beyond its elastic limit is most often conducted with a technique called nonlinear analysis.

While prediction of damage from earthquakes using nonlinear analysis is rooted in science and engineering mechanics, for the most part it is an analysis technique that has been largely developed around --- and designed to predict the behavior of --- modern materials and methods of construction. Archaic, unreinforced masonry structures can be analyzed using nonlinear methods, but those methods require a certain amount of adaptation of existing analysis tools, resourcefulness, and attention to underlying earthquake engineering theory. This is particularly the case for the Washington Monument, in part because the structure of the Monument is so unique.

To our knowledge, application of nonlinear analysis techniques to a structure like the Monument is unprecedented. There is little relevant guidance set forth in earthquake engineering literature as to how to evaluate the seismic adequacy of a 555-foot tall unreinforced stone masonry shaft topped by a faceted thin-walled structure that is supported by arched-frames constructed of unreinforced stacks of stone masonry. The seismic assessment methodology for the Monument was designed to accommodate this void by assembling a reliable basis for predicting how the structure would generally respond to earthquake ground shaking, essentially using the documented performance of the Monument during the August 23 Mineral event. By developing a series of computer models and conducting benchmark analyses on them in which analysis-based predictions of how the structure would respond to the Mineral event could be compared to how it had actually behaved, the models and the nonlinear analysis methods could be validated. Once the benchmark studies were able to validate that the computer models and analysis methods could predict the damage that actually occurred to the Monument during the Mineral event, the models could be re-deployed to assess how the Monument would behave during the Maximum Considered Earthquake (MCE). The MCE is commonly relied on as a basis for seismic assessments of existing structures and seismic design of new structures throughout the United States. In engineering parlance, the MCE has a return period of 2,475-years and a 2% probability of exceedance in 50 years. It is the maximum event currently required to be used by the building codes and other standards for seismic design of new structures and for seismic assessment of existing ones. Even with that, uncertainty would remain, especially in the re-deployment of the models for assessment of structural response during the MCE because prediction of earthquake ground motion is fraught with uncertainty. However, this latter uncertainty is at least common to all seismic assessments and is addressed to an acceptable degree by established methodologies.

As discussed earlier, the Mineral event was used as the benchmark earthquake for this seismic assessment. It is the benchmark earthquake because it provides a known calibration point for correlating a known set of earthquake ground motions with a known catalogue of resulting damage. The availability of information describing the specific motions that occurred during that earthquake on the National Mall, together with the detailed catalogue of the specific damage to the Monument that resulted from those motions, provide a rare and unique opportunity to calibrate a structural computer model for use in generating reliable predictions for future earthquake events. Without either of these subsets of information, there would not be a way to reliably correlate any specific intensity of earthquake shaking to a specific type and severity of damage, or to validate a computer model developed for the purpose of predicting future damage.

The seismic vulnerability assessment included the following primary tasks:

1. Careful study of the type and distribution of physical damage documented subsequent to the Mineral event;
2. Conceptual study of the general behavior of the Monument when subjected to lateral forces;

3. Seismological studies to develop a science-based understanding and mathematical representations of the shaking intensity at the National Mall that actually occurred during the Mineral event;
4. Seismological studies to develop a science-based understanding and mathematical representations of the shaking intensity at the National Mall that might someday occur during future 2,475-year earthquakes;
5. Geotechnical analysis of existing data to develop an understanding of the strength and stiffness properties of the soil supporting the Monument foundation;
6. Development of nonlinear analysis models of the Monument and its support conditions, including a detailed discretization of the pyramidion;
7. Performance of benchmark analyses by subjecting the nonlinear analysis models to the mathematical representations of the shaking that occurred at the National Mall during the Mineral event and using comparisons between the damage predicted by the analyses with the damage documented after the earthquake as a basis for refining the models;
8. Performance of vulnerability analyses by subjecting the nonlinear analysis models to the mathematical representations of the shaking intensity at the National Mall that might someday occur during future 2,475-year earthquakes and evaluating the predicted behavior.
9. As it pertains to a future 2,475-year earthquake, development of findings as the structural adequacy of the Monument and its vulnerability to damage, and development of guidance with regard to the appropriateness of seismically strengthening the Monument.

Conceptual Seismic Behavior and Evaluation

Like all other structures, when the Monument is subjected to ground shaking during an earthquake, it responds by swaying back and forth for numerous cycles, dynamically. The swaying causes deformation of the pyramidion, the shaft and the soils beneath the foundation to occur to varying degrees, and the swaying can be relatively fast or relatively slow, depending on certain subtle characteristics of the shaking during different earthquake events. In other words, some earthquake events from some sources may excite the pyramidion relatively more than the shaft and base of the Monument, but other events may excite the shaft and base more than the pyramidion. All earthquakes will excite all of these “modes” of swaying to some degree. When the swaying is dominated by cantilever behavior of the shaft and deformation of the soil, the lateral displacement of the tip of the Monument is relatively large, and each cycle of swaying takes a few seconds because the Monument shaft is quite tall and slender and the soils that support it are deformable. When the swaying is dominated by local deformation of the pyramidion, the lateral displacement of the tip of the Monument would be relatively small, and each cycle of swaying takes only fractions of a second because the pyramidion structure is relatively squat and stiff. Every earthquake will cause some amount of each of these behaviors.

Conceptually, the mode of swaying that is dominated by cantilever behavior of the shaft and deformation of the soil is common to all high-rise structures and is relatively straightforward to understand and analyze, as long as the masonry in the shaft remains in its linear range, because the structure of the shaft up to 470 feet above the datum is regular and simple. Moreover, the primary structural properties of the masonry in the shaft are estimable, as are the primary structural properties of the soil, and bounds on the likely range of these properties can be established. Base rotation due to soil compression and even a certain amount of rocking at the soil interface is generally desirable as long as the compression capacity of the soil is not exceeded and the structure remains stable.

In contrast, the mode of swaying that is dominated by local deformation of the pyramidion is quite complex because the structure of the pyramidion is quite intricate, consisting as it does of stone arch-

frames of different heights that are interconnected by the tie-beams and the cruciform keystone, as well as interconnected by exterior stone panels which are not themselves structurally interconnected but which form triangular facets that engage each other along their edges. Despite the apparent complexity of the system, there are certain behaviors that can be expected conceptually. Each of these interactions loads the rib teeth and panel lugs because the interactions involve a transfer of forces from one element to the other. These conceptually identified interactions are described below:

1. As described earlier, the teeth provide the gravity support for the inclined panels. The transfer of gravity forces imposes forces into the teeth.
2. As the pyramidion responds to earthquake shaking, the panels, which weigh about 3,300 pounds each, are subjected to out-of-plane acceleration. At its lower elevations, the facets of the pyramidion are too wide to span edge-to-edge, i.e. to the perpendicular facets of the pyramidion, so the forces generated by the acceleration acting on the local mass of each panel must be transferred through the rib teeth and into the ribs. While important for providing lateral support for the panels, this force is judged to contribute less load to the teeth/lug connections than some other behaviors that the teeth are subjected to. The force associated with out-of-plane motion of each panels, and therefore carried by each tooth, can be estimated by multiplying the acceleration of the pyramidion by the weight of each panel and is some fraction of 3,300 pounds.
3. The rib stones themselves have substantial mass, nearly that of each associated panel stone. When a rib stone tries to move in the direction of its minor axis, i.e. in the direction perpendicular to the plane of the ribs, resistance to this motion is initially provided by its supporting bed joint. After the bed joint cracks, however, resistance to this motion is provided only via the teeth and lugs at the extreme end of the rib stone, and by friction. The eccentricity between the center of mass of the rib stone and the location of the tooth creates a torsional moment that can only be resisted by the tooth/lug support and the residual resistance of the bed joint through friction. The connection forces required to resist torsional motion of the ribs is judged to be significant.
4. As the pyramidion sways, the ribs act and deform as frame members until the tensile loads on the bed joints exceeds the capacity provided by dead load and the tensile strength of the mortar. The central ribs behave, by virtue of the cruciform keystone, to some degree as arches; the corner ribs as cantilevers. As the ribs deform and individual rib stones undergo rotation as frame members, they engage additional dead load by pulling up on the adjacent panels, which likely engage yet more load from other panels. The teeth to some degree, therefore act as shear studs that enforce composite action of a sort between the ribs and the facets.
5. The central ribs provide support for greater tributary area than the corner ribs and are more flexible. As they deform in frame action, the canted tie beams transfer load from the center ribs to the corner ribs. The thrust imposed acts to cause spreading of the pyramidion at the elevation of the tie beams.
6. The facets of the pyramidion provide some in-plane shear resistance, although the absence of mortar in the joints limits this mode of behavior. Near the top of the pyramidion, however, where the facets narrow such that in some courses all vertical joints between panels are locked into the rib stones, in-plane stiffness of the panels is likely significant.

Benchmark Ground Motion

On Tuesday, August 23, 2011 at approximately 1:51 PM EDT, a magnitude 5.8 M_w earthquake was recorded by the U.S. Geological Survey (USGS) within the Central Virginia Seismic Zone, centered approximately 84 miles southwest of Washington, D.C. near Mineral, Virginia. The earthquake occurred at an approximate depth of 3.7 miles below the surface and was followed by several after-shocks with

magnitudes that ranged between 2.0M_w and 4.5M_w. Due to the geology of the eastern seaboard of the United States (U.S.), even moderate earthquake events will usually be felt across a far wider region than an earthquake of equivalent magnitude in the west, shaking an inventory of buildings that tends to be significantly older than the building stock in seismic zones in the west and, therefore, generally designed to resist far smaller earthquake forces. The USGS is now reporting that this event was the most widely-felt earthquake in U.S. history.

There are a number of scales that are commonly used to describe the size, magnitude, and intensity of an earthquake. Some measures are more useful for engineering analysis than others. The Moment Magnitude Scale (M_w) is a measure of the energy release associated with an earthquake at its source, and as such, provides more meaningful information about general property of the earthquake as a geological event than about the strength and character of ground shaking at any particular location. The Modified Mercalli Intensity (MMI) scale is a qualitative measure of the general effects of the earthquake in any given locale. While a given earthquake typically has only a single magnitude value associated with it, a Modified Mercalli Intensity level can be assigned to each and every location in a shaken region. The MMI scale narratively describes both a range of human perceptions associated with locally felt ground shaking, as well as the effects of the ground shaking on the built environment. For example, the 5.8 M_w Mineral event caused a shaking intensity at the epicenter of “VII” on the MMI scale, which is defined as “Damage negligible in buildings of good design and construction; slight-to-moderate in well-built ordinary structures; considerable damage in poorly built or badly designed structures, [with] some chimneys broken” on the MMI scale. In the majority of the Washington D.C area, the MMI shaking intensity during the August 23 event corresponded roughly to a “V” on the MMI scale, which is defined as “felt inside by most; some dishes, windows broken; vibrations like large train passing close by”. Structural damage due to MMI V shaking is rare and usually does not occur in competent engineered structures.

The intensity of locally felt ground shaking can also be measured by instruments which record the acceleration of the ground during an earthquake event, thus allowing the shaking intensity of a seismic event to be quantified by measurable data if a recording instrument exists in the locale of interest. While there is undoubtedly a relationship between the acceleration of the ground during an earthquake and the damage caused to buildings by ground shaking, the precise relationship cannot be well-defined because the effects of the earthquake in part depend on the type, configuration and quality of the buildings being shaken. The maximum acceleration of the ground, or “Peak Ground Acceleration” (PGA), is commonly used by engineers to characterize the local intensity of shaking during an earthquake, and can be loosely correlated to the MMI scale using the “Instrumental Intensity” (I_{mm}) map available from the USGS and referred to on their website as a “ShakeMap”. In the absence of instrument data, the USGS /Google Earth ShakeMap in Figure 11 provides some basis for estimating a range for the PGA in Washington DC during the Mineral event. Due to the paucity of actual instrumental data available for the Mineral event, the USGS constructed these ShakeMaps using supplemental internet survey data known as “Did You Feel It?” (DYFI). From the map, it can be seen that the PGA estimated for Washington DC would correlate roughly to a “moderate” level of perceived shaking and a “very light” potential for damage. However, the Monument is a sufficiently unique structural type that it is clearly not the prototypical building on which either the MMI or I_{mm} scales were based when they were developed. There is little reason, therefore, to expect that the Monument would perform in accordance with the expectations set forth in those scales.

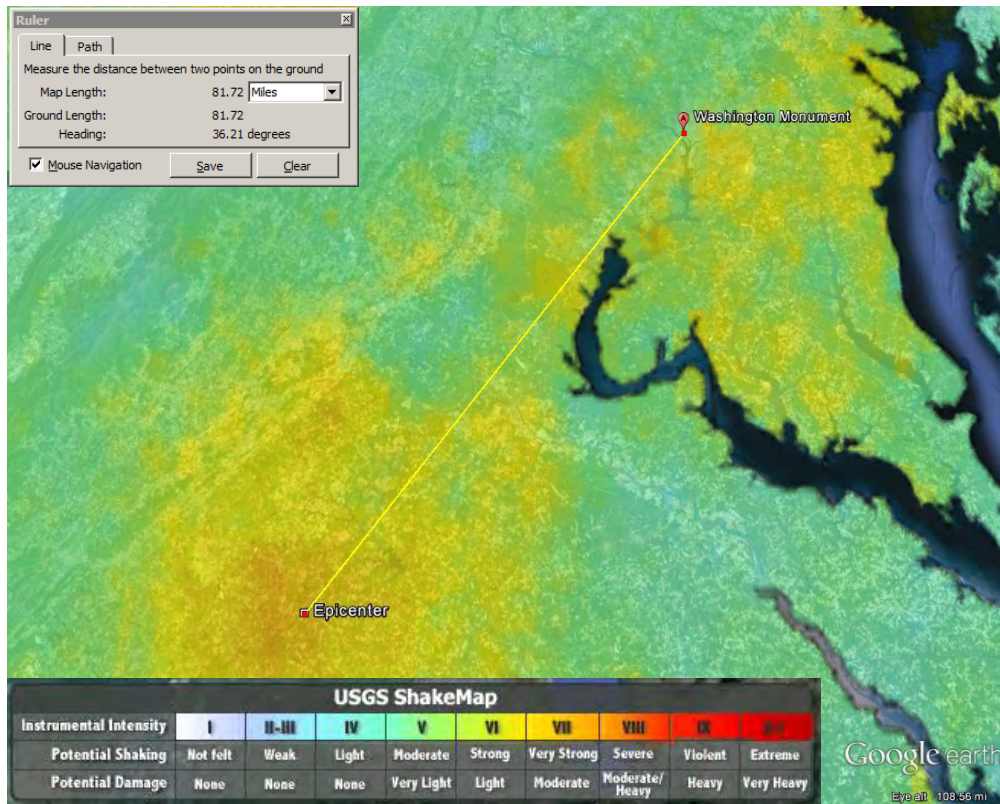


Figure 11. USGS Shake Map of August 23, 2011 for the Mineral, Virginia earthquake

As part of this seismic assessment, WJE retained AMEC as a sub-consultant to provide mathematical representations of the shaking caused by the Mineral event, but specifically at the site of the Monument. Performing this involved, among many other things, obtaining recorded instrumental data of the earthquake shaking and processing it in a manner to make it applicable to the site of the Monument. A combination of published and unpublished data, the latter obtained by WJE, was used. AMEC’s methodology is described in their report, provided herein as Appendix A. WJE and AMEC coordinated efforts to ensure that the seismological and geotechnical data employed for the seismic assessment provided the most usable and relevant information possible.

Representations of the seismic demands on structures sited on the National Mall during the August 23 Mineral event (Benchmark earthquake) are provided in Figures 12 through 14. The data in the plots was developed by AMEC, but the data was reformatted by WJE to provide information more usable for the structural side of the seismic assessment. Figure 12 is called an ADRS response spectrum and it sets forth the magnitude of the expected response --- in terms of spectral acceleration (as defined on the vertical axis) and spectral displacement (as defined on the horizontal axis) --- of a broad range of structures to the ground shaking on the National Mall during the Mineral event. Implicit in the plot is the assumption that the structures remain essentially elastic, i.e. the structures remain undamaged enough that the periods of vibration of the structures do not substantially change. To use the plot to provide structure-specific information, the most important periods of vibration of the structure of interest, must be known. (In the case of the Monument, the periods of vibration were obtained from computer analysis.) The diagonal lines on the plot are the period lines that are used in identifying the spectral demands for any specific structure. From the plot, for a structure with a period of vibration, of say of 0.3 seconds, the 0.3 second

period line can be followed from the origin until it intersects the plotted curve, from which it can be determined that the Mineral event would have imposed a spectral acceleration of almost 0.25g and a spectral displacement at the effective height of the structure of approximately 0.2 inches. Similarly, from the 0.75 second period line, it can be determined that for a structure with a period of vibration of 0.75 seconds, the Mineral event would have imposed a spectral acceleration of about 0.056g and a spectral displacement at the effective height of the structure of approximately 0.3 inches. The plot also shows that the displacement demands from the Mineral event were nearly constant for structures with periods greater than about 0.35 seconds. For example, for a structure with a period of vibration, of either 1.0, 2.0, or 3.0 seconds, the Mineral event would have imposed a spectral displacement at the effective height of the structure of approximately 0.25 inches.

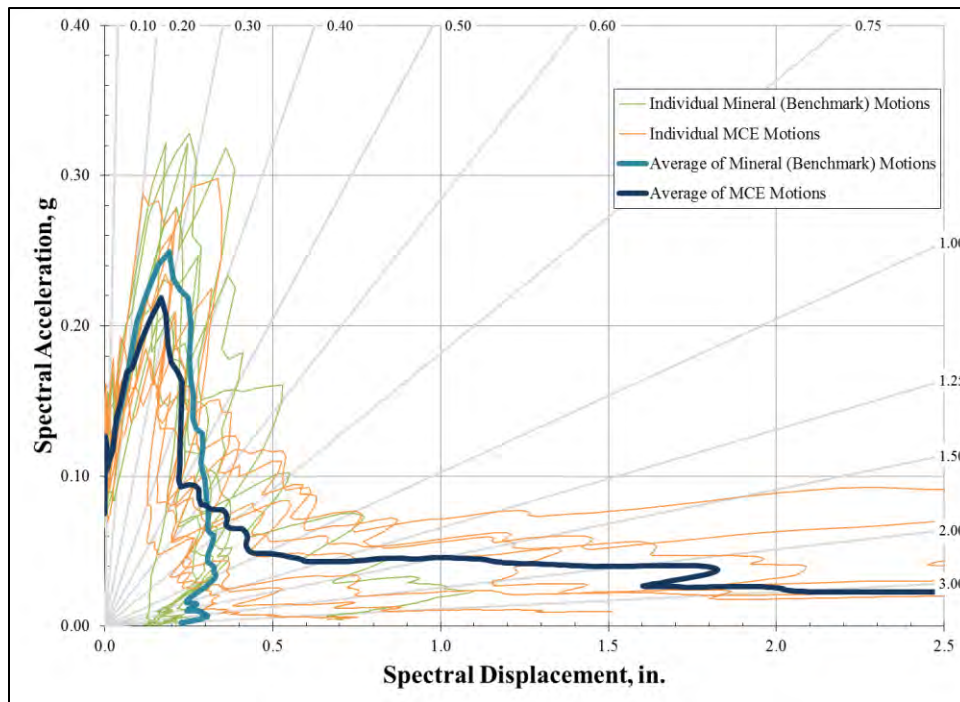


Figure 12. ADRS plot of Mineral (Benchmark) and MCE seismic demands

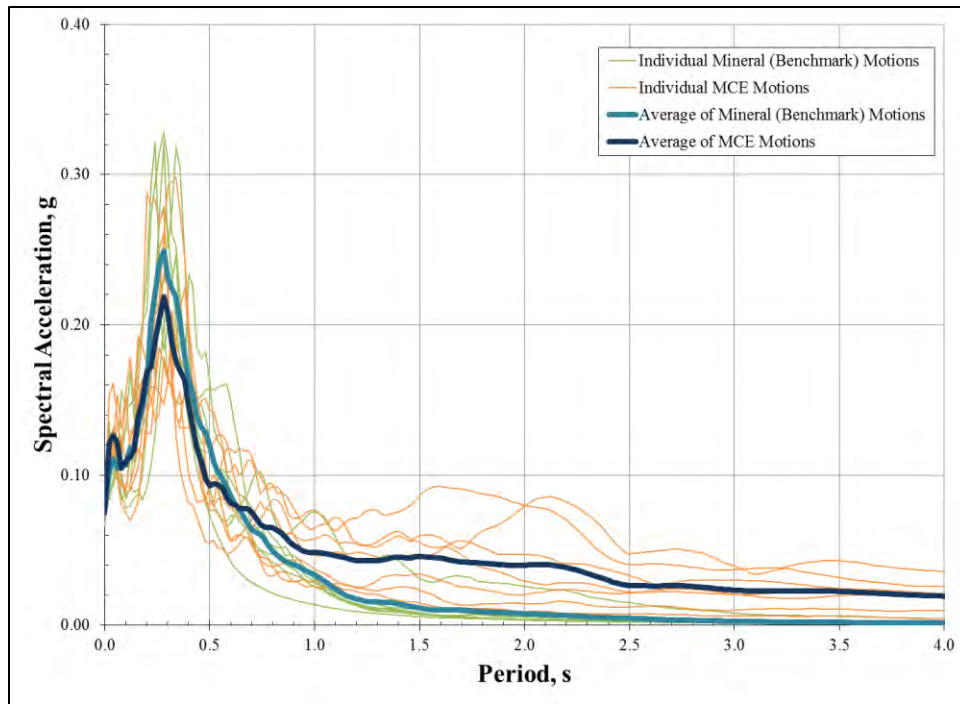


Figure 13. Response Spectrum of Mineral (Benchmark) and MCE seismic demands

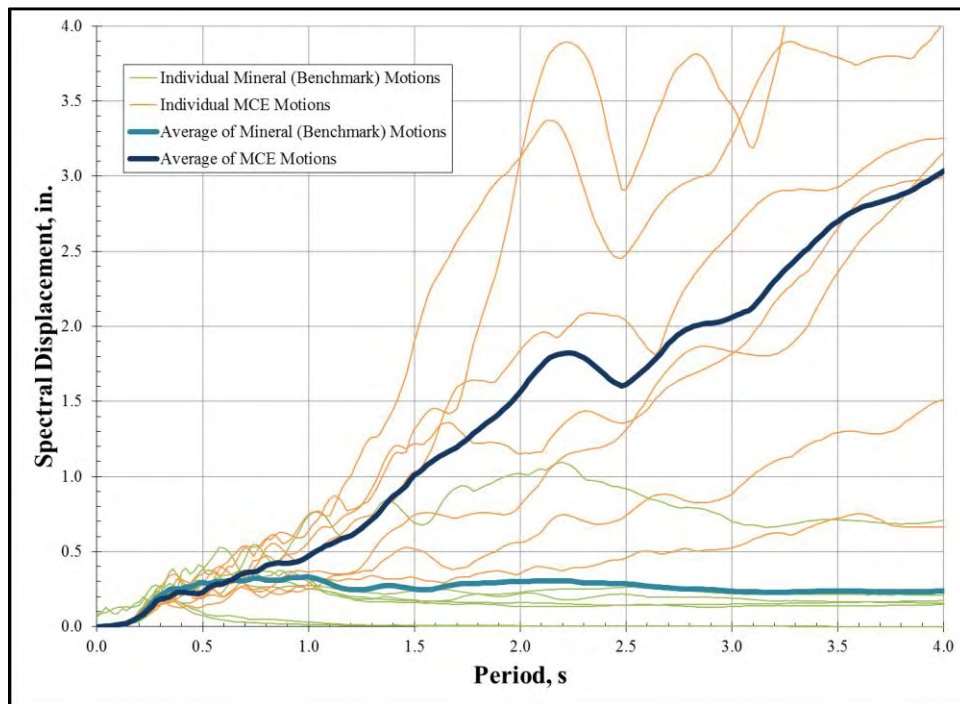


Figure 14. Displacement demand of Mineral (Benchmark) and MCE ground motions

While it will be discussed in greater detail in the analysis section of this report, the computer analysis of the Monument revealed that the primary swaying mode of the Monument shaft is about 3.0 seconds. Thus, assuming that the Monument remained essentially elastic during the earthquake, the displacement demand during the Mineral event on this mode appears to have been significantly less than 1-inch. To conceptually evaluate the structural significance of displacement of a structure, engineers will often compute a “drift ratio” by dividing the displacement demand by the height over which the displacement occurs. This value represents the average deformation over the height of the structure. A 1-inch displacement as a percentage of the height of the shaft, i.e. the “drift ratio” demand for the shaft, is less than 0.0002, which is a trivial value relative to the ability of masonry to deform without ill-consequence. Since the 500-foot tall shaft of the Monument can easily deform this amount without damage, and some portion of this demand was also undoubtedly accommodated by transient deformation of the soils beneath the base, it is relatively easy to understand why the Monument shaft experienced only minor damage during the Mineral event.

A similar conceptual analysis, but with a different outcome, can be undertaken for the pyramidion. The approximate period range for the primary modes that cause deformation of the pyramidion is 0.3 to 0.35 seconds. As discussed above, the displacement demand applicable to this period range is about 0.25 inches. Because the shape of the pyramidion is pyramidal, it has a very stable shape that is relatively resistant to deformation over its height, at least with respect to tip-to-base displacement. The computer analysis demonstrates that the primary mode of deformation in the pyramidion involves frame action of the center ribs and the facets swaying out-of-plane rather than swaying of its tip relative to its base. Moreover, the maximum out-of plane deformation occurs according to the computer analysis near the center of the facets where the center ribs arguably span only a short distance between the pyramidion base to the canted tie beams, and where the facets also span only a short distance. The ribs must therefore accommodate the 0.25-inch displacement over about five bed joints. It is not difficult to see why 0.25 inches of deformation across five or so bed joints of the ribs would necessarily cause damage, including shifting of rib stone blocks and damage to rib-to-panel connections, or why that amount of deformation spread across three or four vertical panel joints would cause damage. This conceptual analysis cannot of course account for nuances of seismic response that were identified during the detailed seismic analysis, but it appears to be generally consistent with the damage documented in the pyramidion after the Mineral event where damage was concentrated over the middle third of the pyramidion height.

Of note, AMEC has concluded that the intensity of ground shaking at the National Mall during the Mineral event, in the period range to which the pyramidion is most vulnerable corresponds to an earthquake with a return period between 2,000 and 3,000 years. From this perspective as well, the pyramidion can be viewed as already having experienced its MCE, or something similar.

MCE Ground Motion

As part of this seismic assessment project, AMEC was charged with developing representations of ground shaking on the National Mall that would be caused by a rare future large earthquake. Their report describes in detail the methodology used to generate these representations. For earthquake-resistant design of buildings in the United States, it is generally accepted engineering practice to consider an earthquake with a return period of 2,475 years as the design-basis event. That event is termed the MCE, or Maximum Considered Earthquake. In actual practice, when buildings are designed the criterion used is equivalent to two-thirds of the 2,475-event. This assessment of the seismic adequacy of the Monument to resist shaking from a future rare event did not employ the one-third reduction normally applied to the MCE but rather, employed the full 2,475-year event.

Representations of the seismic demands on structures sited on the National Mall during the predicted 2,475-year event are also shown in Figures 12 through 14 to facilitate comparison between the demands from the Mineral event and the predicted demands from a rare future event. As was true for the Mineral event, the data for the 2,475-year event curves was developed by AMEC, but the data was reformatted by WJE to provide information more usable for the structural side of the seismic assessment. Several important observations can be made from Figure 12 with respect to the 2,475-year event.

1. For periods less than about 0.5 seconds, the shape and ordinates of the Mineral event spectrum and the MCE spectrum are very similar. The peaks of both spectra coincide at about 0.3 seconds.
2. For structures with periods between about 0.2 seconds and 0.5 seconds, the Mineral event was actually more severe than the MCE. At the peak of the spectra, the Mineral event imposes about 20 percent greater acceleration demand than the predicted MCE. Because the period of the pyramidion is about 0.3 seconds, it therefore appears as if the pyramidion was subjected to something as large, or larger than, the 2,475-year event on August 23. It is therefore reasonable to conclude, at least insofar as this conceptual evaluation of the response spectrum analysis is the basis, that the damage to the pyramidion during the Mineral event is of the same order of magnitude as, or greater than, will occur during the MCE. The detailed seismic analysis described in a later section of this report validates this preliminary finding.
3. For structures with periods greater than the about 0.5 seconds, the displacement demands from the predicted MCE are substantially greater than the demands during the Mineral event. For example, while the displacement demands during the Mineral event were constant for all buildings with periods greater than about 0.5 seconds, the MCE displacement demands increase with increasing periods. For the Monument, whose primary period for response of the shaft in a cantilever bending mode approaches 3.0 to 3.2 seconds for one of the sets of material properties that were analyzed, the MCE spectral displacement demand is approximately 2.2 inches (See Figure 14), which would be accommodated partially at the foundation/soil interface and partially as deformation along the height of the shaft. It is therefore reasonable to conclude, at least insofar as this conceptual comparison between the Mineral event and the predicted MCE is the basis, that the shaft will be subjected to substantially greater movement during the MCE than it was during the Mineral event, for which the spectral displacement demands at 3.0 seconds was about 0.25 inches. In terms of acceleration, the MCE demands on the shaft also appear to be substantially greater in percentage terms than were the demands during the Mineral event, but the MCE demands still appear to be quite modest, about 0.03g. The detailed seismic analysis described in a later section of this report was used to determine if the predicted increased demands on the shaft during the MCE would be sufficient to cause damage to the shaft.

Of note, AMEC has found that the Charleston, South Carolina earthquake in 1886 shook the National Mall with an intensity equal to or greater than the hazard associated with the MCE in the period range greater than 1 second, which is the range to which the shaft of the Monument and the soils supporting the Monument are most vulnerable. From this perspective, the shaft and soils beneath the Monument can be viewed as already having experienced their MCE, or something similar, in 1886, shortly after the construction of the Monument was completed.

WASHINGTON MONUMENT ANALYTICAL MODELING

Overview

Analytical modeling of the Monument took various forms; proceeding from simple single degree-of-freedom systems and prismatic cantilever frames, to parametric studies employing detailed three-dimensional nonlinear finite element models subjected to time history analysis. The analyses were focused on characterizing the behavior and performance of the Monument under two seismic loading regimens: one representing the Mineral event “benchmark”, and another representing the Maximum Considered Earthquake (MCE) with a return period of 2,475 years. The Monument’s construction employing massive stacked blocks of stone with thin layers of mortar, especially the unique stone arch/frame assemblies in the pyramidion, rendered traditional modeling and analysis methods ill-suited for seismic assessment of the Monument as traditional methods are unable to capture the nuances of behavior of these systems. The finite element models ultimately relied on for this assessment incorporated variability in material properties through a series of parametric exercises that bounded structural behaviors, and employed available historic and more recent material testing along with field data. The benchmark ground motions allowed for a direct comparison between analysis output and observed conditions that informed the selection of modeling techniques, geometric configurations, and material properties. In certain respects, the finite element model is a product of the earthquake damage assessment and survey: many of the relative movements, displacements, offsets, and damage to the Monument documented by WJE field personnel after the Mineral event informed the assembly of the finite element model.

The three-dimensional finite element model is mainly comprised of three different types of elements: contiguous three-dimensional solid elements, three-dimensional solid elements modeled as sliding effectively rigid blocks, and shell elements modeled as effectively rigid panels with deformable joints. The model was subjected to various linear and nonlinear, static and dynamic analyses, including an Eigenvector Modal Analysis to determine the undamped free-vibration mode shapes, and a Nonlinear Modal Time History Analysis utilizing AMEC provided ground motions.

Model Development

Layers of complexity were successively added to the Monument analysis and modeling effort, starting from hand calculations, single degree-of-freedom models, and prismatic cantilever frames, to large three-dimensional finite element models. The software package utilized to create the models was SAP 2000 Version 14, an industry standard for complex three-dimensional structural modeling and seismic analysis. Although several ancillary studies were performed on features of the models such as verification of three-dimensional solid aspect ratios for meshing operations and submodels of nonlinear friction-pendulum isolators, the only models that are described below are the final finite element models that were used to perform the analyses on the Monument.

The modeling discussion below is sub-divided to facilitate distinct presentations of the primary areas of study along the vertical height of the Monument, namely 1) the bearing materials at the foundation/soil interface, 2) the shaft from 0 feet to 470 feet, 3) the shaft from 470 feet to 500 feet, 4) the pyramidion rib stones, 5) the pyramidion panels. Here, as elsewhere in the report, the vertical datum of 0 feet is taken as the bottom of the shaft of the Monument, which is approximately at grade level.

Soils and Monument Foundation

The Monument was modeled with the as-built geometry of its stone and concrete foundation bearing on compressible soil. The properties of the compressible soil were provided by AMEC based on various historic and contemporary logs of soil borings taken from nearby on the National Mall. AMEC defined the load-displacement response of the soil for both static (gravity loading only) and dynamic (transient loading due to seismic response) from zero to 30 inches of vertical displacement (Figure 15). The vertical component of soil response was judged to be the only mode of soil response with potentially significant influence on the global behavior of the Monument.

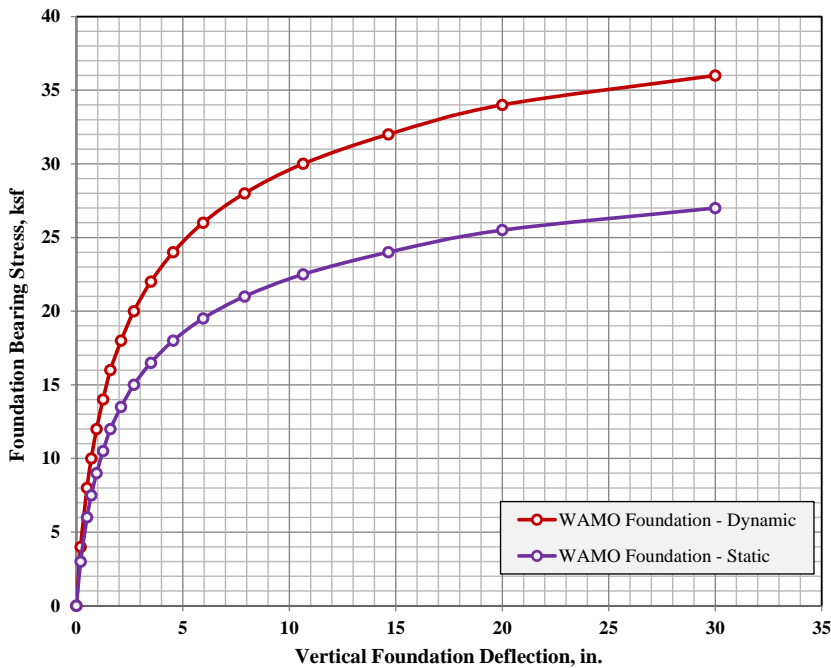


Figure 15. AMEC provided soil load-displacement relationship

As recommended by AMEC, the seismic increment in soil response was modeled as linear-elastic extending from the static to the dynamic curve. On the static side, linearization begins at the bearing stress due to dead load (approximately 10.5 ksf) calculated using the static load-displacement relationship. From this point, the relationship extends to the dynamic curve to the predicted maximum bearing pressure of approximately 16 ksf, determined using an iterative procedure. This method resulted in an elastic soil stiffness of 15 ksf/in, shown in Figure 16 as a green line. During preliminary model development, a range of soil stiffnesses was input into the model as a bounding exercise and shown to have only minor effects on the behavior of the pyramidion and the shaft. The soil stiffness of 15 ksf/in is associated with the higher side of the range considered, especially as it relates to the static tangential soil stiffness at the bearing stress due to dead load. The stiffness value that results from the AMEC recommendation appears to track the instantaneous dynamic soil response at the origin of the load-displacement relationship.

Vertical soil stiffnesses were modeled as surface springs applied to the downturned face of the three-dimensional solids that were used to model the Monument's foundation construction (and discussed in more detail below). Analysis and hand calculations determined that sliding at the base of the foundation

was not a likely failure mode and that horizontal deformation of the soil mass at the sides of the foundation under lateral loading would be insignificant to the global response. Therefore, the base of the model was restrained laterally and passive earth pressures were not distributed vertically along the sides of the foundation.

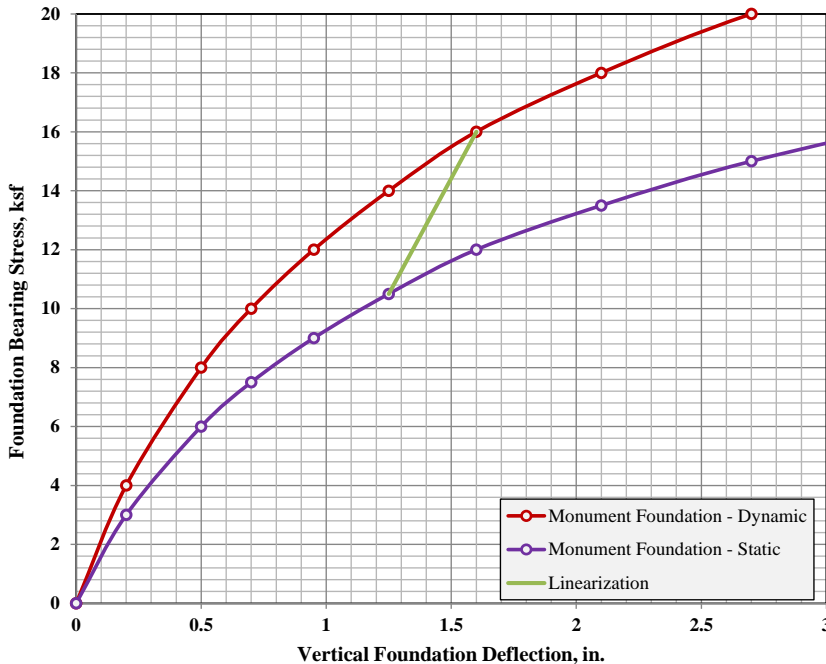


Figure 16. Linearization of static-to-dynamic soil behavior

The foundation of the Monument is comprised of three different materials from two different eras of construction. The original stone foundation was reportedly 80 feet square in plan and approximately 23 feet deep. The outer courses were constructed of dovetailed blocks of blue gneiss stone bonded with mortar, the inner courses are a more rubble-like ashlar-coursed stone masonry infill (Oehrlein and Associates 1993, Paul 1986). This foundation supported the original shaft to the 156 foot level when construction was halted. Prior to the continuation of construction of the shaft in 1880, the foundation was buttressed and underpinned with concrete. The concrete buttressing was performed in stages after the underpinning work, resulting in a complete encasement of the original blue gneiss stone (Figures 3 and 4). The new foundation depth was 13.5 feet deeper than the original footing and encompassed an area approximately 126 feet square in plan. The foundation in SAP 2000 is shown in Figures 17 and 18 with the original stone foundation in blue and the concrete buttressing and underpinning in grey.

The influence of the flexibility of the foundation on the overall behavior of the Monument is minor compared to the flexibility of the soil. The foundation was modeled as having two different elastic moduli, the blue gneiss stone and mortar composite having an effective elastic modulus of 1200 ksi and the concrete portion of the foundation having an elastic modulus of 2500 ksi. The two vintages of foundation construction were meshed using three-dimensional solid elements meshed together as a single linear-elastic deformable object.

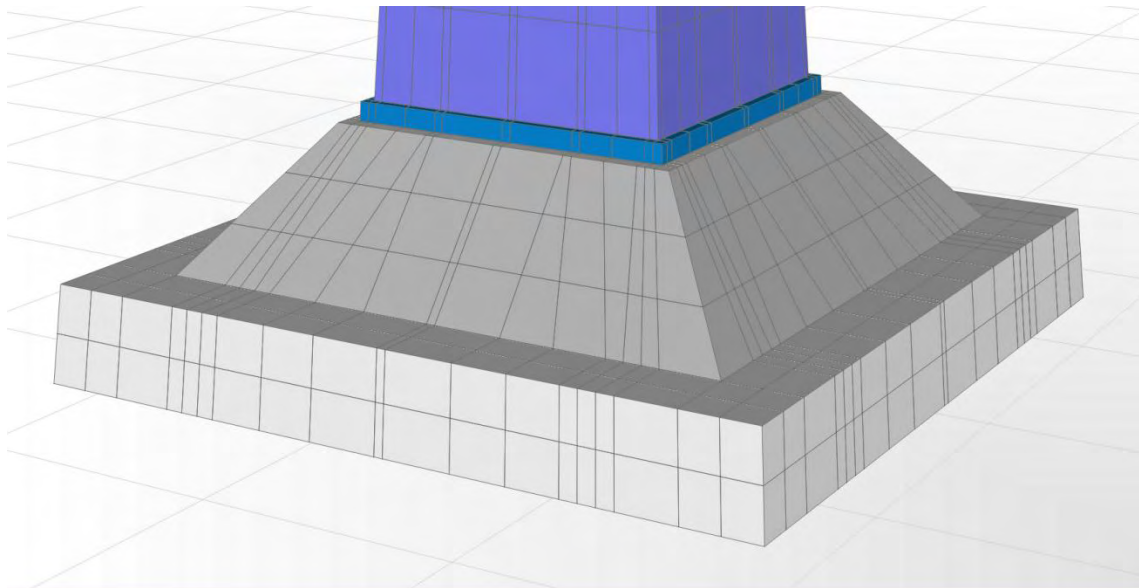


Figure 17. The Monument foundation in SAP2000

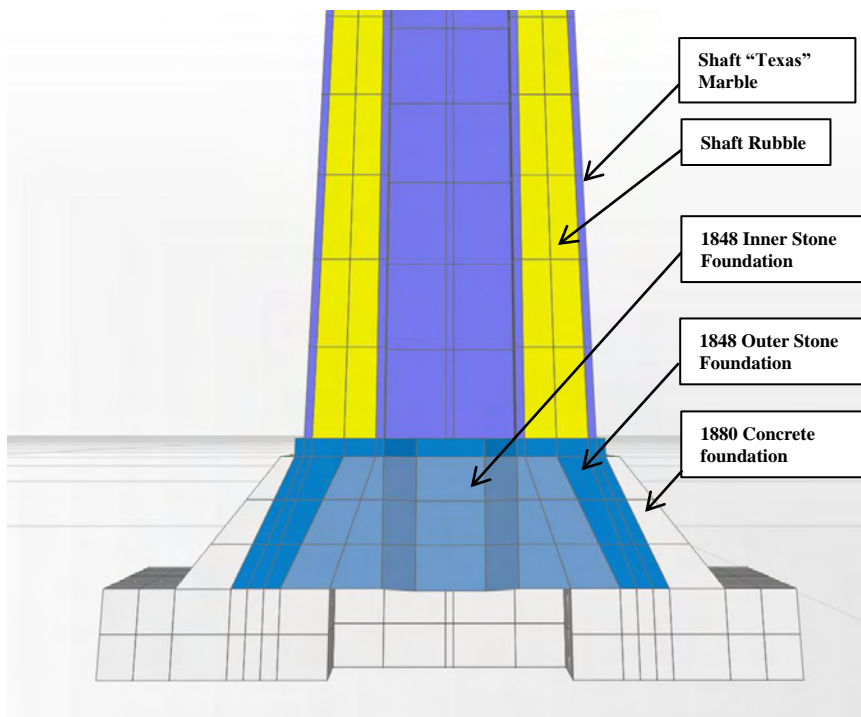


Figure 18. Cross-section of the Monument foundation and lower portion of shaft in SAP2000

Shaft

The shaft of the Monument gradually tapers between the ground level datum located at 0 feet and the beginning of the pyramidion at an elevation of 500 feet. This portion of the Monument was modeled in three different ways to correspond with the different construction types encountered along the shaft's height.

Shaft from 0 feet to 150 feet

From ground level to an elevation of 150 feet the masonry shaft of the Monument consists of three well-integrated wythes of different construction: an outer wythe of high-quality stacked ashlar “Texas” white marble, an inner wythe of gneiss, and an inner cavity filled with stone rubble masonry (Figures 18 and 19). The masonry in this portion of the shaft was constructed with natural cement mortar. Although the stone in the various wythes has different properties, the properties of the natural cement mortar dominate the behavior of the masonry in general and the interior rubble wythe --- which contains a far greater amount of mortar than the exterior wythes --- dominates the behavior of the wall construction overall. Recognizing the highly variable nature of masonry, even within an individual wythe, and after studying the effects of modeling each wythe with a different material property on the model behavior, as a base value, an elastic modulus of 1000 ksi was assumed for all materials. It is our judgment, based on our prior experience in testing masonry structures, with additional insight provided by other industry standards and codes, including ACI 530 (American Concrete Institute 2011), that this value is a reasonable average property for the masonry stiffness. Each of the different masonry layers was modeled using a continuous mesh of three-dimensional solid elements, which was intended to capture the high degree of articulation and keying that exists between the two exterior stone layers and the rubble masonry.

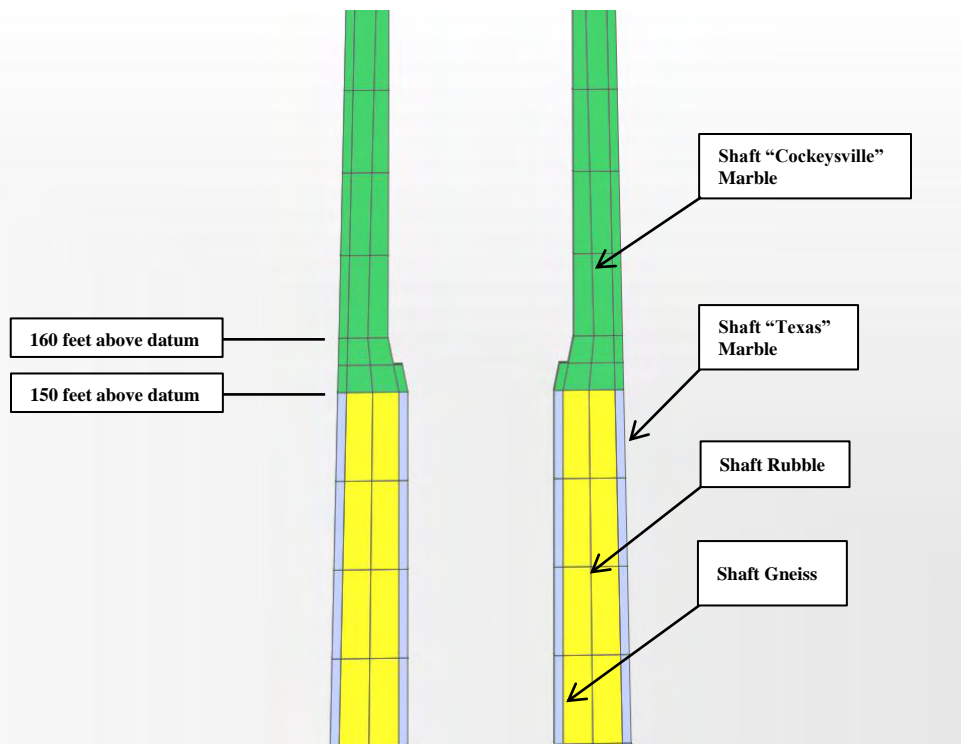


Figure 19. Cross-section of the Monument at 150 foot transition level

Shaft from 150 feet to 470 feet

From an elevation of 150 feet to 160 feet, the shaft transitions from marble-rubble-gneiss construction to an all-marble coursing, and the stone type and mortar type change (Figure 19). “Cockeysville” marble, without rubble, was used to construct the full wall thickness above 150 feet of elevation to the pyramidion and the mortar is Portland cement based. Stone cubes of marble and gneiss were compression tested at the

time of construction and determined to have unadjusted strengths of 12.7 ksi and 18.7 ksi, respectively (Army Corps of Engineers 1878, Army Corps of Engineers 1879).

The shaft from 150 feet to 470 feet is modeled similar to the section below with a continuous mesh of three-dimensional solid elements (Figure 20); horizontal continuity in the structure throughout this section is provided by marble header courses that interconnect two or three wythes of blocks. With the wall masonry constructed hewn stone rather than stone rubble, a stiffness of 2000 ksi was assigned as a base value to the masonry that exists from an elevation of 150 feet to 470 feet. Parametric studies were also conducted to test the sensitivity of the global behavior to this value. The only connection between courses of masonry in this section of the shaft is the bed joint mortar.

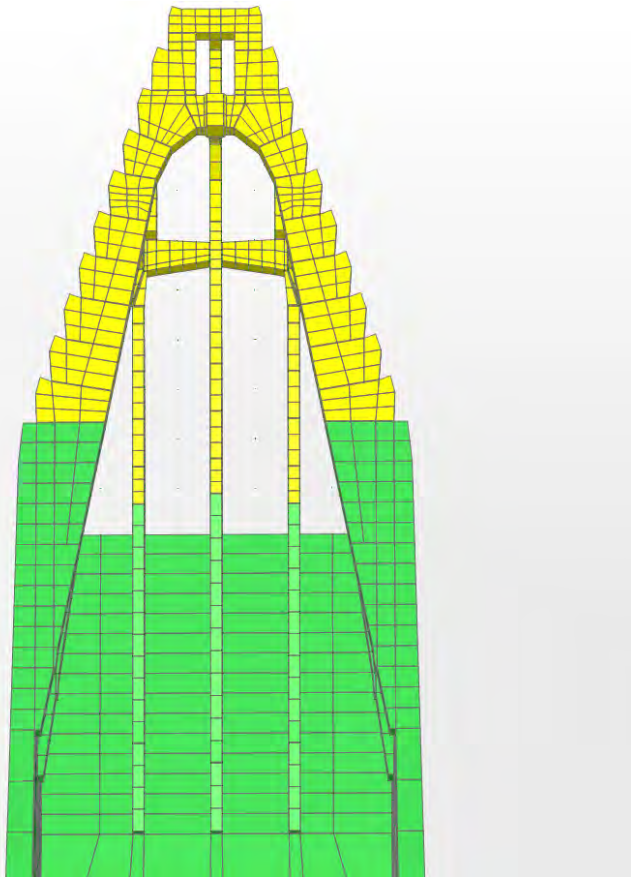


Figure 20. Cross-section of the Monument from approximately 450 ft to 540 ft

The space within the hollow core of the Monument is occupied by an elevator at the center and a staircase around its perimeter. Ten-foot-tall flights of stairs are located on the East and West interior faces of the Monument. At the top of each ten-foot flight of stairs is a steel landing framed with rolled steel I-beams and channels. The framing members are typically let into the interior shaft stones a sufficient distance to allow for a simple bearing-type connection (Figure 21). Little positive connection between the landings and the stone shaft exists. The beams making up the elevator hoistway are supported laterally by the stairs and landings and vertically by cast iron columns. Because of the limited positive connection between the landings and the shaft masonry, the lack of a direct connection between the elevator framing and the

shaft, and the relatively small sizes of the members relative to the massive masonry, the structural aspects of the steel and cast iron framing were not modeled.



Figure 21. Photograph of bearing-type connection between floor framing and stone wall

Shaft from 470 ft to 500 ft

At 470 feet above the datum, the marble coursing of the Monument shaft changes to accommodate the lowest manifestation of the integration between the shaft and the pyramidion ribs. Between 470 and 500 feet, all twelve horizontal ribs in the pyramidion exist as “rib projections” that extend inwards from the shaft wall and provide the vertical support for the ribs above. The shaft wall and these rib projections were explicitly modeled as a continuous mesh of three-dimensional solid elements. The masonry construction and the stone and mortar materials of this section of shaft are similar to the section below, except that between 470 and 500 feet, the blocks have mortise and tenon joints that cross the bed joints and steel “cramps” that interconnect adjacent blocks horizontally. These details are believed to have been included to help resist lateral spreading. In the actual structure, damage from shaking during the Mineral event occurred in this section of the shaft. Figure 22 shows a typical interior elevation of the shaft wall between 470 feet to 500 feet developed by WJE’s post-earthquake damage survey; it shows locations of pre-earthquake damage (denoted with prefix “E”) and presumptive earthquake damage. The arrows in the figure are indicative of damaged head joints and the appearance of “spreading”. We did not typically observe out-of-plane offsets of stones forming the shaft wall, although minor offsets were observed in the rib projections. This type of behavior is difficult to model nonlinearly, as the head joints and bed joints must both be modeled in a nonlinear fashion to accurately represent the behavior. To attempt to model it simply, we created a trial model with nonlinearity in the bed joints only, but the behavior under seismic loading predicted horizontal offsets (that did not occur due to the Mineral event) and not any sort of lateral spreading (which did occur due to the Mineral event). We therefore decided to model the section from 470 feet to 500 feet elastically with the same meshing and element types as the section of the shaft

below, but with a reduced stiffness to represent the damage to the masonry that was observed to have occurred.

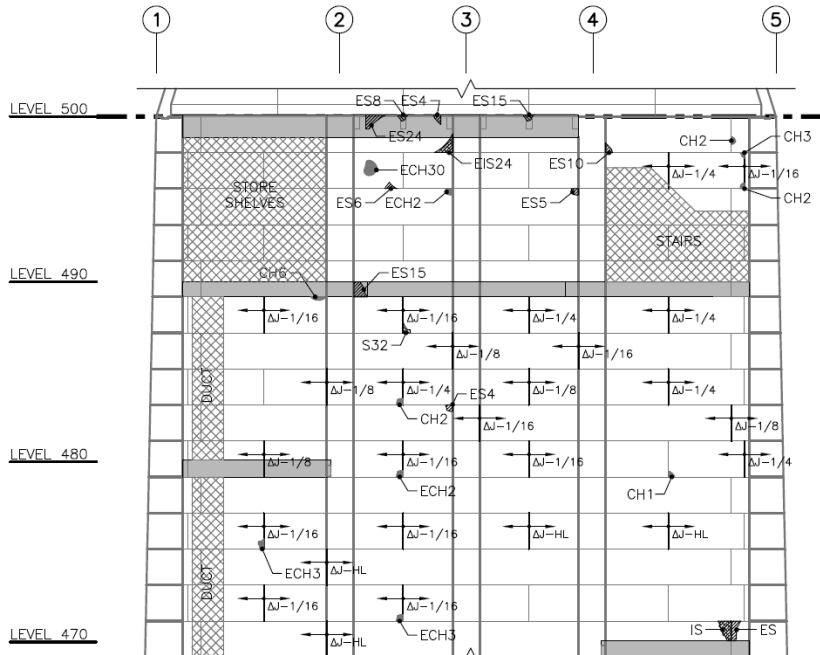


Figure 22. Typical interior elevation of WJE earthquake damage survey from 470 feet to 500 feet

Pyramidion Rib Stones

At an elevation of 500 feet above ground level where the pyramidion begins, the rib projections and marble blocks of the shaft become twelve marble ribs of stacked rib stones and 7-inch thick marble panels (Figure 23). In each rib, the rib stones, each having approximate dimensions of 12 inches wide by 4 feet tall, are stacked one atop another, one stone per course, with a thin mortar bed joint and a small (in relation to the size of the block) mortise and tenon joint. At the pyramidion and as described in detail below, to simulate the ability of the stacked rib stones to rock and/or slide relative to adjacent stones, the analytical model changes from one with contiguous three-dimensional solid elements to one containing nonlinear links capable of emulating rocking/sliding behavior of the individual rib stone blocks. Consistent with this modeling technique, the relatively rigid rib stones were modeled with a modulus of 5700 ksi, substantially stiffer than the masonry in the shaft below for which the mortar properties were smeared into the element properties formulation.

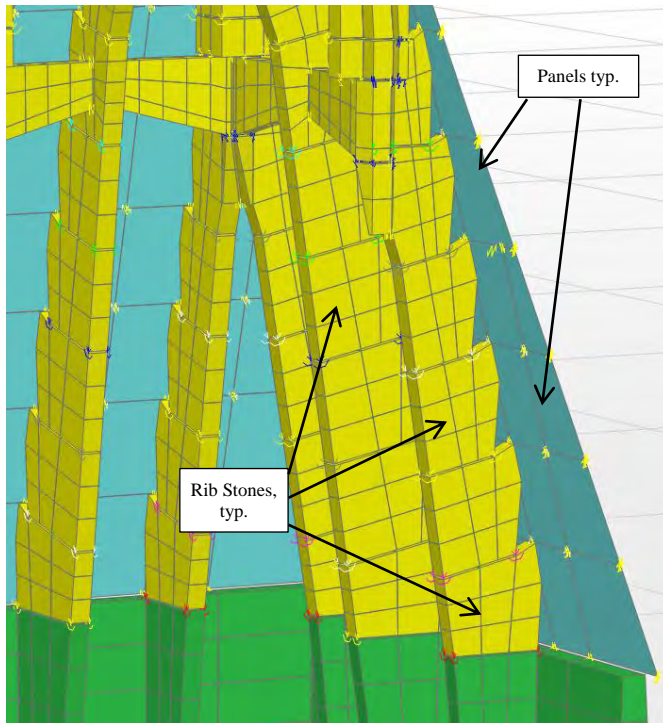


Figure 23. Isometric cross-section of lower pyramidion

During the post-earthquake damage survey, we observed a number of locations where relatively small horizontal offsets, up to a maximum of 3/4-inch, occurred between adjacent rib stones (Figure 24). These offsets appear to be the manifestation of sliding, a dominant mode of response within the pyramidion. This type of behavior poses an interesting problem from a structural engineering standpoint in that it is a type of non-linear behavior that is not easily captured by traditional computer modeling techniques. The slipping and resulting residual relative displacement, for the purposes of this model, was idealized as behaving in accordance with the Coulomb model for frictional response. Functionally, the model simulates an interaction between axial force across the bed joints and the frictional resistance provided by the bed joint. Specifically, friction-pendulum isolators, which obey the load-displacement curve shown in Figure 25, were used to model the interface between rib stones. The properties of the friction-pendulum isolators are such that, for a given axial load and coefficient of friction, there is a critical value of lateral load at which additional deformation can occur without any additional lateral load. This is the point at which “slip” occurs. When the lateral load is removed, the elastic deformation is recovered, but a residual plastic deformation can remain.



Figure 24. Horizontal offset between rib stones documented at the observation level

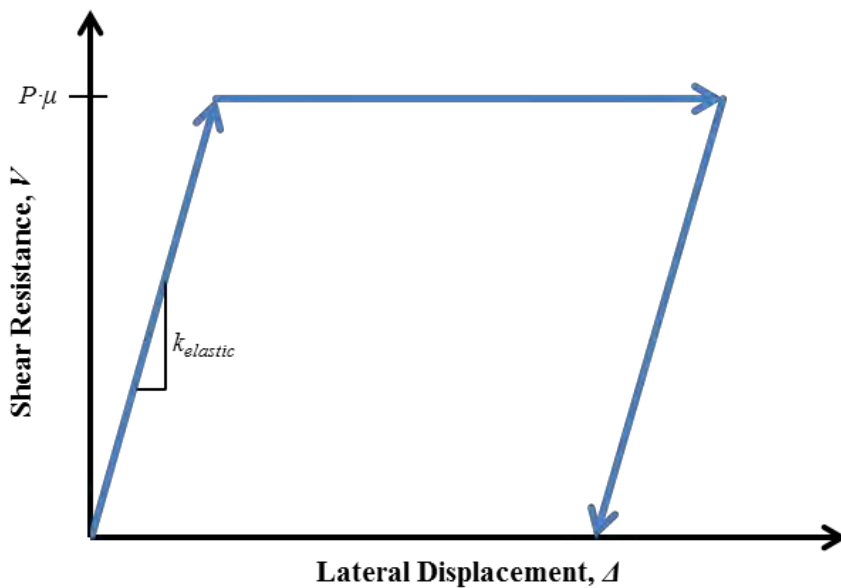


Figure 25. Diagrammatic representation of response of friction-pendulum damper to axial and lateral loads; P = axial load, μ = coefficient of friction, V = lateral load, $k_{elastic}$ = elastic stiffness, and Δ = lateral displacement of the friction-pendulum damper

In order to facilitate modeling of this sliding behavior, one-inch gaps were provided between the discretely modeled rib stones to allow for the inclusion of the friction-pendulum isolator links (Figure 26). A total of four isolators were placed in the gaps between all rib stones, which permitted the rib stones to translate in any direction, uplift at any corner or side, and rotate torsionally. They were generally placed in (or near) the corners of the stones. To facilitate the connection between the three-dimensional solids and the link element, rigid body constraints were applied to each node on all faces of rib stones in contact with other rib stones (Figure 27). The result of applying the body constraints was that the mated faces of rib stones in contact with one another were forced to stay planar (though the two faces were not constrained to stay parallel or square to each other). Since the modeled stiffness of the rib stones, at 5,700 ksi, is already much larger than that of the bed joint isolators, this is not an unreasonable assumption.

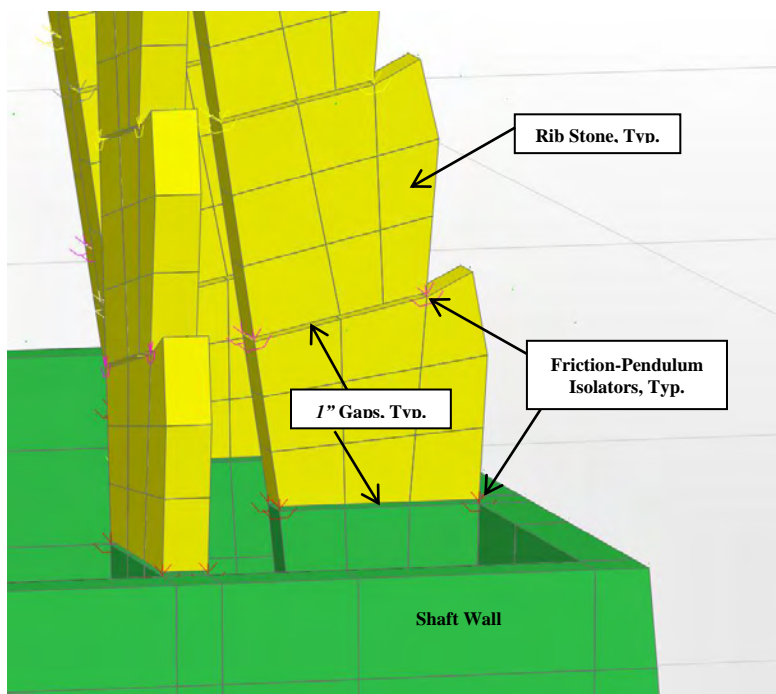


Figure 26. Cut-away view of model at 500-foot level showing as-modeled connections from rib stone to rib stone, and from rib stone to shaft wall. Panels not shown for clarity

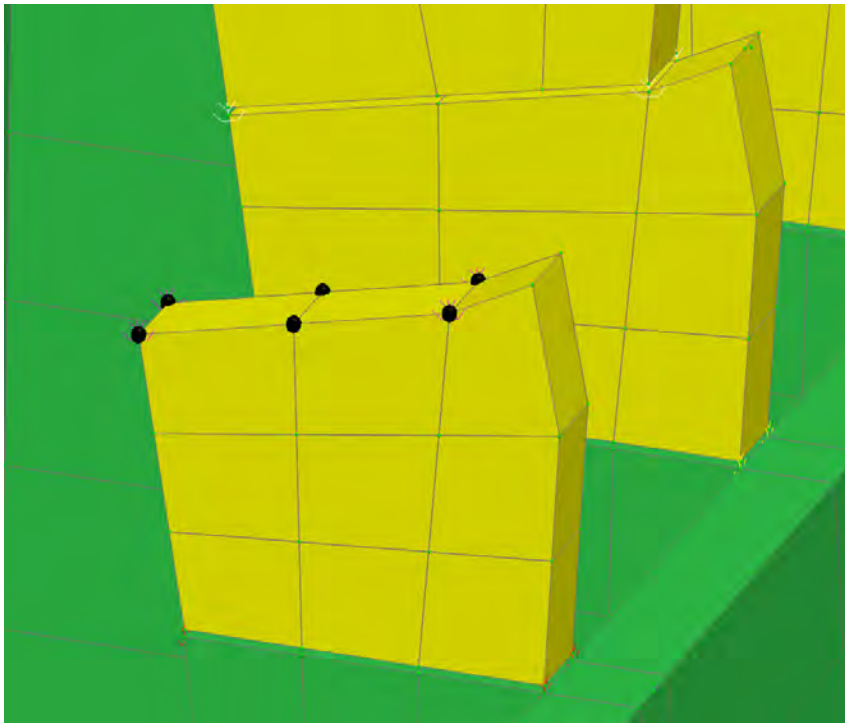


Figure 27. Rib stone showing nodes with a rigid body constraint applied (black dots); rib stone above and panels not shown for clarity

The nonlinear links in the bed joints between the stacked rib stones were assigned axial and shear stiffnesses calibrated based on the known damage conditions encountered during our earthquake damage survey, however, as with other aspects of the model, these parameters were also varied to test sensitivity of the results to different assumptions. A typical elevation from the WJE earthquake damage survey is shown in Figure 28. Using an iterative procedure, the offsets and residual displacements in the bed joints after subjecting the model to the benchmark ground motions were compared with the WJE earthquake damage survey and approximately matched. Other items also informed the selection of the link properties including mortar material properties, cyclic behavior of the mortar, and mortar-stone sliding behavior. The input parameters employed for friction-pendulum isolator elements within the SAP2000 model of the pyramidion include mass, moments of inertia in the three rotational degrees of freedom, elastic stiffnesses (k , $k_{effective}$), viscous damping parameters (ζ , $\zeta_{effective}$), coefficients of friction (μ_{fast} , μ_{slow}), a rate parameter, a sliding surface radius. Table 1 shows values assigned to the parameters of interest; they were both computed from known or estimated properties and calibrated based on model output and field observations of the Monument. The sign convention is as follows: the “1” direction lies parallel to the friction-pendulum damper element (i.e., perpendicular to the sliding surface), the “2” direction is parallel to the short direction of the rib stones (i.e., out-of-plane with respect to the major axis of the ribs), and the “3” direction is parallel to the long direction of the rib stones (i.e., in-plane with respect to the major axis of the ribs).

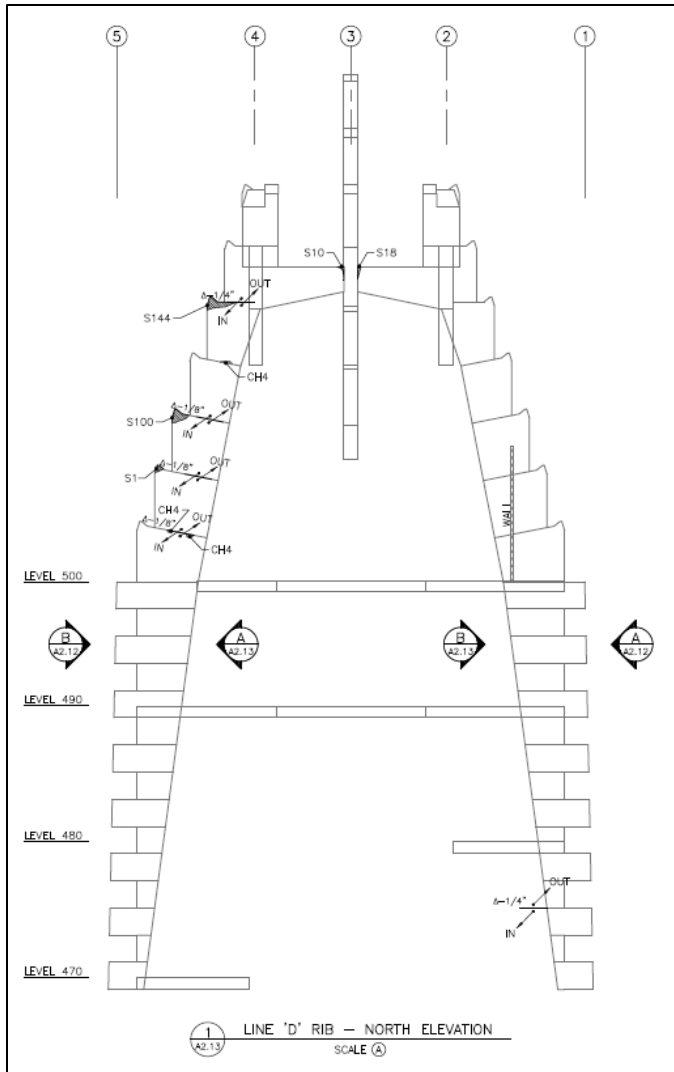


Figure 28. Typical elevation for WJE rib stone damage survey

Table 1: Rib Stone-to-Rib Stone Isolator Properties

Degree of Freedom	Property	Value	Unit
All	<i>Mass</i>	0	<i>kip-s²/in</i>
All	<i>Weight</i>	0	<i>kip</i>
U1	<i>k, k_{effective}</i>	1000	<i>kip/in</i>
	<i>ξ, ξ_{effective}</i>	0	<i>kip-s / in</i>
U2, U3	<i>k, k_{effective}</i>	500	<i>kip/in</i>
	<i>ξ, ξ_{effective}</i>	0	<i>kip-s / in</i>
	<i>μ_{fast}, μ_{slow}</i>	0.5	-
	<i>Rate Parameter</i>	0	-
	<i>Radius of Sliding Surface</i>	0	<i>in</i>
R1, R2, R3	<i>No response parameters defined</i>	N/A	N/A

As the pyramidion reduces in size toward the tip, the geometry of the masonry become extremely complex, and the ribs and rib stones become interconnected in various ways (Figure 29). The details of each of these connections were modeled based on the original drawings and their behavior due to the Mineral ground motions as predicted by the analysis was compared with the documented post-earthquake damage. In general, each rib stone was vertically connected using the friction-pendulum isolator elements; a summary of some of the other types of connections are provided below:

1. Tie beam to center rib - gap elements
2. Cruciform stone to center rib connection - friction-pendulum isolators
3. Side rib to tie beam - linear-elastic springs
4. Corner stone to side ribs - friction-pendulum isolators

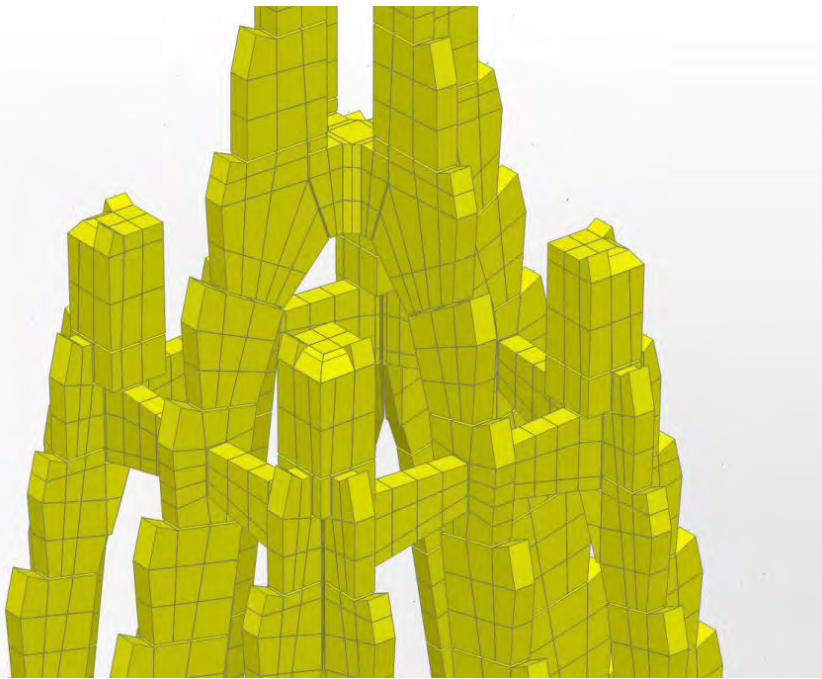


Figure 29. Upper portion of pyramidion; pyramidion panels and link elements not shown

Pyramidion Panels

Two hundred sixty two marble panels having dimensions 7 inches thick, approximately 7 feet wide and 4 feet tall make up the exterior walls of the pyramidion. Each typical pyramidion panel is connected to and are supported by the rib stones in two locations, where the lug connection primarily provides vertical support and the “let” connection primarily provides in-plane keying. At the lowest course, the base of each panel is supported directly on the shaft. Above that level, the typical panels are gravity-supported by lugs which project from the interior face of the panels and which bear on teeth extending from the rib stones. Lead shims, 3/32-inches thick, are placed within this bearing interface. Horizontal panel-to-panel joints are shiplapped. Typical interior vertical joints are also shiplapped. Though not in direct stone-to-stone bearing and though not mortared, the vertical and horizontal joints have the potential to transfer some loads via materials located in the joints; materials which include lead shims, oakum, and various sealants. The panels at the corners of the pyramidion are dovetailed, creating a more rigid connection than the vertical or horizontal joints. The modeling approach allowed for certain joints to be given unique properties. For example, the vertical joints at rib stones were verified by field investigation as having been well-filled with molten metal and hence were modeled with the ability to transfer larger forces.

The pyramidion panels were modeled as semi-rigid elastic shell elements having material properties similar to the rib stones and connected with deformable joints. The layout of the pyramidion panels lends itself to the modeling approach shown in Figure 30 through Figure 32, wherein most panels were modeled as a sub-assembly of two rigidly-connected shell elements. Gaps 0.1 inches wide were modeled between each panel sub-assembly to accommodate linear-elastic link elements that were placed in these gaps to connect adjacent panels. The meshing permitted definition of joint-specific structural properties for these links depending on whether the orientation of the joint was horizontal, vertical or at a corner.

It is noted that the employment of linear-elastic links to represent the pyramidion panel joints is a relatively crude idealization that is not capable of capturing the deep complexity of the behavior of the pyramidion’s construction; the joinery and construction of the pyramidion fascia is complex and so fundamentally nonlinear that a highly detailed model of it would quickly overwhelm the capabilities of almost any currently available analysis environment. The modeling of these joints is therefore intended to be an approximation designed to provide insight into the behavior of the panels but not to precisely quantify that behavior. In fact, the model appears to be capable of predicting the global pyramidion behavior reasonably well, in large part because the stiffnesses of the horizontally and vertically oriented links were first estimated based on in-situ conditions and then calibrated based on comparison of the predictions from the model subjected to the Mineral earthquake motions with the damage documented in the pyramidion after the Mineral event. In other words, the observations of the behavior of the structure during the Mineral event informed the construction of the model and enabled it to be tuned. As with a number of other features of the model, to determine if the model response was inordinately sensitive to the “calibrated” link properties and in order to attempt to bound the problem, the properties of the links were also varied and the effects of those variations considered.

The analysis runs whose results are presented later in this report employed stiffnesses for panel-to-panel link elements as provided in Table 2. The “1” direction corresponds to the axial direction of the link (opening and closing of gaps between panels), the “2” direction corresponds to the in-plane shearing direction of the links with respect to the plane of the panels, and the “3” direction corresponds to out-of-plane movement of the stone panels. The link configuration within each joint is depicted in Figure 30 which shows that the link orientation is typically orthogonal to the joint orientation, i.e. horizontal joints are modeled with vertically oriented link elements.

Table 2. Panel-to-Panel Link Properties

Link Description	Property	Value	Unit
Horizontal Joints	k_{U1}	200	kip/in
	k_{U2}	200	kip/in
	k_{U3}	10	kip/in
Vertical Joints	k_{U1}	200	kip/in
	k_{U2}	0	kip/in
	k_{U3}	0	kip/in
Vertical Joints at Rib Stones	k_{U1}	200	kip/in
	k_{U2}	200	kip/in
	k_{U3}	200	kip/in
Corner Joints	k_{U1}	200	kip/in
	k_{U2}	200	kip/in
	k_{U3}	200	kip/in

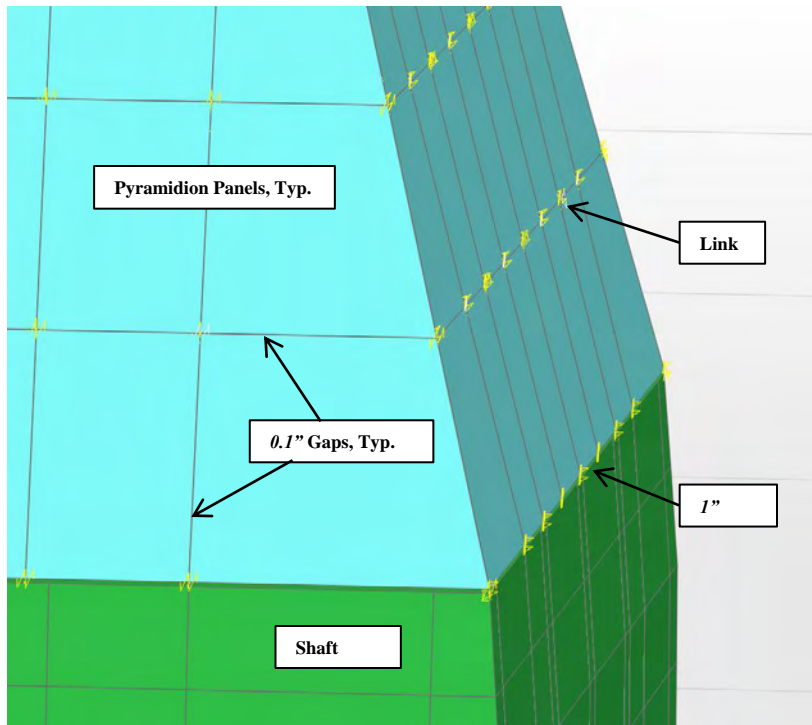


Figure 30. Pyramidion panels above shaft

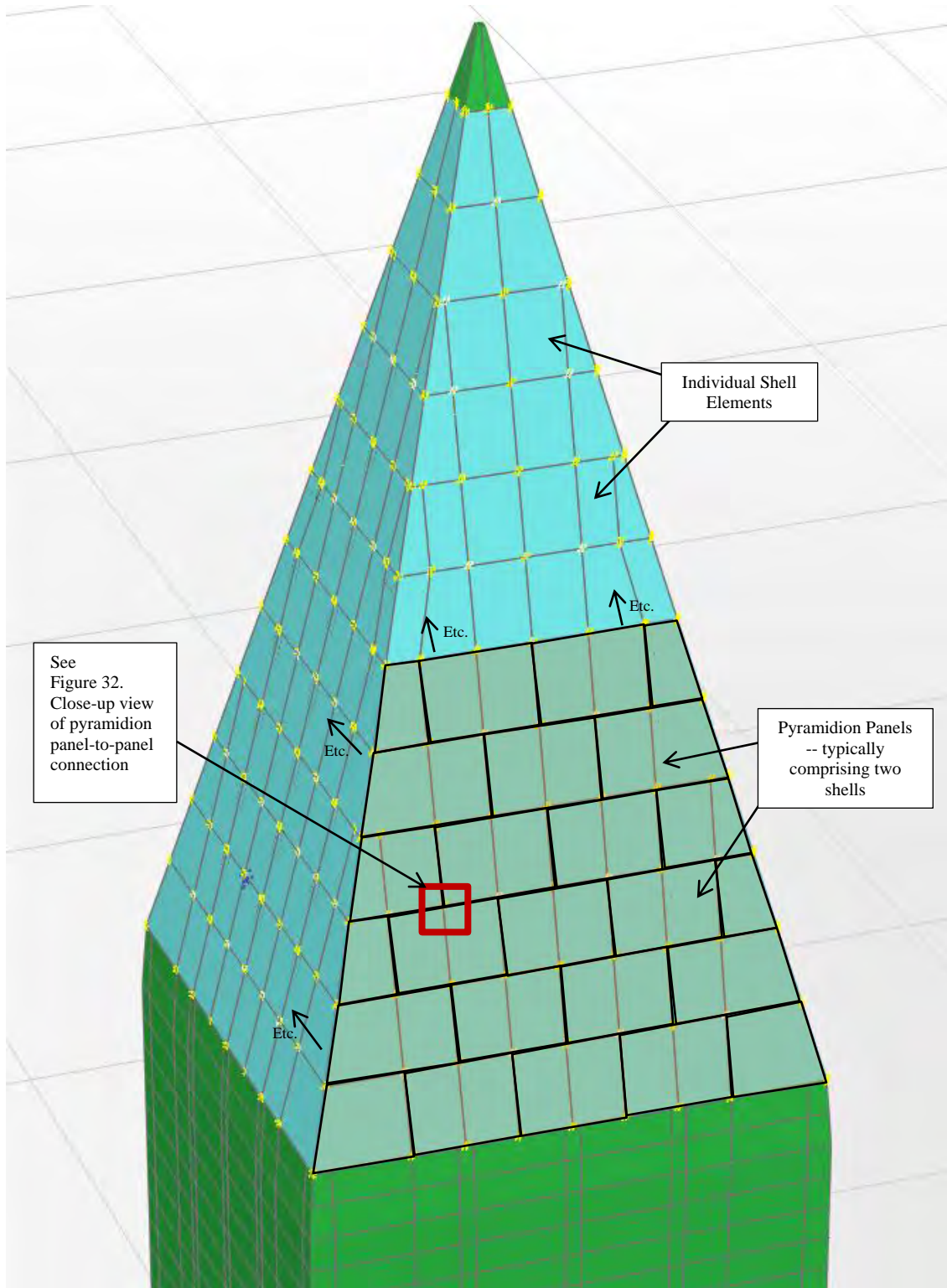


Figure 31. View of pyramidion showing panels in running bond superimposed on mesh

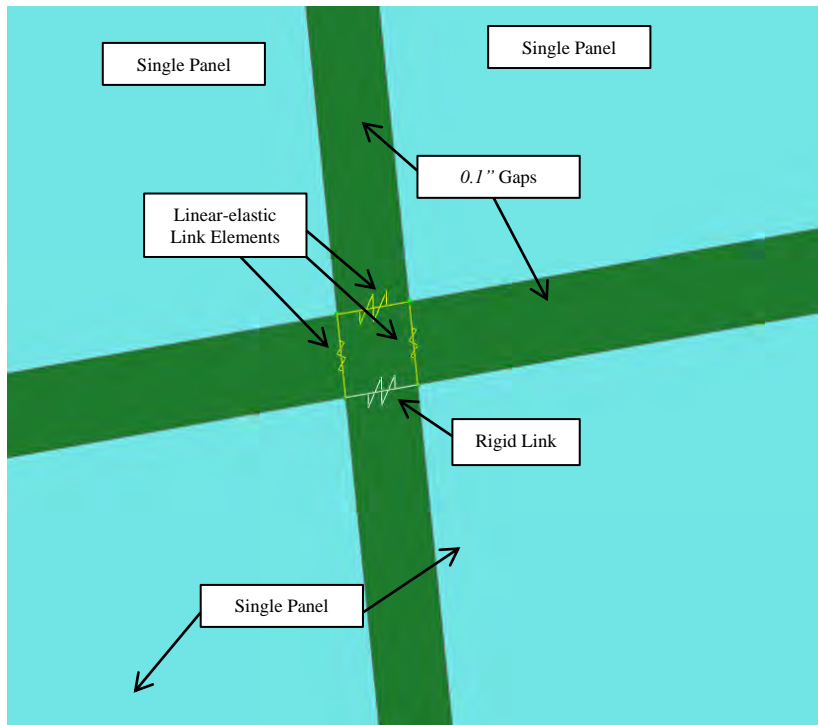


Figure 32. Close-up view of pyramidion panel-to-panel connection

Connections between the lugs and “lets” of the pyramidion panels and the teeth of the rib stones were modeled using linear-elastic link elements as shown in Figures 33 and 34. As with the links employed to model the joints between panels, the use of links with linear-elastic properties is an idealization necessary to keep the size of the analysis problem manageable. In the model, link elements extend from the center of each rib stone tooth to each of the shells making up the pyramidion panels adjacent to the tooth, meaning there are typically four links per tooth. The properties of the links vary depending on whether the links support the base of the panel at the lug or the top of the panel at the “let”, defined herein as the lower and upper connections, respectively. Table 3 sets forth the properties assigned to these links in the analyses whose results are presented later in this report. These tabulated properties correspond to links that enable only minimal transfer of horizontal shear between the panels and the teeth. The link properties were also varied parametrically so the sensitivity of the analysis conclusions to the properties of these links could be assessed and the problem could be bounded. The “1” direction corresponds to the axial direction of the link (out-of-plane movement of the stone panels), the “2” direction corresponds to vertical movement of the stone panels, and the “3” direction corresponds to the in-plane shearing direction of the links with respect to the plane of the panels.

Table 3. Panel-to-Tooth Link Properties

Link Description	Property	Value	Unit
Lower bearing connection at lug	k_{U1}	200	kip/in
	k_{U2}	0	kip/in
	k_{U3}	0	kip/in
Upper connection at "let"	k_{U1}	200	kip/in
	k_{U2}	200	kip/in
	k_{U3}	0	kip/in

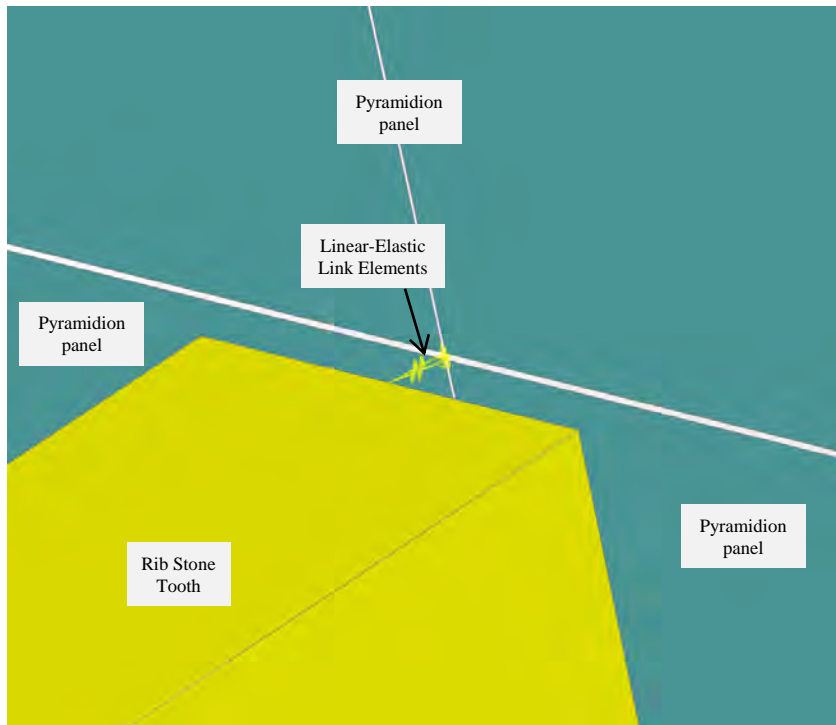


Figure 33. Rib-to-panel connection

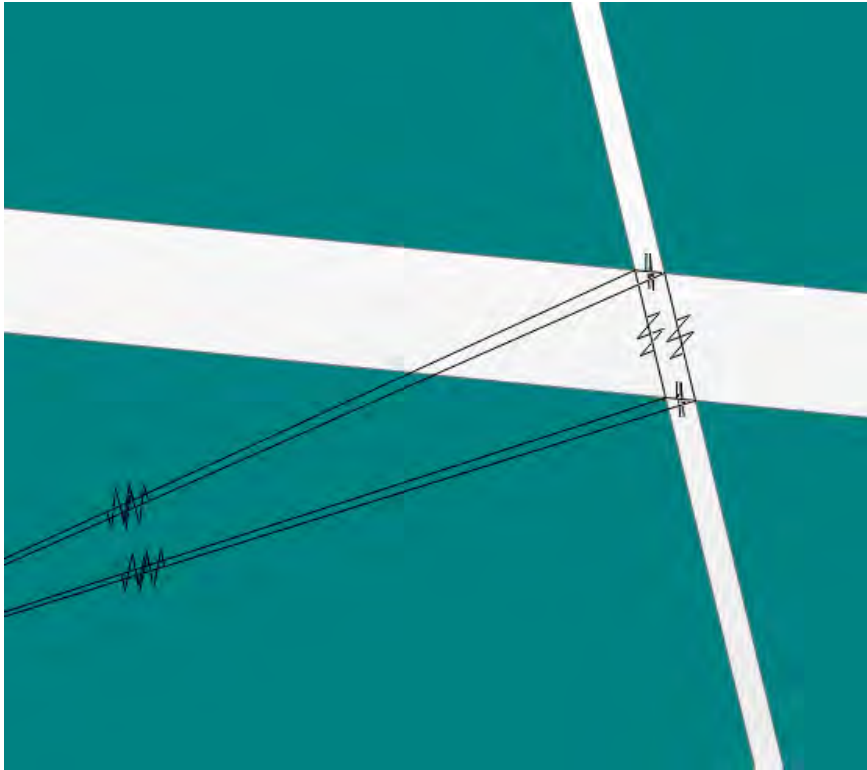


Figure 34. Rib-to-panel connection

Analyses

The finite element model of the Monument was subjected to various linear and nonlinear, static and dynamic analyses to better understand its behavior under seismic loading. As mentioned in the “Model Development” section, some analyses were performed concurrently with the development of the model in an iterative fashion so that the response of the Monument to the benchmark ground motions informed the selection of modeling parameters. Two of the analysis methods used are described below: Linear Modal Analysis and Nonlinear Modal Time History Analysis.

Modal Analysis

A Linear Modal Analysis using eigenvectors was performed on the finite element model to develop insight into dynamic behavior of the various portions of the Monument as well as into its global behavior. Visually demonstrative, the free vibration modes provide information that was used to preliminarily identify regions of the structure where deformations concentrate and where accelerations are most amplified. Moreover, the Linear Modal Analysis provides basic information that was used to develop preliminary estimates of acceleration and displacement demand by comparing the output from these analyses with the Mineral event (“benchmark”) and MCE response spectra developed by AMEC.

Some results of the modal analysis for one particular model are shown in Table 4 where a brief description of the mode shapes generated by SAP2000 are provided along with each period in seconds and the modal mass participation ratios. The fundamental period of free vibration for one particular model of the Monument, a “cantilever” mode dominated by the bending of the shaft and the deformation of the supporting soil, was found to be around 3.16 seconds, with second and third modes occurring around 0.89

and 0.45 seconds respectively, for one of the softer models. Relatively softer and relatively stiffer models were also studied. The second mode shape is shown in Figure 35. The third mode has a shape where the shaft remains nearly vertical but the pyramidion appears to be heavily displaced or “whipped” towards a corner of the structure. The amplified motion in the pyramidion is repeated in the fourth mode shown in Figure 36, where the pyramidion is shown with the panel stones removed for clarity. As the periods of the identified modes get shorter, other mode shapes in the pyramidion are encountered such as a torsional mode and a several “pinching” modes where the top of the shaft walls breathe in or out (Figures 37 and 38).

The mean spectral acceleration versus period response spectra for the Mineral and MCE ground motions are provided in Figure 39. These response spectra were developed from the AMEC provided time histories and conveniently summarize the peak response of all possible linear single-degree-of-freedom systems to mean ground motion. Also provided on this figure as red dashed lines are the locations of several of the relevant free-vibration modes of the Monument including the fundamental (or first) mode and second mode that dominate the response of the shaft, along with a grouping of modes that are the predominant ones for the pyramidion. As can be seen from the figure, the MCE ground motions are higher than the Benchmark ground motions in two period regions: 1) from 0 seconds to 0.1 seconds, and 2) from 0.6 seconds to 3.5 seconds. The Mineral ground motion is higher than the predicted MCE motions at a period region from 0.1 seconds to 0.6 seconds, a region that coincides with the modes most relevant to the pyramidion. Therefore even without adding nonlinearity to the model, the Linear Modal Analysis predicts that the MCE motions will likely not cause as much damage to the pyramidion as was already caused by the Mineral event.

Table 4: Modal Analysis

Mode in SAP2000	Period (sec)	Modal Mass Participation Ratio N-S direction*	Modal Mass Participation Ratio E-W direction*	Behavioral Description
1, 2	3.16	0.21	0.12	Fundamental mode
3, 4	0.89	0.11	0.07	Second mode
5, 6	0.45	0.04	0.03	Third mode, pyramidion “whipped” towards corner
7	0.41	0.00	0.00	Torsional mode
8	0.33	0.00	0.00	Vertical mode
9	0.32	0.00	0.00	“Pinching” near top of shaft walls
Mode in SAP2000	Period (sec)	Modal Mass Participation Ratio N-S direction*	Modal Mass Participation Ratio E-W direction*	Behavioral Description
10, 11	0.31	0.03	0.02	Fourth mode, pyramidion “whipped” towards corner
12	0.27	0.00	0.00	Torsional mode at pyramidion
13, 14	0.22	0.00	0.00	“Pinching” at pyramidion tie beam
15, 16	0.21	0.03	0.02	Fifth mode, pyramidion “whipped” towards corner

* Many mode shapes repeat in the orthogonal direction producing higher total mass participation

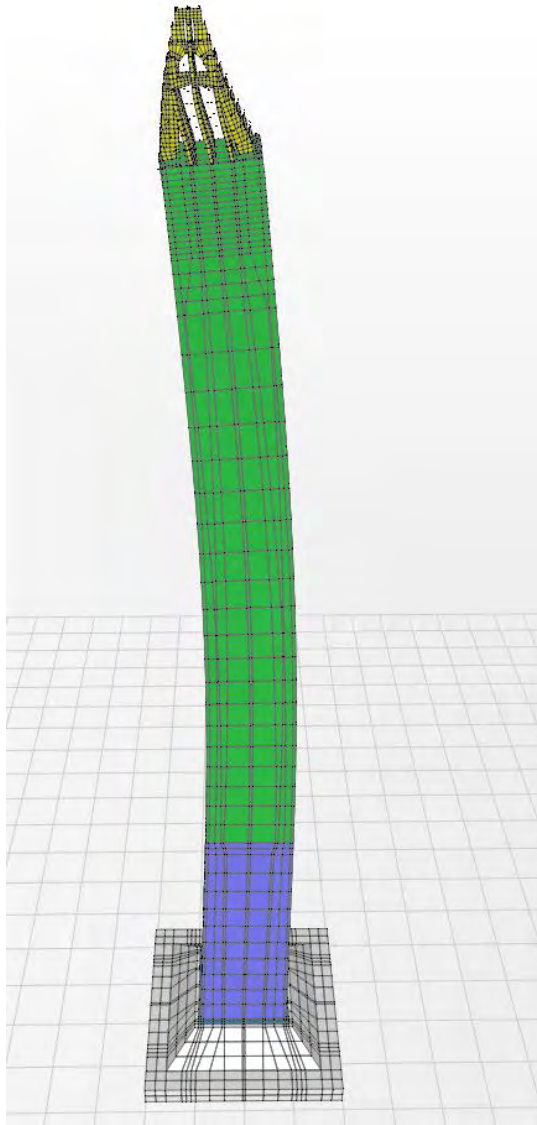


Figure 35. Second mode behavior of Monument from modal analysis, $T=0.89$ seconds (displaced shape greatly exaggerated for clarity)

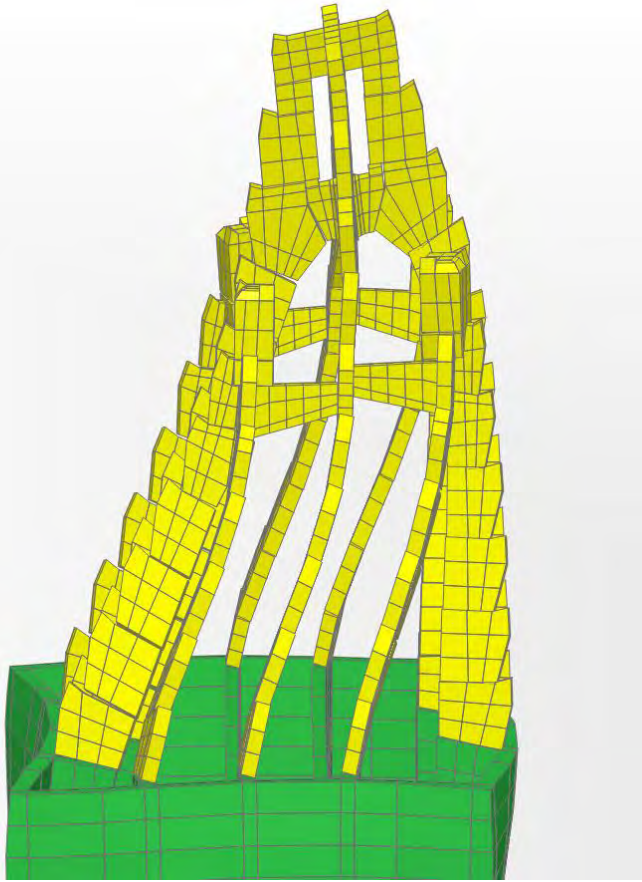


Figure 36. Fourth mode behavior, pyramidion “whipped” towards corner of shaft, $T=0.32$ seconds (displaced shape greatly exaggerated for clarity)

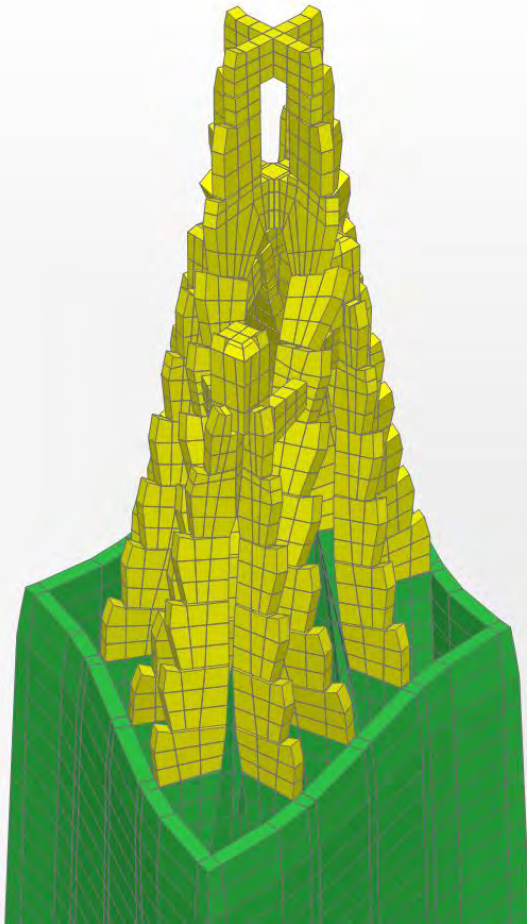


Figure 37. "Pinching" behavior at top of shaft walls in mode 9, $T=0.32$ seconds (displaced shape greatly exaggerated for clarity)

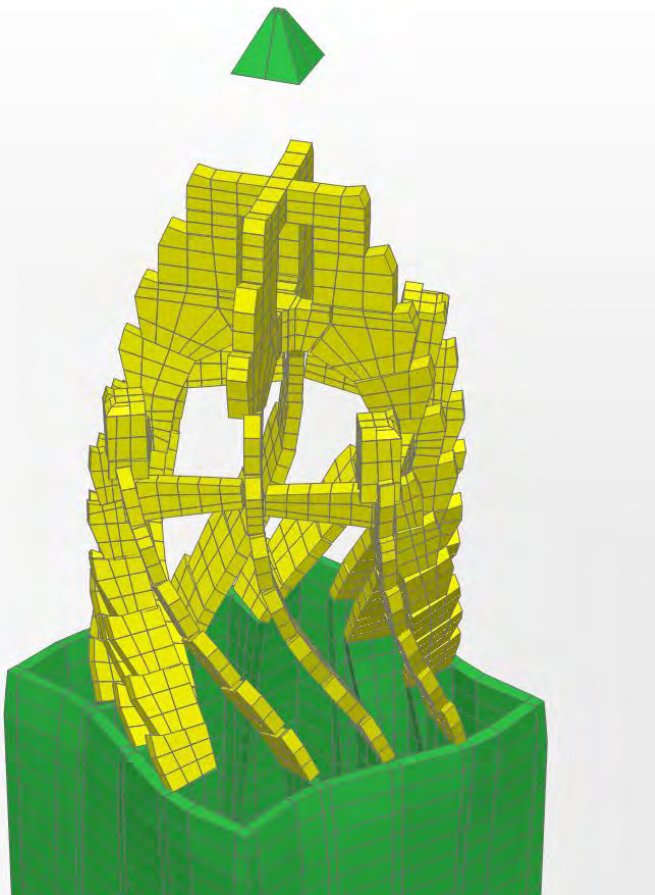


Figure 38. Torsional mode at pyramidion in mode 12, $T=0.27$ seconds (displaced shape greatly exaggerated for clarity)

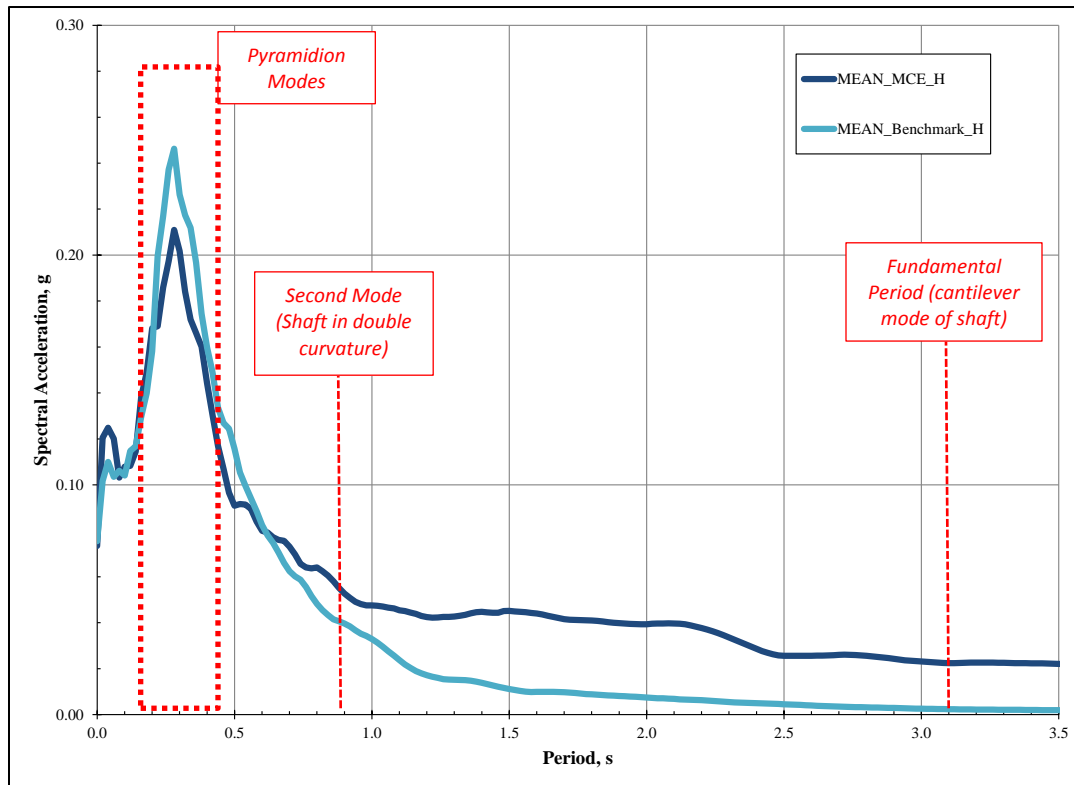


Figure 39. S_a versus T plot of Benchmark versus MCE

Nonlinear Modal Time History

Nonlinear Modal Time History (also called Fast Nonlinear Analysis, or FNA) is an efficient method to analyze structures which are predominately linear-elastic but which have a number of pre-defined nonlinear link/support elements (Computers and Structures 2011). The accuracy of the predicted response of a structure using FNA is dependent on being able to adequately represent nonlinear forces by modal forces. This requires an appropriate number of modes to be used to ensure that the static modal load participation ratio of each nonlinear degree of freedom approaches 100 percent. The number of nonlinear degrees of freedom in our model was quite large, requiring many hundreds of Ritz-vector modes to be solved to adequately represent all nonlinear responses. The nonlinear dynamic FNA follows from a quasi-static dead load FNA, applied using a ramp function and high modal damping.

As mentioned in previous sections, time and computing constraints limited the number of nonlinear link elements that could be used to model the structure. The locations of the insertion of nonlinear elements into the model were concentrated where damage from the Mineral event was found and in similar regions even if damage was not found. We created several different FNA models and conducted parametric studies for a variety of reasons, but primarily to bound the behavior of the Monument and fully consider potential nonlinear behavioral characteristics that were modeled with linear elements. Different FNA models were also created to bound the behavior of the pyramidion in a future postulated MCE event. Two methods were used to accomplish this:

1. *Broken Teeth*. Our field investigation revealed that 28 teeth were damaged in the Mineral event. The proposed repair of the teeth involves securing the panels to the rib stones at the broken teeth

with steel angles and epoxied bolts. This type of repair reestablishes the lost strength of the broken tooth, but cannot completely restore the lost stiffness due to the fracture. In order to capture the effect of this in the computer model, the stiffness of the broken teeth was reduced in the model to 5% of their pre-earthquake values for the MCE FNA runs.

2. *Load Sequencing.* Nonlinear analyses were conducted assuming that the Monument was an undamaged structure when subjected to both the Mineral and MCE events, and also conducted assuming that the Monument was subjected to the Mineral event and the MCE events in series. As mentioned in the “Benchmark” and “MCE” sections, AMEC produced suites of seven pairs of time histories for both the Mineral event and the Maximum Considered Event. As a baseline, we ran each of the fourteen pairs of time histories starting from residual forces and deformations established from the dead load only case. Due to the presence of certain features in the SAP 2000 finite element software used for this assessment, however, it is also possible to restart an FNA analysis using residual forces and deformations from a previous FNA analysis. Since the MCE ground motions are postulating a future event and the Mineral earthquake motions are predicting a past event, it was deemed appropriate to also start MCE runs from the endpoint of the dead load plus Mineral event analyses, i.e. with the residual forces and deformations from those analyses. Load sequencing in this fashion helped to determine whether the Monument behavior, and its residual offsets and displacements, is significantly impacted by prior earthquake events.

The basic matrix of Nonlinear Modal Time History runs conducted as part of this assessment is shown in Table 5.

Table 5. Nonlinear Modal Time History Models

Descriptor	MCE or Benchmark	Broken Tooth Stiffness Reductions	Load Sequencing Prior to Final Run
Full 79	Mineral	NO	Dead Load Only
Full 84	Mineral	YES	Dead Load Only
Full 80	MCE	YES	Dead Load Only
Full 82	MCE	NO	Dead Load plus Whittier 2 (Mineral) Time History

To bound the problem and account for variability in the material properties of stone masonry, each of the models shown in Table 5 was run twice -- once with the modulus of stone masonry in the region between 150 to 470 feet above datum set equal to 1000 psi, and another set of runs with the modulus set equal to 2000 psi.

Analysis Results | General

The analysis results presented in the following sections were generated primarily by the Nonlinear Modal Time History (or FNA) analyses described above. In certain instances, where results from the Linear Modal analyses are brought into the discussion, the narrative so states.

FNA analysis results are presented primarily in the form of stress plots and tabulated data, supplemented by narrative engineering interpretation. Of note, the results relied on to support the conclusions reached

during this seismic assessment are generally the averages of the maximum predicted envelope forces, displacements and stresses experienced by the Monument in response to each of the seven pairs of time histories in the two suites of ground motions --- one representing the Mineral event and the other representing the MCE--- that were developed by AMEC. Reliance on the average maximum response values, as opposed to the maximum values predicted from any of the ground motions, is prescribed in essentially all recognized seismic design and evaluation guidelines, codes and standards for new and existing structures in the US, including the Tall Buildings Initiative Guidelines (TBI 2010), ASCE 7-10 and ASCE 41-06.

In addition, the Tall Buildings Initiative Guidelines uniquely recognize that for a response mechanism that is brittle, reliance on average maximum values implies a significant --- and perhaps an unacceptable -- probability of failure, along with any consequences associated with that brittle failure mechanism. To account for this, the Tall Buildings Initiative Guidelines sets forth certain multipliers that should be used to amplify the average maximum values. From a technical perspective, we consider this explicit recognition of the potential risks associated with brittle response mechanisms to be an insightful improvement over other available performance-based engineering documents.

Despite the fact that none of these documents ever contemplated the specific type of construction used in the Monument, there is little question about the presence of potentially brittle failure mechanisms in the Monument, even if many of these mechanisms would be difficult or impossible to actually reach given the relatively low intensity postulated ground motions, and even if some number of these mechanisms do not appear to have attendant unacceptable consequences. Essentially, this implies that the philosophy embedded in the Tall Buildings Initiative Guidelines could be applied to the Monument, but the specific means by which it should be applied is debatable. This seismic assessment therefore sought to maintain the more-stringent spirit of the Tall Buildings Initiative Guidelines, relative to ASCE 41-06. The selected approach involved a combination of techniques, including selection of the full unreduced MCE in lieu of two-thirds of the MCE and selectively examining the maximum maximum responses in lieu of the average maxima when the consequences of failure were judged to be particularly significant. We interpret this approach as consistent with the spirit of the Guidelines as they pertain to brittle modes of failure.

The above discussion notwithstanding, for presentation purposes in this report, the stress plots of the various demands are not the average maxima of the seven time histories in each of the ground motion suites studied; instead, the predicted responses that are plotted are the results from just two of the fourteen provided ground motions, Whittier2 and ChiChi2, representing the Mineral event and the MCE, respectively. Although the average maxima predicted by the analyses were also closely studied as a part of this assessment, plots of structural response parameters to individual ground motion records are usually more physically meaningful than plots of envelopes. The Whittier2 and ChiChi2 results were specifically selected for presentation as appropriate surrogates for the average maxima because these particular ground motions have spectral shapes that are close to the mean of the seven ground motions for the Benchmark (Whittier2) and the MCE (ChiChi2). As such, the predicted responses of the Monument to these specific records are reasonable representations of the average maximum values.

As the plots of results are presented and discussed, it is important to keep in mind that they represent the actual predicted average maxima from the seven pairs of motions in each suite of time histories (or appropriate surrogate values) without any reductions incorporated therein. This distinction is highlighted because in typical earthquake engineering practice involving normal structures, a variety of reductions are normally taken. Each of the above-mentioned guidelines and standards, for example, requires that seismic design and evaluation only consider two-thirds of the MCE, rather than the full, unreduced MCE, when

protection of life safety is the engineering goal. However, due in part to the high visibility of the Monument, and in part due to unique structural issues presented by the Monument, this reduction was intentionally not implemented during this assessment, meaning that only the full, unreduced MCE was employed to represent future seismic input motions. Significantly, since the assessment of the Monument employed the full unreduced MCE in lieu of 2/3 of the MCE, the input motions being considered are effectively 50 percent greater than would be required by any of these documents for other structures. This difference ought to be factored into deliberations regarding the need for and extent of any recommended seismic improvements. That said, it should also be understood that protection of life safety --- the performance criterion linked to employment of 2/3 of the MCE in the above-mentioned documents --- is not analogous to prevention of structural damage. Some structural damage is expected to occur even to new, code-compliant structures during intense earthquakes and that damage is considered acceptable by modern-day design and evaluation criteria as long as it does not present a serious threat to safety. While, the acceptability of damage to the Monument during a future strong earthquake is a subject that also ought to be carefully considered, employment of the full, unreduced MCE in this assessment assists in understanding the consequences of earthquake shaking that is more intense than two-thirds of the MCE.

As mentioned earlier, several different models were created in which the “tooth” material properties were varied to simulate teeth that had been damaged during the Mineral event, and some of these models were “re-started” with the MCE motions after analysis of the Monument subjected to the Mineral event terminated. The variation between these models only affects the pyramidion; the results for the shaft and foundation are not affected by these modifications.

Analysis Results | Soils and Monument Foundation

The average soil bearing stress predicted from analyses in which the only loading was self-weight is estimated to be 9.0 ksf over the entire footing area. When subjected to the MCE-level earthquake, the maximum expected soil bearing pressure under the Monument increases to be approximately 15 ksf which is very low relative to the compressive capacity of the soil and generates no concern for the stability of the Monument even during maximum predicted ground motions. When subjected to the August 23 Mineral motions, the predicted compressive stress in the soil is only nominally increased over the self-weight condition, which indicates that no damage to the soils supporting the Monument could have occurred during the Mineral event.

The analyses also predict that the maximum compressive stresses in the stone and concrete materials comprising the Monument foundation are nearly the same for the dead load case, the Mineral earthquake ground motions and the MCE-level ground motions around 150 psi. These stresses are trivial in comparison to the compressive strengths of the materials from which the foundation and shaft are constructed, and are therefore also not of concern. A stress plot of the vertical compressive stresses in the foundation and the base of the shaft are shown in Figure 40 for the MCE motion ChiChi2; the stresses in the figures range from -300 psi (red) to 0 psi (blue), which are very small relative to the likely compressive strength of any of the masonry or concrete in the lower elevations of the Monument. The negative sign indicates that the stress is compressive. The soils supporting the Monument and the foundation itself is thereby concluded to be adequate to assure the stability of the Monument during a 2,475-year event.

Of note, no uplift of the foundation is predicted to occur during the MCE level shaking, meaning that the behavior of the Monument does not involve “rocking”. “Rocking” is a common means by which structures dissipate energy during earthquakes, but the Monument is apparently stable enough that it will

not engage in rocking behavior even during an MCE event. While the analysis results suggest that some limited, localized tensile stresses occur at the construction interface of the original blue gneiss and the concrete buttressing at the base of the shaft, this tension dissipates with depth due to the significant weight of the foundation masonry. In any case, the stresses in this location are consistent with only small uplift forces and stress concentration anomalies from modeling, not predicted earthquake distress. A stress plot of the envelope tensile stresses at the top of the foundation is shown in Figure 41 for the Benchmark motion Whittier2; the stresses in the figure range from 0 psi (purple) to about 20 psi (red).

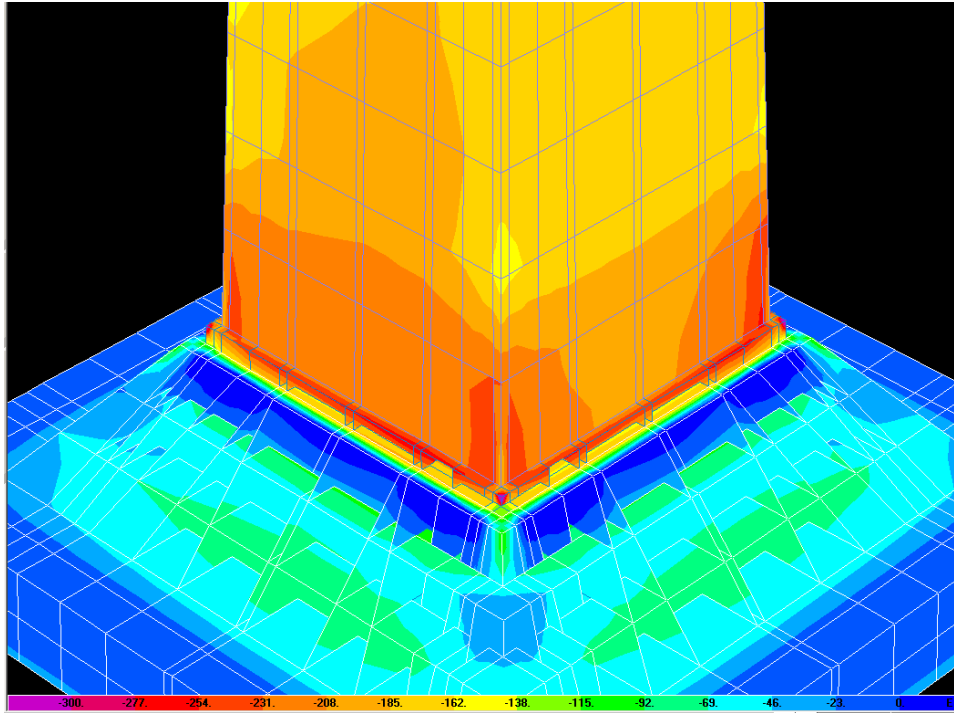


Figure 40. Envelope compressive stresses in vertical direction of the shaft due to MCE motion ChiChi2

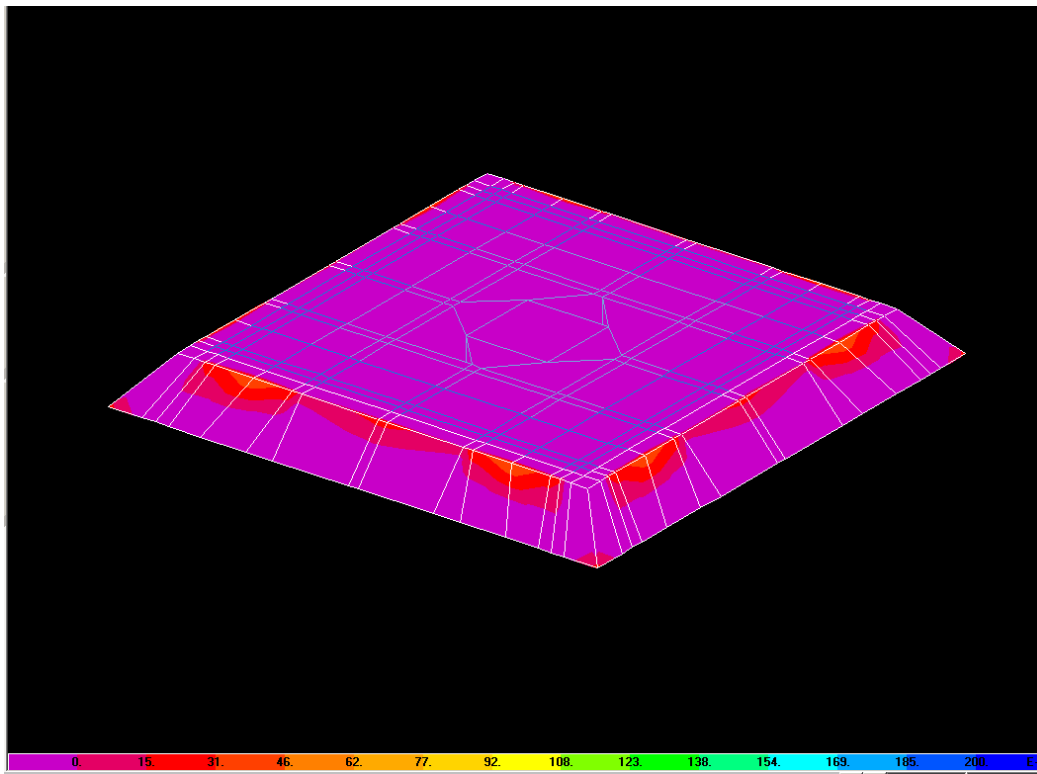


Figure 41. Envelope tensile stresses at cross section of solids at the top of foundation due to Benchmark motion Whittier2

Analysis Results | Shaft

The vastly different dynamic input between the Mineral and the MCE ground motions makes scrutiny of the Monument shaft an important exercise, especially because the shaft is responsive primarily to longer period motions that were insignificant during the Mineral event but are predicted to be much greater during the MCE. Damage to the shaft between grade and 470 feet above the datum from the Mineral event was minor and included damaged mortar joints, re-opening or extension of various repaired cracks and dislodgement of previous spall repairs. The damage to these previous repairs of questionable competence occurred even though the shaft in this elevation range was subjected to very little seismic excitation. Little damage to competent masonry was observed between grade and 470 feet above the datum from the Mineral event.

Because the spectral acceleration input at the fundamental mode period from the mean MCE event --- although itself small --- is predicted to be more than 8.5 times the mean estimate of the Mineral event at this period (0.023g vs. 0.0027g), it is reasonable to expect that other spall repairs may experience damage in an MCE event, although the question of how spall repairs of highly variable quality will behave in the MCE was somewhat beyond the scope of this assessment. Instead, the assessment focused on the ability of the shaft's competent masonry to withstand the MCE. It is clear both from the Linear Modal Analyses and from the FNA analyses that the MCE will result in greater response of the shaft and the foundation --- with respect to shear, tension, and compression stress, local deformation and global displacement --- than did the Mineral event. Therefore, this assessment focused on conditions that might have the potential to lead to permanent displacement or other severe damage that might pose a potential safety hazard.

As described above, the Nonlinear Modal Time History models were analyzed multiple times to bound the likely range of responses. Included in this bounding approach were models in which the modulus of the stone masonry in the region 150 to 470 feet above datum was set equal to 1000 psi, and another set of runs with the modulus set equal to 2000 psi. In general, the increased flexibility of the shaft observed for the 1000 psi runs was beneficial to the Monument response, with stresses in the shaft predicted to be significantly lower than for the 2000 psi runs. As is typical for masonry of any type, during a very large seismic event, when the stone masonry in the Monument begins to be damaged, it will “soften” as the mortar joints degrade and its effective modulus will reduce. The range of analysis results represented by the 2000 psi and 1000 psi runs is therefore not an unreasonable representation of the range of possible responses of the Monument --- due not just to variability of the type and quality of the masonry, but also to the occurrence of damage such as might be postulated for a very large earthquake event. Therefore, to most readily identify regions of the shaft that might be most prone to being damaged during the MCE, the results that are presented herein are those from the analyses in which 2000 psi was used for the modulus of elasticity of the masonry.

Tension stress is a primary measure of potential damage to masonry because masonry is far weaker in tension than it is in compression. In the following sections we explore the predicted tensile stresses, oriented in the vertical and in the horizontal directions. The envelope tensile stresses (S33) in the vertical direction are shown in Figures 42 and 43 in the upper part of the shaft for the Whittier2 (Mineral) and ChiChi2 (MCE) motions, respectively. These are the motions most representative of the average of the seven pairs of time histories. Tension stresses with this vertical orientation below the 470 foot elevation are an indication of bending of the shaft and the potential for the bending to overcome dead load and cause a horizontal crack in the shaft (above the 470 foot elevation, the stress field is complicated by interaction with the pyramidion). Figures 42 and 43 show that both the MCE and the Benchmark motions create regions of vertically-oriented tensile stress in the shaft. For the shaft below the 470 foot elevation, the stresses in the “Mineral” figure range from 0 psi (purple) to 20 psi (red) while the stresses in the “MCE” plot range from 0 psi (purple) to about 70 psi (orange). We note that the vertically-oriented tensile stresses appear to be heavily dependent on the input flexibility of the shaft. In particular, and as shown in Figure 44 where the MCE ChiChi2 ground motion is applied to the model with a “softened shaft”, i.e. with a modulus of 1000 psi, the vertically-oriented stresses below 450 feet diminish radically. At a minimum, this indicates that the system is somewhat self-correcting although reliant on minor nonlinearity. If the vertically-oriented tensile stresses are high enough to cause cracking in the shaft, cracking would occur in the mortar joints, the effective modulus of the shaft would reduce locally, and the stresses would diminish. As discussed in the following paragraph, the predicted 70 psi stresses for the “unsoftened” model do not create any concern as to safety or stability of the Monument.

As shown in Figure 43, for the MCE ground motions with “unsoftened” shaft, the maximum vertically-oriented tensile stresses occur at around 360 feet above the datum. Further analysis reveals that stresses of this magnitude only occur at the outer face of the corner of the walls and would be unlikely to generate a crack of any significant length or of any significant concern (Figure 45). In particular, at 70 psi, these stresses are relatively small and are expected to be below the strength of the Portland cement mortar in the bed joints at this elevation. In addition, at this elevation, the masonry already includes header courses that extend the full thickness of the walls. These full thickness header courses combined with the large blocks of stone in the typical courses will effectively resist degradation of the wall in the event that a horizontal crack forms, and the weight of the Monument will cause the crack to close when the earthquake shaking ends.

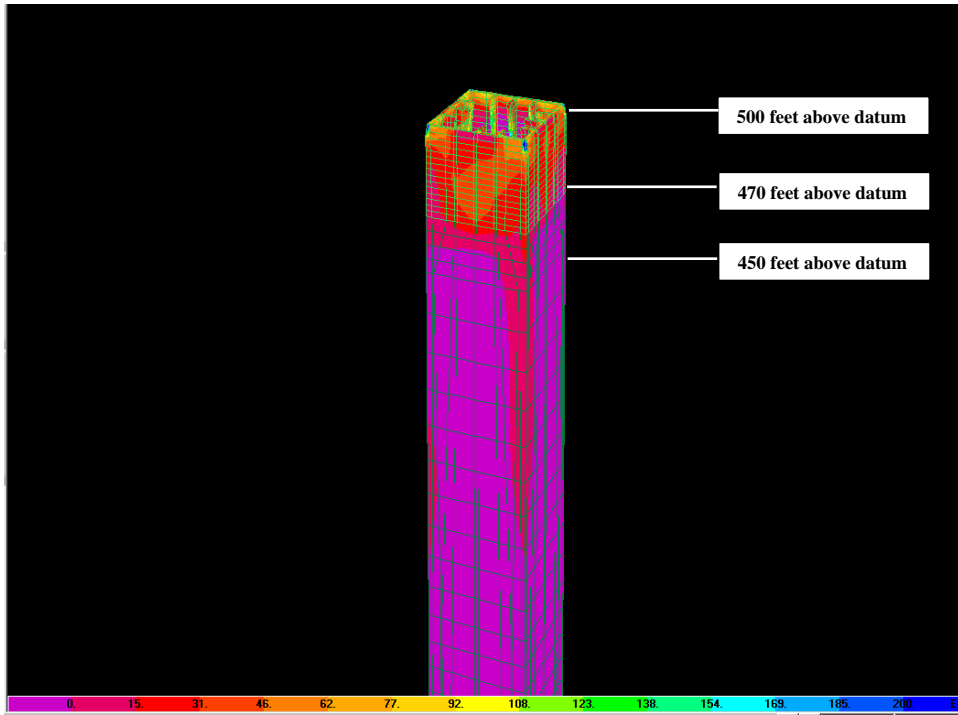


Figure 42. Envelope tensile stresses in vertical direction of the shaft due to Mineral benchmark motion Whittier 2

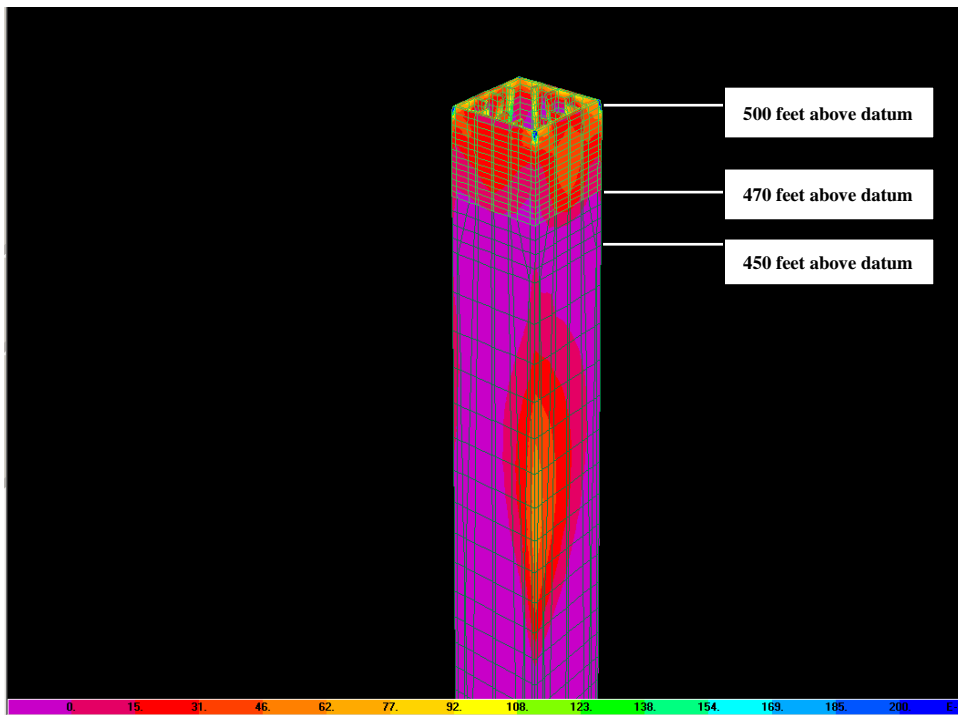


Figure 43. Envelope tensile stresses in vertical direction of the shaft due to MCE motion ChiChi2

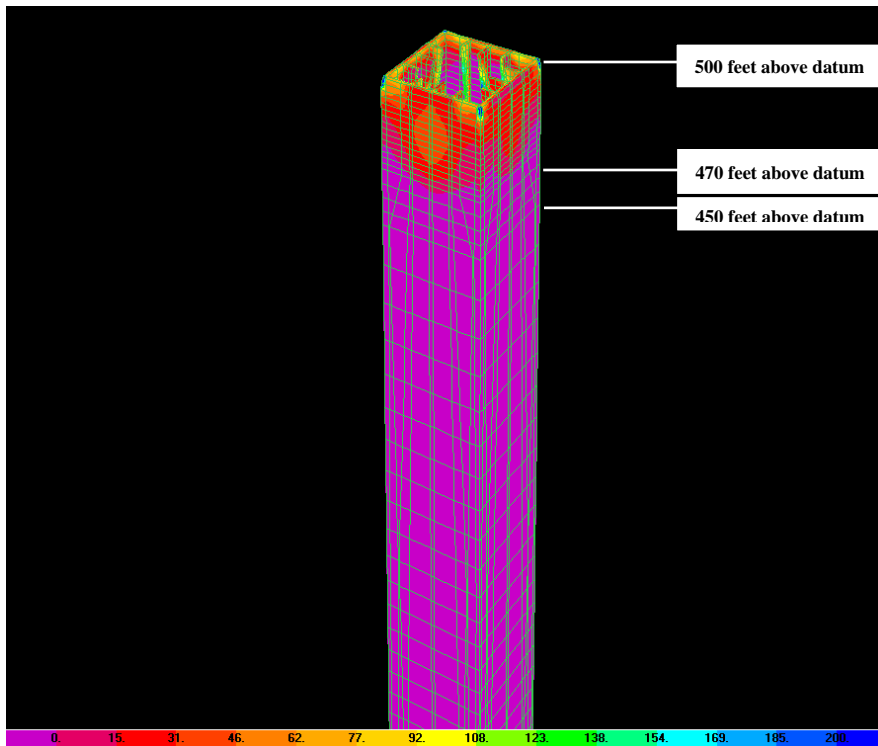


Figure 44. Envelope tensile stresses in vertical direction of the shaft due to MCE motion ChiChi2 for softened shaft stiffness

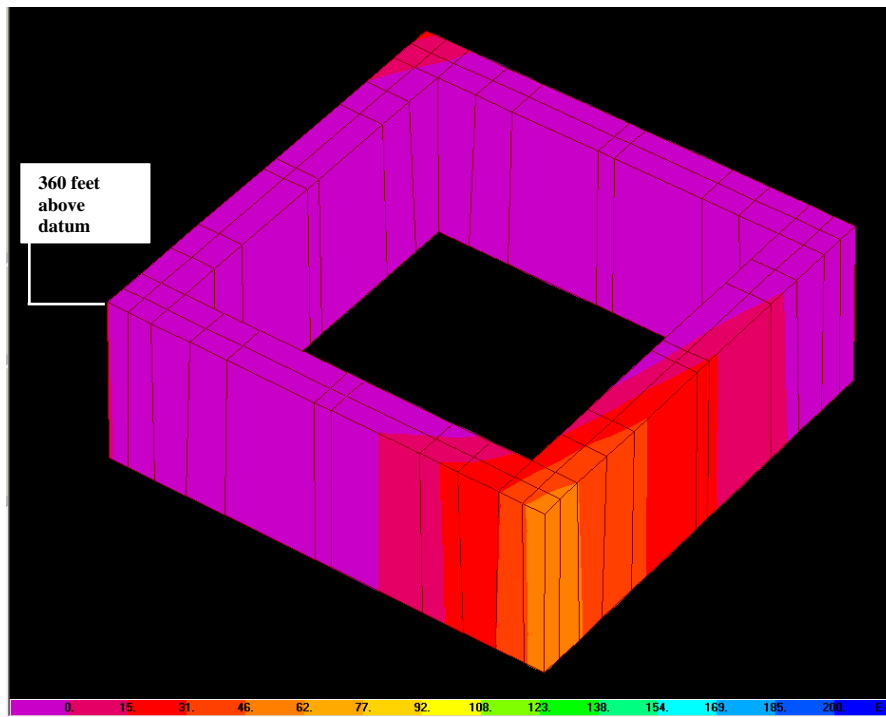


Figure 45. Envelope tensile stresses in vertical direction of a cross section of the shaft around 360 feet above the datum due to MCE motion ChiChi2

Stresses in the upper portion of the shaft walls influenced by the pyramidion are quite complex and deserving of special focus. Damage after the Mineral event was observed to the shaft walls above 450 feet, particularly cracking in and loss of mortar from vertical joints. In the following paragraphs, vertically-oriented and horizontally-oriented tensile stresses are discussed.

The largest vertically-oriented tensile stresses occur due to a modeling simplification: the “tying down” of the lowest course panels of the pyramidion to the shaft, which creates a local stress concentration at the corners. In reality, the pyramidion panel-to-shaft connection is a continuous rabbet and is unable to transmit vertically-oriented tension. As shown in Figure 42 and 43 for the model with the “unsoftened” shaft, the region from 470 feet to 500 feet above datum has considerably higher vertically-oriented tensile stresses than regions below. These tensile stresses are around 70 psi for the Benchmark motions and 60 psi for the MCE motions. For the models with a “softened” shaft, the tensile stress values have similar magnitude and location (Figure 44). These tensile stresses are considered to be below the likely strength of Portland cement mortar.

In contrast, the cracking in and loss of mortar from vertical joints in the upper regions of the shaft are largely a manifestation of “working” and “spreading” of the shaft masonry, i.e. related to horizontally-oriented tension. Conceptually, such actions would result from resolution of compression forces along the lines of action defined by the edges of the pyramidion. Such actions likely also result from migration of lateral forces from the pyramidion and the ribs --- which flex and transmit shear forces --- into the walls of the shaft and rib projections. The rib construction is well integrated into the shaft wall construction throughout the upper thirty feet of the shaft. Figures 46 and 47 depict horizontally-oriented tensile stresses (S11), which are the indicator of the “spreading” potential, due to the Whittier2 and ChiChi2 motions. The stresses in the figures range from 0 psi (red) to 200 psi (blue) and the difference in stress magnitude on walls orthogonal to each other is the result of the three-dimensional solid global stress orientation. Our analysis demonstrates that the “spreading” stresses are predicted to be of a similar intensity in the MCE as they were during the Mineral event, approximately 150-200 psi if the vertical joints are not modeled as degrading elements. In the Monument, “spreading” stresses are initially resisted by the tensile strength of the mortar in the vertical joints. After the mortar cracks and ceases to transmit tension, the horizontally-oriented tensile stiffness of the shaft wall drops dramatically and the reduced tensile stresses that result are resisted by tension in the cramps, iron rods that interconnect blocks of stone in the upper fifty feet of the shaft. Cramps exist at every course and are understood from historical documents to be 3/4 inch galvanized iron bar (Brewer, date unknown). Based on non-destructive testing by which we found evidence of cramps about six inches from the interior of the shaft masonry, we suspect that there may be two rows of cramps in each course, giving them a capacity to single-handedly resist a tensile stress of around 70 psi. It should also be mentioned that the concentration of horizontally-oriented tensile stresses below 450 feet above the datum shown in Figure 47 are largely a function of the abrupt change in the as-modeled shaft stiffness in this location; this is demonstrated in Figure 48 where the MCE load case with a “softened” shaft does not show these concentrations.

While it is noted that the predicted 150 psi horizontally-oriented tensile stress is strongly influenced by continuous meshing of the shaft stone masonry, which did not explicitly allow for softening of the structure once cracking of the vertical joints occurred, the Mineral event caused lateral offsets in these joints of up to 3/8 inch. Although during this assessment no models were created that included vastly reduced horizontal tensile stiffness of the upper shaft walls as a result of cracking in the vertical joints, it is possible that if an MCE-type earthquake occurred, the offsets at the upper vertical joints would increase slightly, but these types of offsets are judged to not appreciably impact the ability of the structure to carry the required loads.

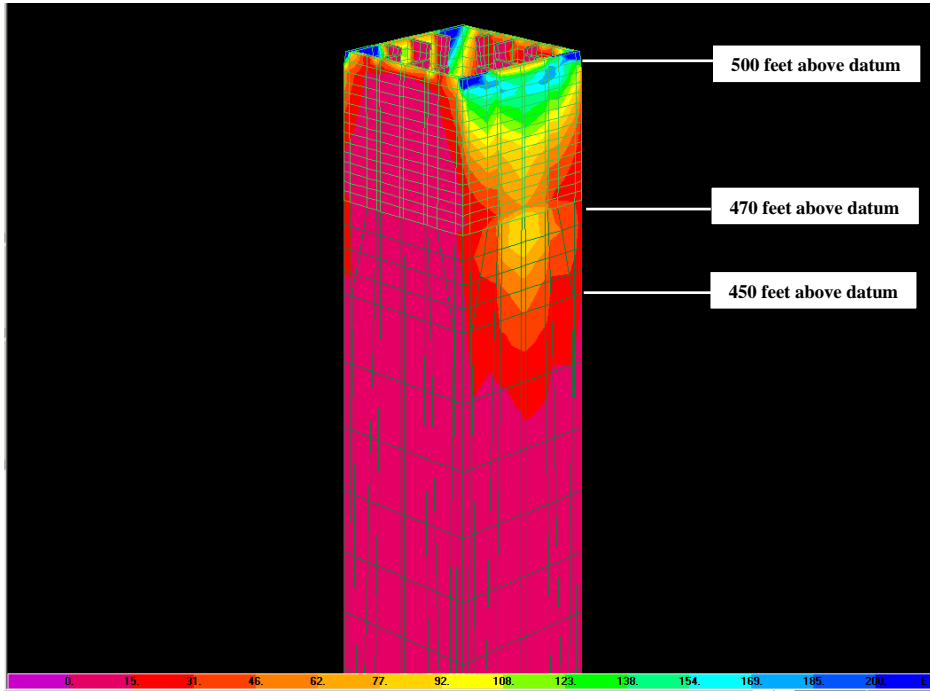


Figure 46. Envelope horizontal tension stresses in the shaft due to the Benchmark motion Whittier2

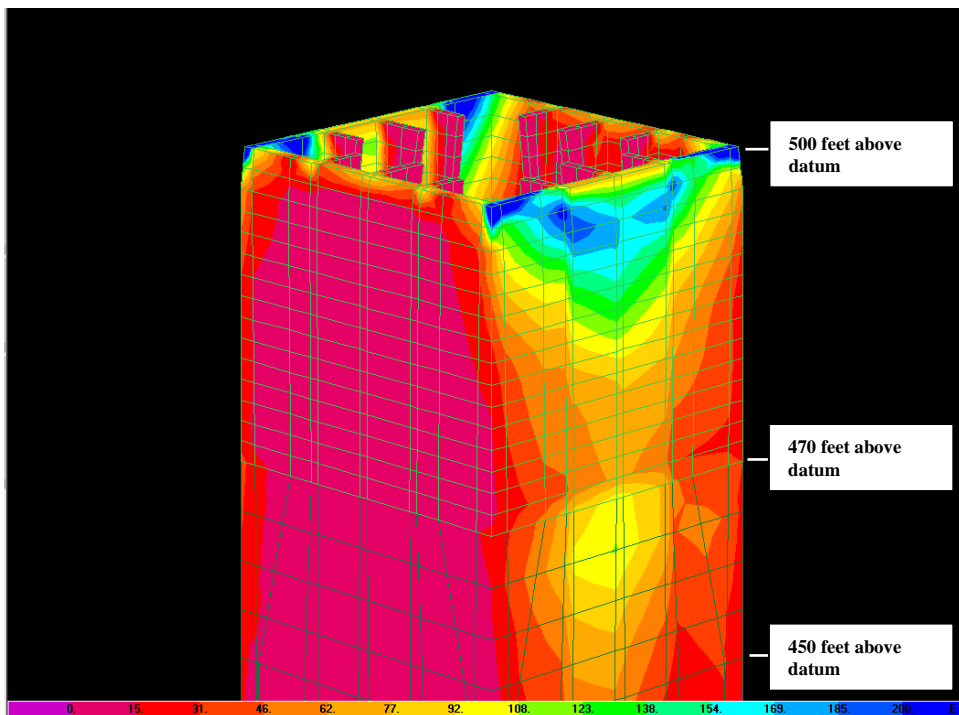


Figure 47. Envelope horizontal tension stresses in the shaft due to the MCE motion ChiChi2

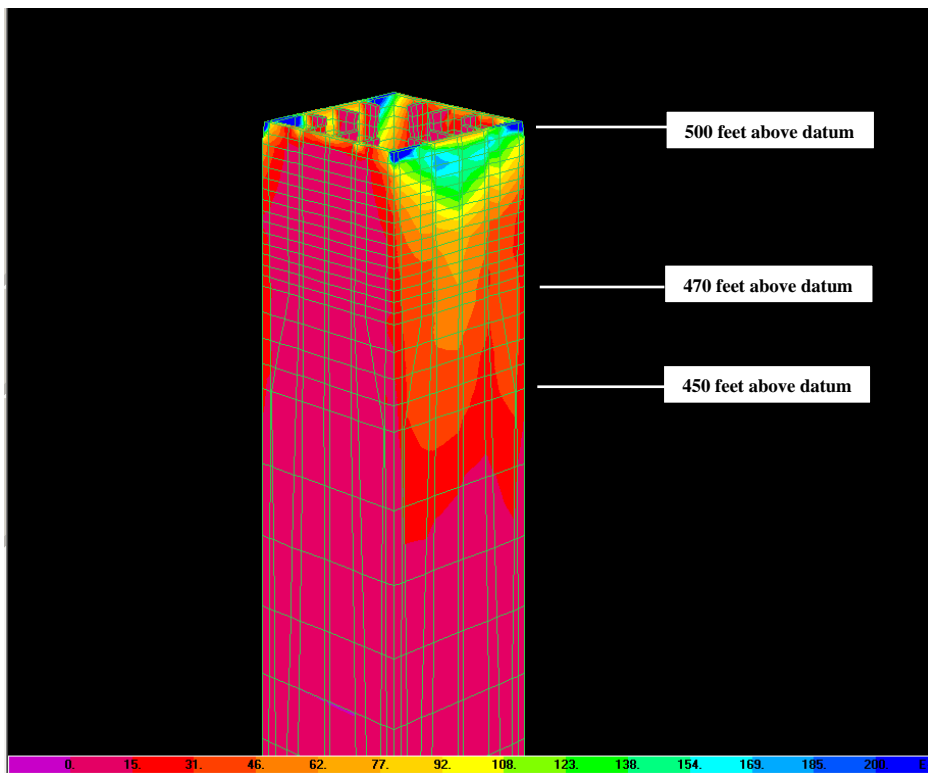


Figure 48. Envelope horizontal tension stresses in the shaft due to the MCE motion ChiChi2 for softened shaft stiffness

Because compressive stress in masonry can also be a potential concern, the vertically-oriented compressive stresses in the shaft for the Mineral and MCE events were examined. Maximum compressive stresses at the base of the shaft are approximately the same for the dead load case, the Mineral load case and the MCE load case, and are approximately 250 psi. Figure 49 shows the maximum compressive stress at the base of the shaft for the MCE ChiChi2 ground motion. The compressive stresses in the figure range from -250 psi (red) to 0 psi (blue). The compressive capacity of the stone masonry at the bottom of the shaft substantially exceeds the combined gravity plus seismic demands from either the Mineral or MCE ground motions.

The shear stresses in the model were also evaluated and found to be small with relation to the capacity of the Portland cement stone masonry. In the main body of the shaft, the maximum shear stresses due to the MCE ground motions are around 30 psi. Limited areas of shear stresses of 70 psi occur near the very top of the shaft at the corners as a result of the migration of “spreading” forces from the edges of the pyramidion above.

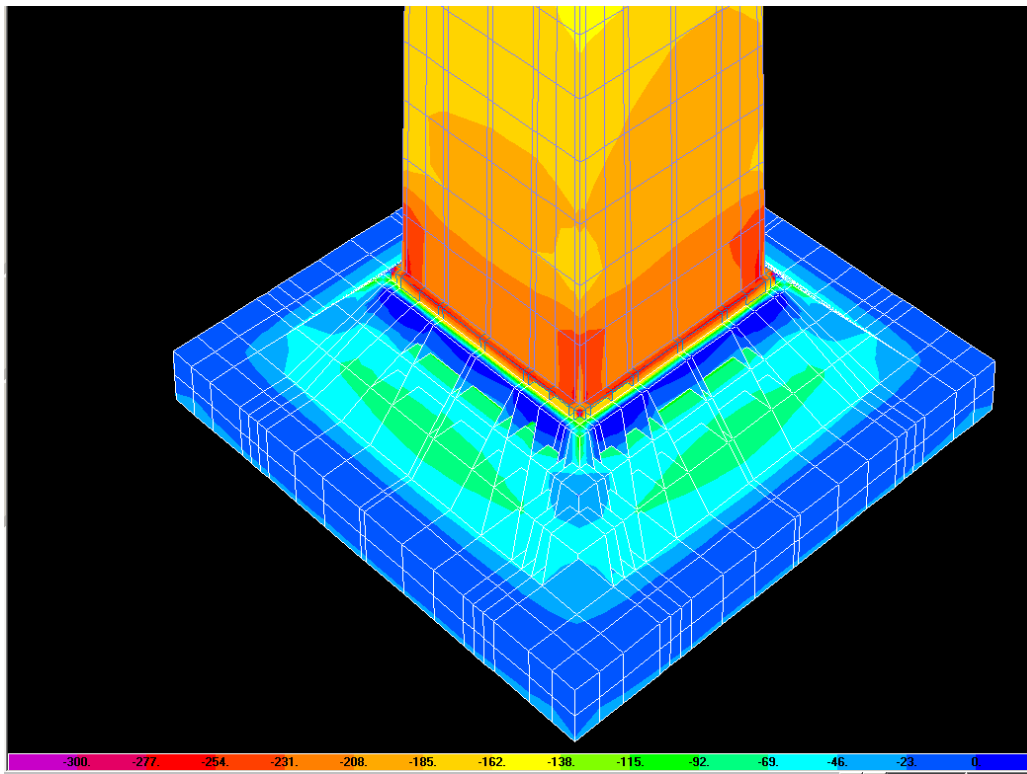


Figure 49. Envelope vertically-oriented compressive stresses at the base of the Monument due to the MCE motion ChiChi2

The overall lateral displacement, or drift, of the tip of the Monument due to seismic forces is mainly driven by cantilever action of the shaft, which in turn is influenced by the material properties of the shaft masonry, the stiffness of the supporting soils and by the ability of any particular earthquake to cause the shaft to respond (i.e. the spectral shape of the input motion). The pyramidion contributes relatively little to the tip displacements in the MCE, but contributed far greater in a relative sense during the Mineral event, which did not excite the lower portion of the Monument to any significant degree. Parameters such as the type of FNA run (broken tooth or with residual load sequencing) were studied but found to have little effect on the overall building drift although they affect the “story drift” of the pyramidion itself. As described above, given the much greater spectral acceleration input into the shaft of the Monument for the MCE ground motion as opposed to the Mineral motion, the predicted tip displacements are much larger for the MCE. A summary of relative displacement output from the Monument FNA runs is provided in Table 6 at the base of the pyramidion (500 feet above datum) and the top of the Monument (555 feet above datum). These maximum displacements do not necessarily occur at the same instant in time during any particular record. The analysis results show that the average displacements for the Mineral ground motion are 0.83 inches and 1.82 inches at the base of the pyramidion (500 feet above datum) and at the top of the pyramidion (555 feet above the datum), respectively. The MCE ground motions produced displacements at the base of the pyramidion that, on average, were approximately 6 times greater than the ground motions representing the Mineral event.

Table 6. Analysis output | Relative translational displacements

Ground Motion Series	Ground Motion	Maximum relative displacement at 500 feet above datum (inches)*	Maximum relative displacement at 555 feet above datum (inches)*
Benchmark	Sag1	0.71	1.49
	Sag2	0.77	1.99
	Sag3	0.53	0.90
	Whittier1	0.69	1.24
	Whittier2	0.69	2.00
	Georgia	1.84	3.61
	N Palm	0.58	1.52
	Average	0.83	1.82
MCE	Duzce	4.48	5.28
	Landers	7.86	9.49
	Kocaeli	3.71	4.47
	ChiChi1	6.85	8.19
	ChiChi2	2.13	3.24
	ChiChi3	1.48	2.04
	ChiChi4	8.39	9.86
	Average	4.99	6.08

* Values in the table are maxima that may not occur at the same instant in time. See pyramidion results section for discussion of pyramidion drifts.

Analysis Results | Pyramidion

As described earlier, the mode of swaying dominated by local deformation of the pyramidion is quite complex and was modeled using an intricate network of three-dimensional solids, nonlinear isolator elements, link elements, and linear-elastic shell elements. Even with that degree of discretization, the modeling of the pyramidion is only a crude idealization of its complexity. The geometric layout and material properties of the elements in the model were determined in part from an iterative procedure where the effect of the variables were each assessed and then assigned based on damage metrics observed at the Monument after the Mineral earthquake. In addition, due to uncertainties and variability associated with actual properties of the extant construction, the material properties of many of the elements in the model were adjusted in order to assess the sensitivity of the results to the input assumptions and to attempt to bound the problem. In keeping with the over-arching modeling and analysis approach used throughout, the assessment of the seismic adequacy of the pyramidion was based on analysis results that

were derived from a variety of models, including models in which the properties of the shaft were varied. With respect to the results for the pyramidion presented herein, the model incorporating the “unsoftened” shaft was used, as described in an earlier section, unless otherwise noted. The analyses demonstrated that the results from the “unsoftened” and “softened” shaft were nearly interchangeable. Bounding of the results was also performed based on two methods described that were also described earlier, 1) Broken teeth, and 2) Load sequencing.

Several general categories of output -- including “tooth forces” and “rib stone residual displacements” -- have been selected for presentation of pyramidion results in this report; of all the categories of analysis output that could be presented, these appear to be the most revealing with respect to explaining the damage that occurred due to the Mineral earthquake and the damage that could occur due to a future 2,475-year earthquake. These categories of output are discussed in detail below.

Our field investigation revealed that fractures judged to be of significance that they required repair occurred in 24 of the rib stone “teeth” during the Mineral earthquake. To assess the vulnerability of the teeth, the model development included bounding of the interlocking properties of the rib stone-to-panel connection, particularly the in-plane flexibility. Analysis of models in which these interlocking properties had greater flexibility achieved better correlation with the damage observed after the Mineral-event than analysis of models with less flexibility. For models with greater flexibility of the interlocking properties, the in-plane forces in the panels are mainly carried by the panels themselves while the out-of-plane forces are mainly transmitted through the panel-to-rib connections. For models in which the links capable of transferring “in-plane” forces between the panels and teeth had the greatest flexibility, predicted values of “in-plane” and “out-of-plane” tooth forces on the east and north elevations of the pyramidion during the Mineral earthquake are shown in Figure 50. These values are average maxima from the suite of seven pairs of Mineral records. The figure also identifies the locations of teeth with fractures.

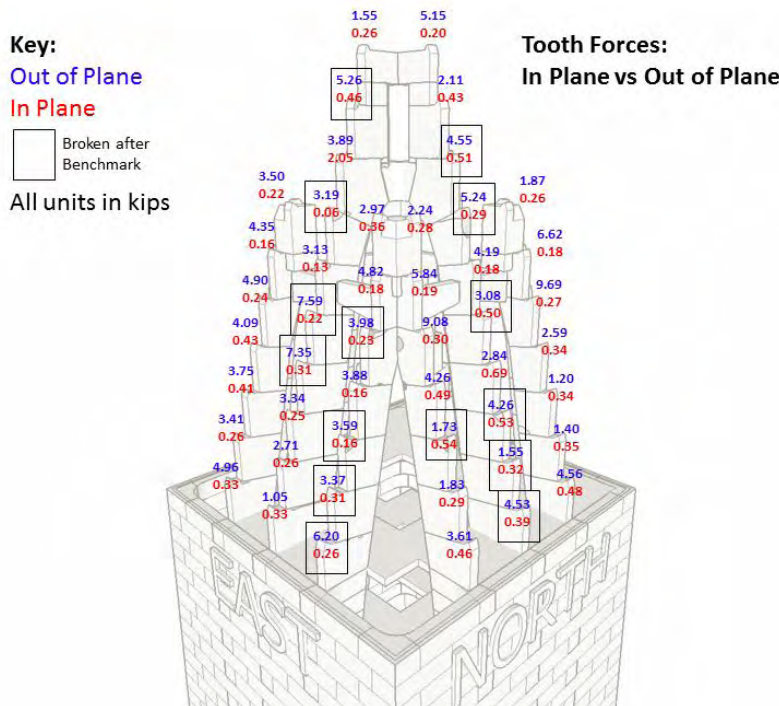


Figure 50. Typical in-plane versus out-of-plane tooth forces

The out-of-plane tooth forces that occur between the rib stones and pyramidion panels are comprised of either locally generated inertial forces, or forces resulting from distortions in the pyramidion structure (e.g. sliding or rocking of the rib stones with respect to one another). For the Mineral load case, the location of the largest “average maximum” tooth forces correlate reasonably well with the locations of the teeth that were found with fractures during the post-earthquake survey, especially given that each panel-to-tooth connection is fit-up somewhat differently (Figure 50). For the MCE load sequence analyses in which the model simulated “broken teeth” from the Mineral event, some average maximum “tooth” forces are predicted to be larger than what occurred during the Mineral event but these generally occur in the vicinity of the “broken” teeth which suggests that the broken teeth, as modeled, are shedding load to the adjacent teeth in the MCE load cases (Figures 51 and 52). Because the connections at “broken teeth” were modeled with only the stiffness of the added steel brackets and assuming that the existing teeth provide no support or stiffness, these results likely overestimate the degree to which load will be shed. On a more global level, the magnitude of the out-of-plane tooth forces for the Mineral ground motions varies between approximately 11 kips and 1.0 kips, for the MCE with “broken teeth” they vary between 9.0 kips and 0.5 kips. These results are not significantly affected by changing the rib stone-to-panel connection flexibility.

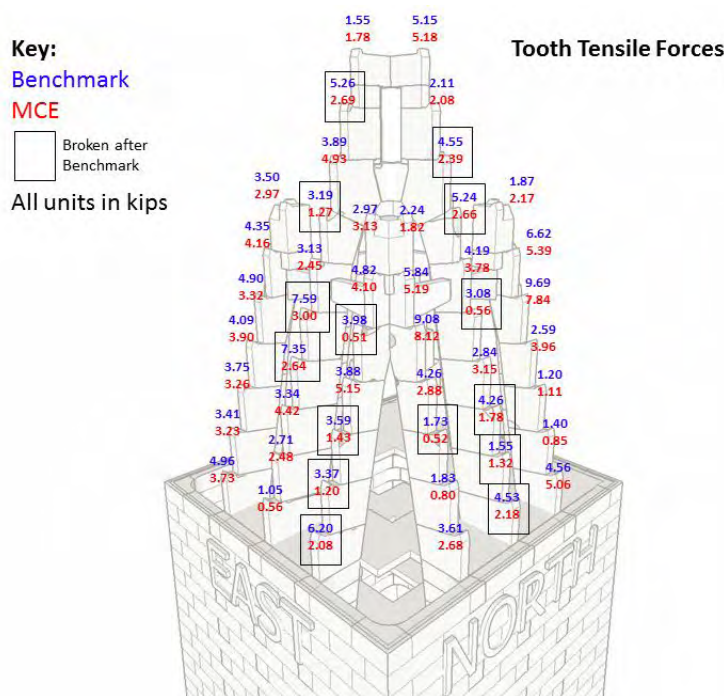


Figure 51. Typical out-of-plane tooth forces in the pyramidion East and North facing ribs

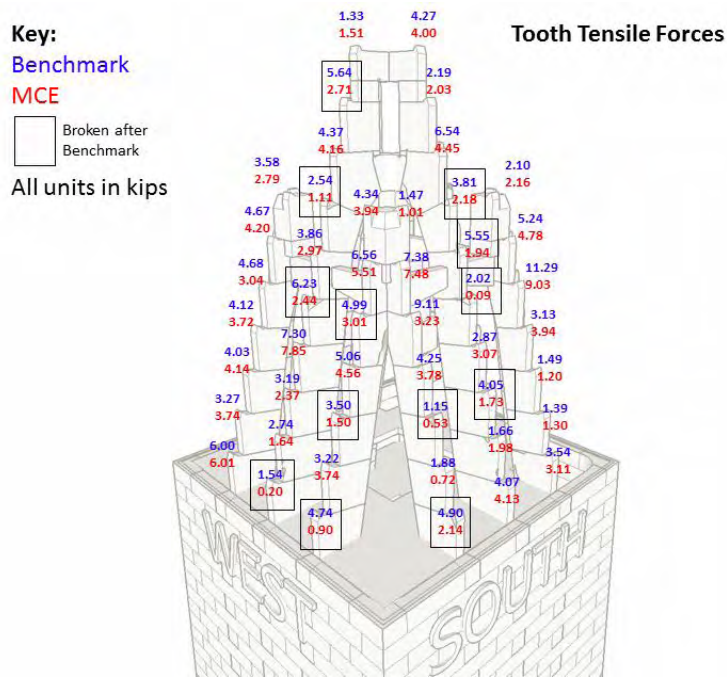


Figure 52. Typical out-of-plane tooth forces in the pyramidion West and South facing ribs

Although “average maximum” values are the appropriate output values to examine when structural response to suites of seven pairs of time histories is evaluated, it can also be informative to compare the average maximum with the maxima from each of the seven pairs of ground motion inputs. Such an examination quantifies the variability of forces resulting from the different pairs of ground motions, though all represent either the Mineral event or the MCE. For a corner rib stone-to-panel connection immediately below the tie beam elevation, for example, the seven pairs of Mineral ground motions generate an average maximum value of 9.08 kips, as shown in Figure 51. In comparison, the maximum value for each of the seven input ground motions, however, varies from 11 kips to 5 kips. This variation demonstrates that the out-of-plane forces in the teeth are dependent on the specific characteristics of the individual ground motions, although some locations -- such as the course just below the tie beam -- are clearly predicted to experience larger forces, on average, than others.

Certain variables with the potential to influence other aspects of the pyramidion behavior, such as the effect of load sequencing, are predicted to have a relatively minor influence on the magnitude of the “tooth forces”. Comparing out-of-plane tooth forces predicted from the MCE runs restarted from the dead load plus Whittier2 (Mineral) ground motion (i.e. the load-sequenced analyses) to the MCE runs with only dead load previously applied, some tooth forces are higher; some are lower; and some tooth forces are actually negative (Figure 53 for “softened” shaft). Negative forces in this case indicate that the Mineral motion resulted in sliding of rib stones, which imparted compression in the link elements connecting the ribs to the panels. The magnitude of the MCE load-sequenced tooth forces is related to the residual deformation of the isolator elements (i.e. the sliding blocks) due to the selected Mineral ground motion. For example, the Whittier2 and Landers ground motions result in substantially different residual rib stone offsets and, therefore, also substantially different MCE load-sequenced tooth forces when restarted.

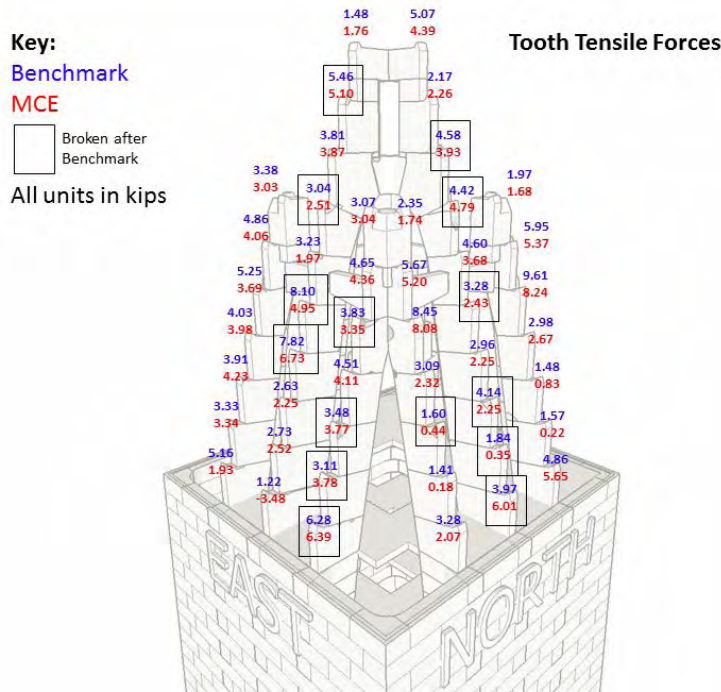


Figure 53. Typical out-of-plane tooth forces in the pyramidion for Benchmark v. MCE load-sequenced analysis (“softened” shaft)

The finite element models utilize friction-pendulum isolators to simulate sliding of the rib stones with respect to one another. To compare the analytically predicted sliding from the Mineral load case to the WJE earthquake damage survey, we employed isolator residual displacements, which represent the “last step” or final displacements that exist after the time history run is completed. Specifically, we used these values to calibrate the model to the residual shifting of the rib stones actually observed in the Monument after the Mineral earthquake. Figures 54 and 55 and Figures 56 and 57 show the predicted In/Out and Side/Side residual displacements due to the Mineral and MCE load cases for both side ribs and center ribs, respectively. The values shown are the average maxima, in line with earlier discussions, and are presented as the largest value of the four isolators that exist at each rib stone. This largest value thus captures the maximum shift, including any torsional response of the rib stones. For clarity, only predicted offsets greater than 0.1 inch are shown in the figures. The figures validate behaviors observed in the field such as: 1) In/Out residuals have smaller magnitude than Side/Side residuals, 2) some of the largest offsets occur just below the tie beam level between courses D and E, and 3) magnitude of predicted offsets generally match observed with maximum around 0.75 inches.

In general, the isolator residual displacements predicted for the MCE load case occur in similar locations to the Mineral load case and have magnitudes that are the same or slightly greater. The slightly larger MCE residuals are likely due to the MCE ground motions being spectral-matched and therefore having characteristics that impart short-, intermediate- and long-period dynamic input to the finite element model at the same time. In other words, if the shaft is being excited and is swaying back and forth at its relatively long fundamental period, the pyramidion rib stones will be subjected to acceleration cycles related to that motion. If at the same time the pyramidion is being excited by motion coinciding with its own short period fundamental modes, these two effects will combine. Therefore, even though the MCE ground motions have less average spectral accelerations in the short period range to which the pyramidion

is most sensitive compared to the MCE motions, they result in a greater tendency for sliding of the rib stones. This is one of the problems inherent in spectral-matched time histories and is an artifact of the method used to generate the ground motions; they synthesize seismic input that combines maximum energy throughout the spectrum rather than representing the energy content of any single earthquake. As a result, we conclude that the residuals predicted for the MCE exceed what will really occur during any real MCE event. In any case, we note that the analysis predictions for the overall magnitude of residual displacement from the MCE motions are low enough that they are not likely to lead to instability of the pyramidion. As will be discussed in the “Recommendations” section, the use of “scenario” ground motions to predict the earthquakes occurring from specific sources could improve the MCE predictions of residual displacement.

As a worst-case evaluation of rib stone residual and transient displacements, we extracted the maximum observed residuals from all of the MCE ground motion analyses (i.e. the maximum maximum as opposed to average maximum) when the MCE ground motions were applied as load-sequenced (i.e. restarted from a dead load plus Whittier2). The maximum shifting of the centroid of any rib stone under this sequenced analysis is approximately 2.7 inches and occurs just below the tie beam level. This value substantially exceeds the average maximum for any earthquake. For a rib stone with base dimensions of 12 inches by 30 inches, a shift of 2.7 will not jeopardize stability, particularly at the elevation of the tie-beams where the gravity loading is relatively minor.

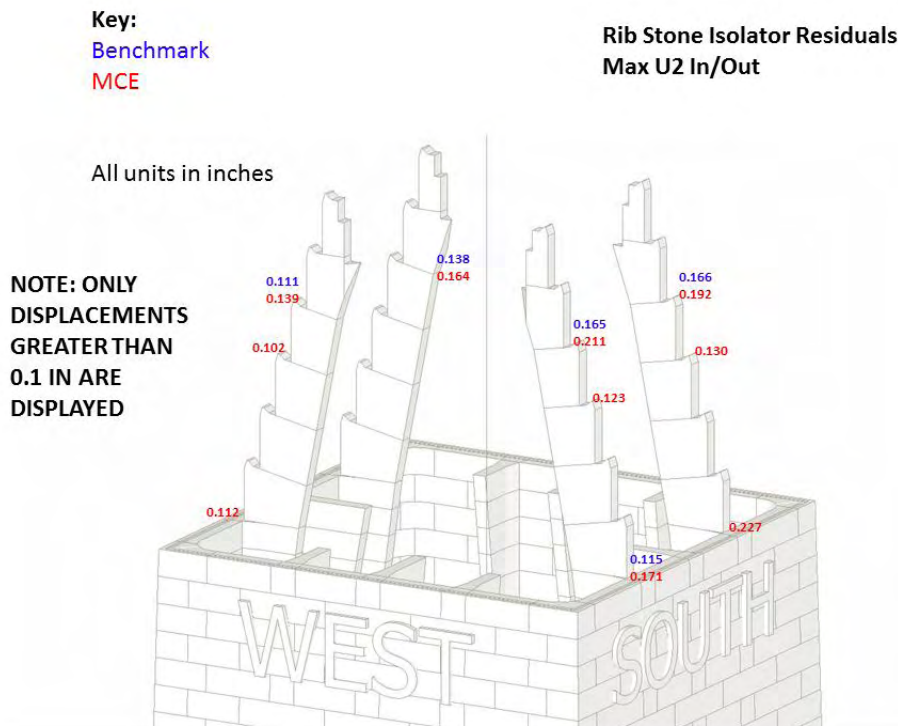


Figure 54. Typical side-rib isolator in/out residuals

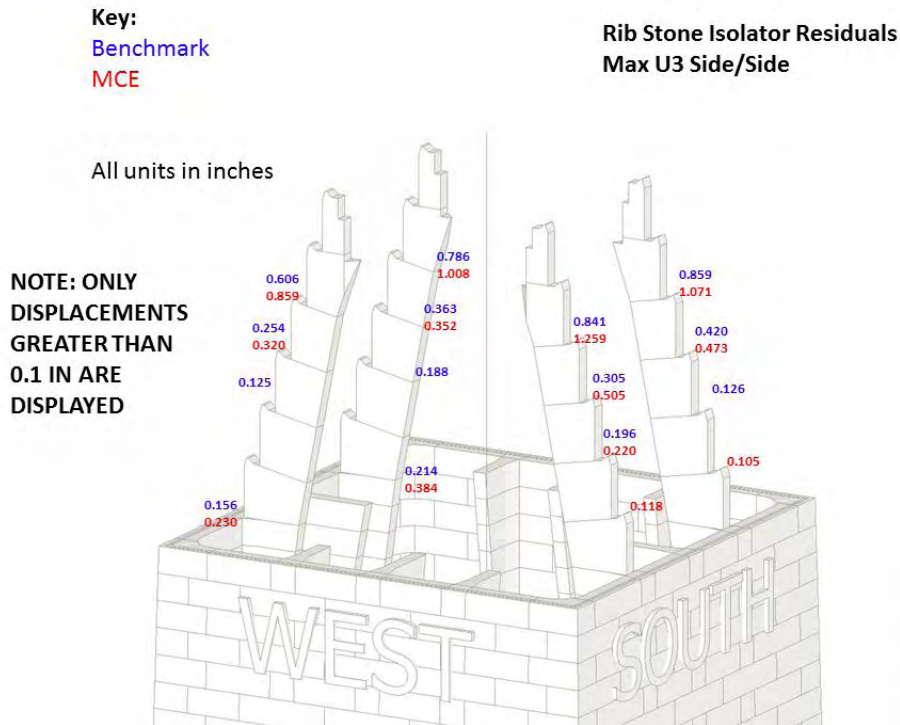


Figure 55. Typical side-rib isolator side/side residuals

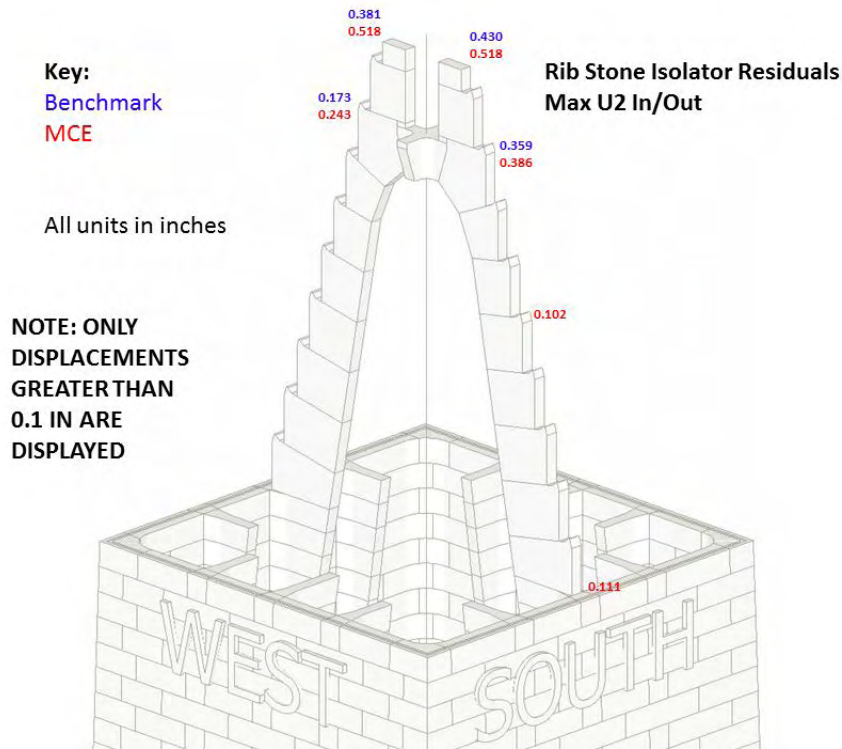


Figure 56. Typical center-rib isolator in/out residuals

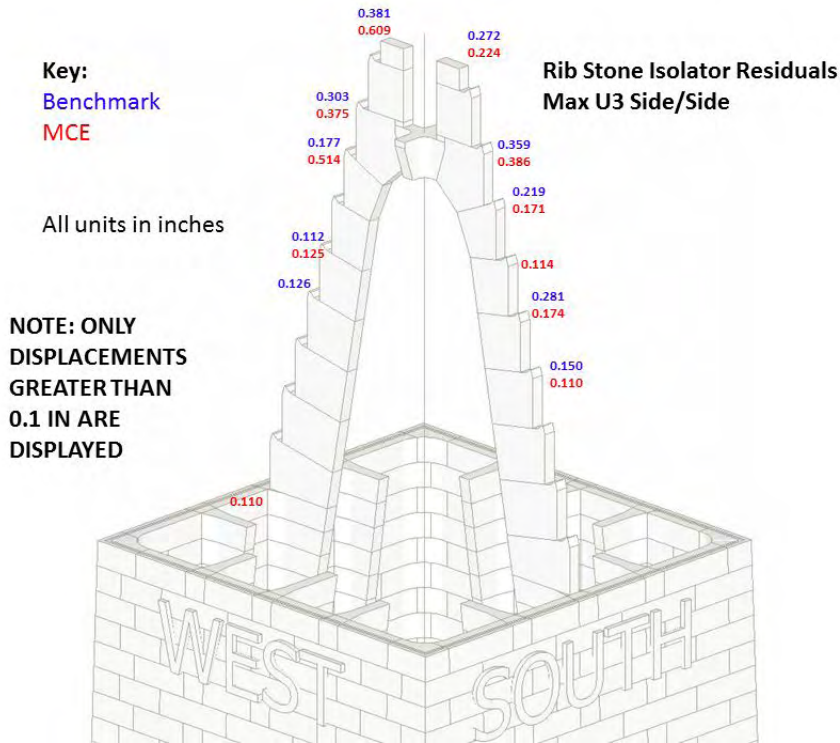


Figure 57. Typical center-rib isolator side/side residuals

The pyramidion cruciform stone is cross-shaped in plan but keystone-shaped in elevation; the joints between it and the four ribs that extend to the elevation of the cruciform are sloped to retain the keystone under gravity loads and contain mortise and tenon joints. The cruciform exhibited several smaller spalls and chips after to the Mineral event, but more significantly, an adjacent rib stone experienced a large spall that exposed one of the cruciform's mortise and tenon joints. The joints between the cruciform and adjacent rib stones were modeled with isolators. Figures 58 and 59 provide analysis results for these isolators, specifically the maximum transient and residual displacements due to the Mineral and MCE load cases (i.e. the maximum of the maxima for each ground motion) in the vertical and horizontal directions. The results show that the maximum predicted residual displacements in the isolators after the Mineral time history analyses are not large, on the order of 0.2 inches. In contrast, the maximum transient displacements predicted over the duration of the Mineral time histories, are much larger, on the order of 0.8 inches in both the vertical and horizontal directions for the Mineral load case. Although these transient values are smaller than for some rib stones below, the cruciform is wedged between rib stones that subject it to a complex set of internal forces. It is not unreasonable to expect that the 0.8 inches of maximum displacement in either direction during the Mineral earthquake could cause the cruciform to lock up between competing ribs and cause spalling. The maximum predicted transient and residual displacement for the MCE motions are similar or somewhat larger.

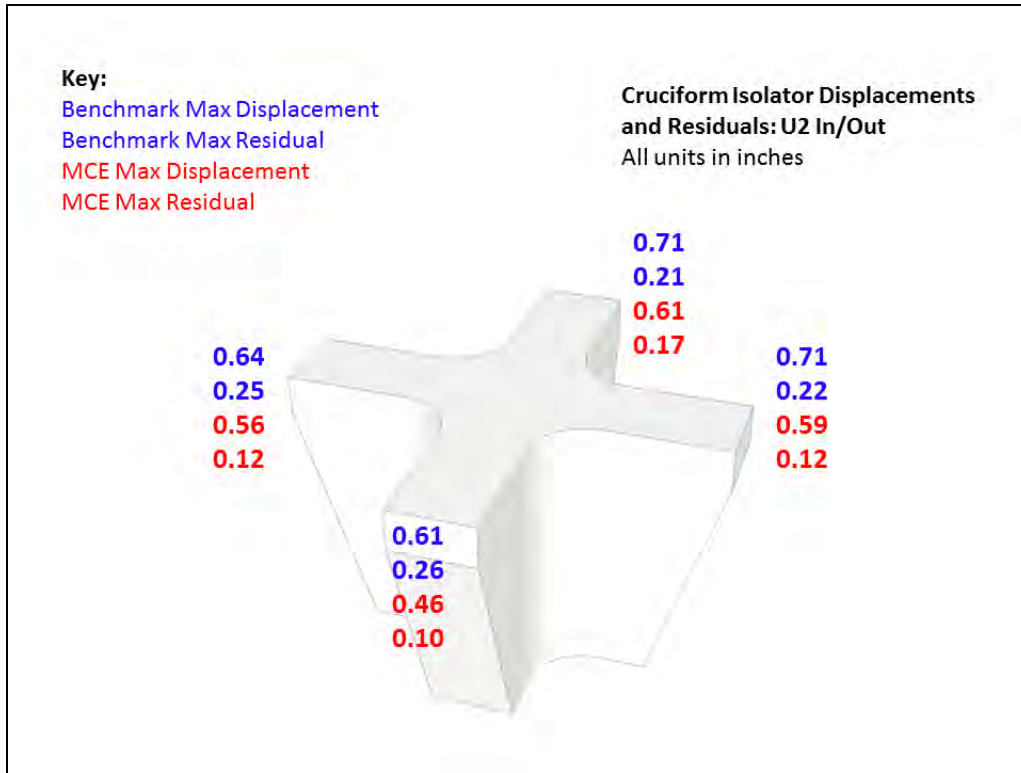


Figure 58. Typical center-rib isolator side/side residuals

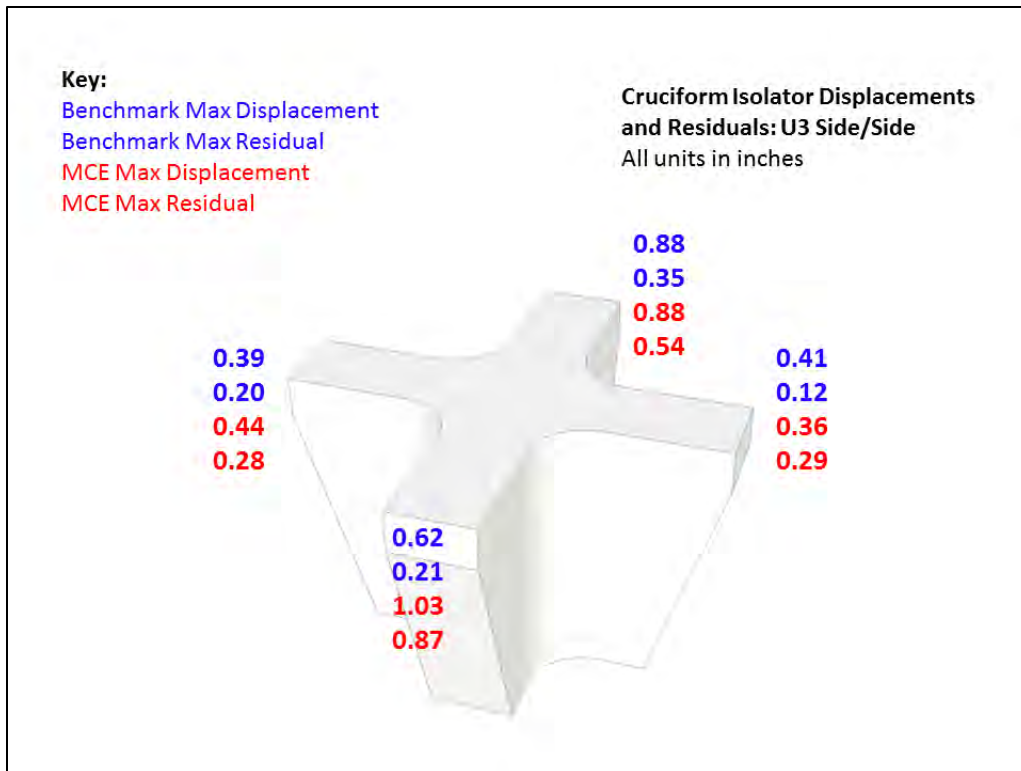


Figure 59. Typical center-rib isolator side/side residuals

Eight stone tie-beams roughly 12 inches by 30 inches with a span of 6 feet interconnect the center and corner ribs at elevation 523 ft above datum (Course F). One of them was significantly damaged adjacent to the connection with a center rib. Although the complicated joinery at this location -- particularly where the tie beams, corner ribs and cornerstones intersect -- led to the use of many linear-elastic link elements to idealize the region, the general behavior of the tie beams was consistent with the conceptualized behavior as restricting and transferring loads between the arched-frame ribs. The envelope of the horizontally-oriented tensile stresses for the Whittier2 (Mineral) ground motion is shown in Figure 60. The stresses in the figure range from 0 psi (red) to 200 psi (blue). The envelope plot is showing the tie beams in bi-axial bending, which is mainly associated with relative movements between the center and corner ribs. A likely source for much of differential movement between the ribs is out-of-plane distortions at the top of the shaft wall, and differential frame-related displacements due to the varying vertical spans of the rib stone arches. The maximum predicted horizontally-oriented tensile stresses for the MCE motions are similar or somewhat smaller than stresses due to the Mineral motions.

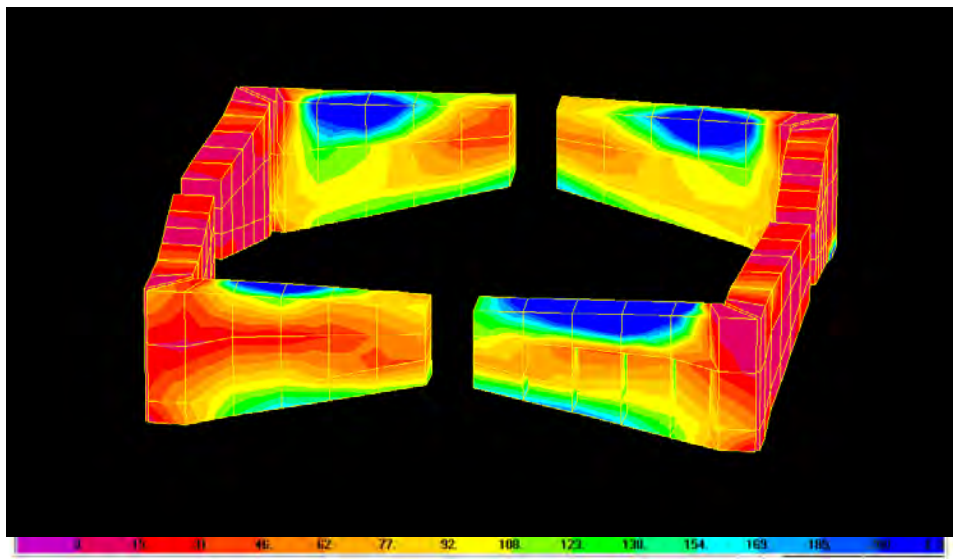


Figure 60. Envelope of horizontally-oriented tensile stresses in tie-beam for Whittier2 (Mineral) ground motion

Some of the 7-inch-thick pyramidion panels experienced through-panel cracking during the Mineral event; the analyses appear to be reliable indicators of that cracking. The earthquake cracking in the panels is always associated with the thinner section of the panel where the tooth is “let” into the panel; it presents the appearance of cracking induced by out-of-plane moments. The cracking is inclined, suggesting that it could be initiated by moments about either a horizontal or vertical axis. The panels were modeled using shell elements, allowing for visualization of out-of-plane moments due to the various input ground motions. Both moments about the vertical and horizontal axis were considered, but for this discussion we present only the moments about the horizontal axis which the analyses indicate had larger demands during the Mineral earthquake. The maximum envelope moments for the Whittier2 Mineral ground motion and the ChiChi2 MCE ground motion are shown in Figures 61 and 62. The moments in the figure range from 0 kip-foot-per-foot (red) to 5 k-ft/ft (blue). The results demonstrate that the maximum moment demand on the pyramidion panels occurs near the center-rib-to-panel connections at the course at the tie-beam, the lowest level where only the center ribs are available to provide out-of-plane support for the facets. This is the same location where cracking was observed in the pyramidion panels on the west

elevation after the earthquake (Figure 63). Simple hand calculations indicate that 5 k-ft/ft is sufficient demand to crack the stone panels.

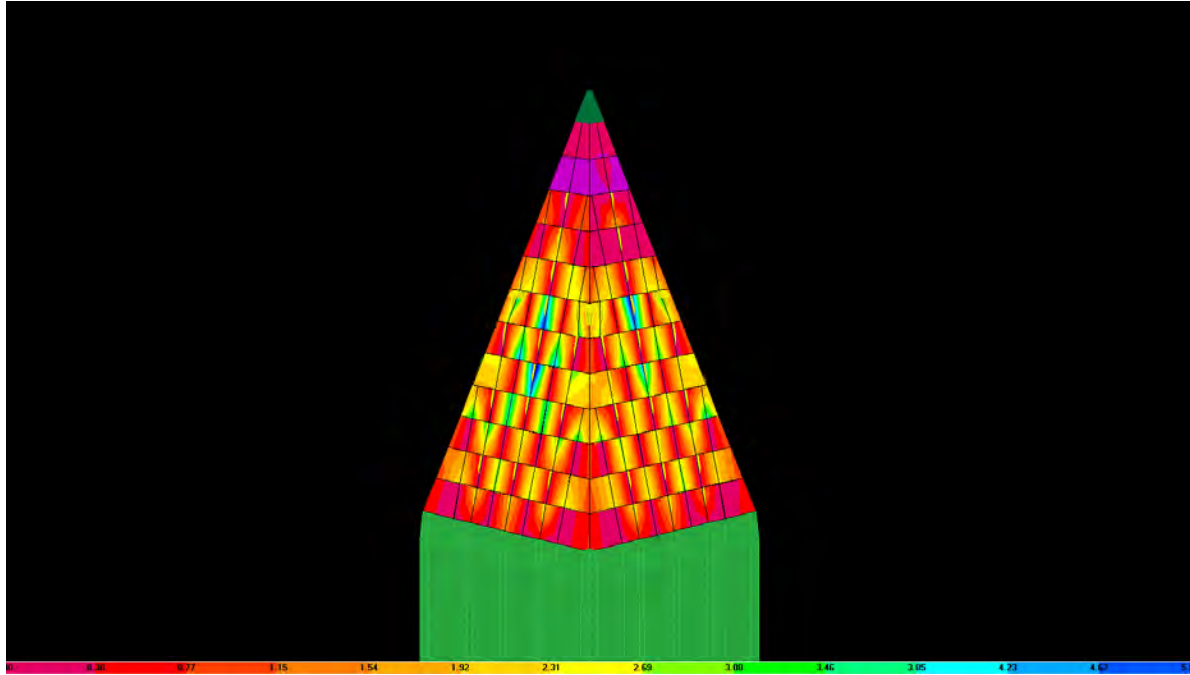


Figure 61. Maximum envelope moments about the horizontal axis for Whittier2 Mineral ground motion

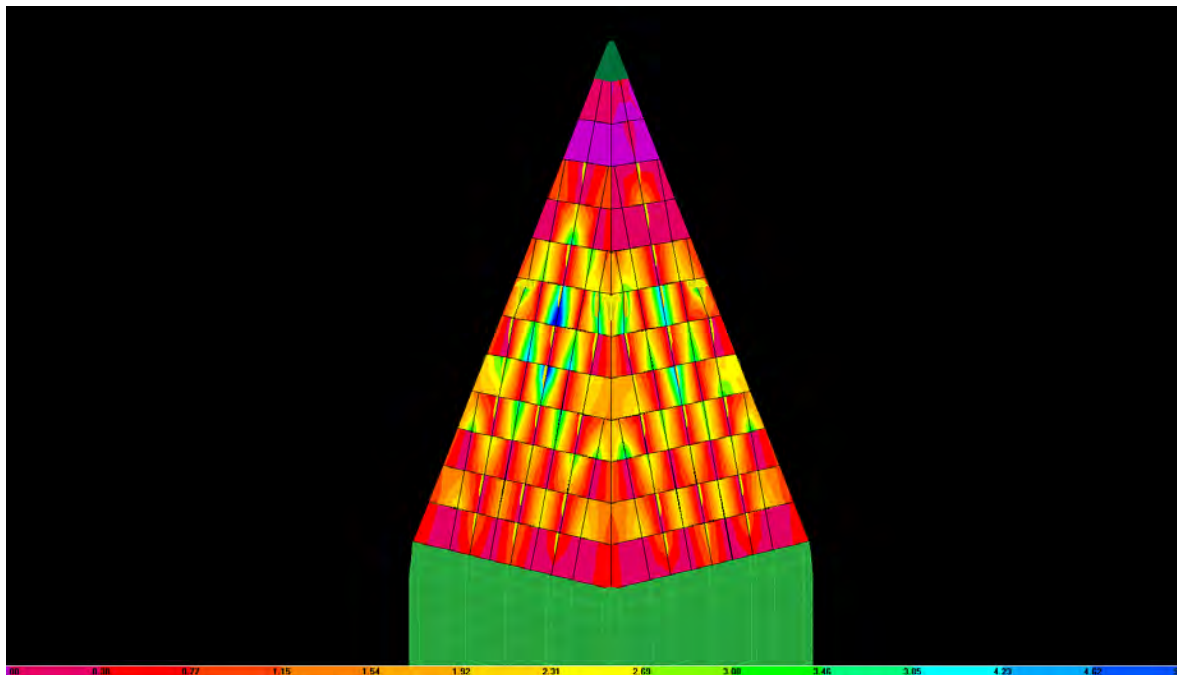


Figure 62. Maximum envelope moments about the horizontal axis for ChiChi2 MCE ground motion

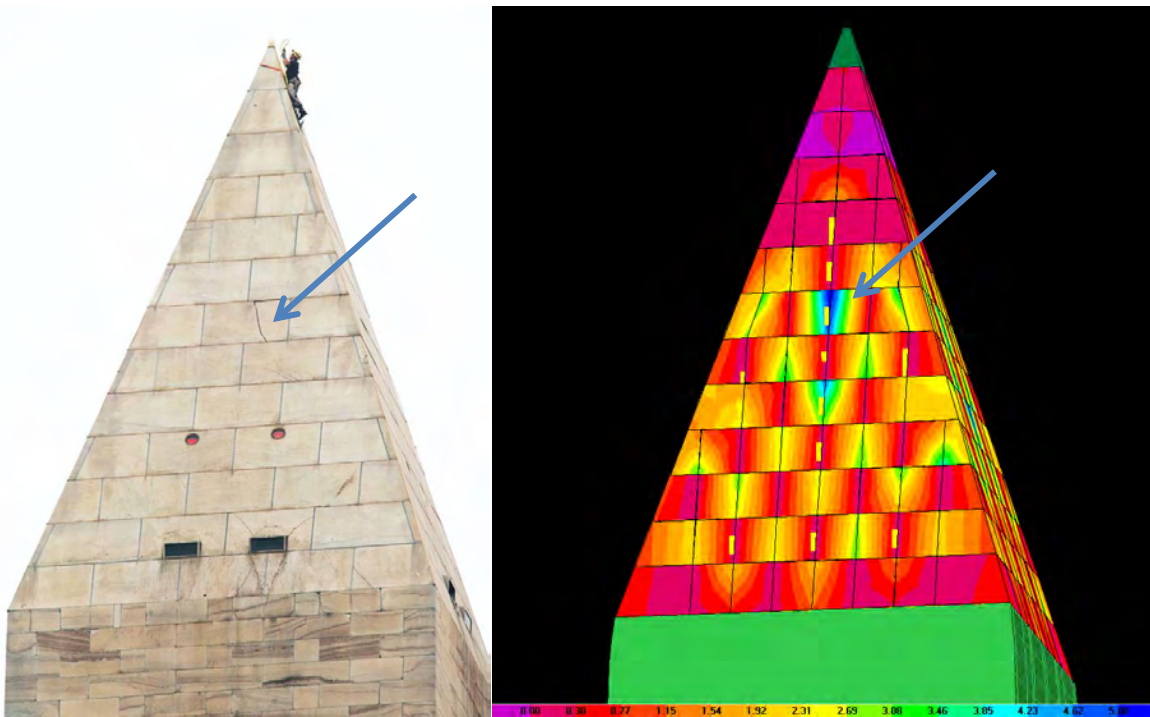


Figure 63. Comparison between a photograph of the pyramidion after the Mineral earthquake to the predicted maximum envelope moment

Supplemental Analysis Confirmation

As part of this seismic assessment project, a supplemental analysis confirmation study was performed in parallel by Tipping Mar (TM). TM describes their work in detail in a report that is attached as Appendix B. WJE and TM coordinated and engaged in interim contact to ensure that the basic analytical approaches did not diverge, but the modeling methods and analysis software employed differed and the analyses were conducted independently. A primary goal of this parallel analysis approach was to enable the comparing and contrasting of independently-derived analysis results in order to facilitate the confirmation of significant seismic safety problems where they existed or the confirmation that there are no significant seismic safety problems. Broadly speaking, the computer models developed by TM and by WJE yielded remarkably similar results, despite the fact that the models were independently developed and were vastly different in many ways including the computer software employed, the element types used to construct the models, and levels of discretization and nonlinearity available to the model. For example, the modal results developed from WJE’s analysis and presented in Table 4 align well with the modal results presented by Tipping Mar (TM) in their supplemental analysis confirmation report for their “lower bound” stone stiffness. The differences between the specific corresponding values of period for each mode shape are attributable to the different analytical approaches and computer software packages used by each firm and are within expectations for these types of analyses.

The computer model developed by TM confirmed that the WJE analysis model and results are an appropriate and accurate representation of the seismic behavior of the Monument. This is exemplified by the comparable major findings: 1) the pyramidion experienced shaking during the Mineral earthquake that equaled or exceeded the shaking predicted to occur during the MCE, 2) the pyramidion will experience a degree and type of damage during future strong earthquakes similar to what occurred during the Mineral

event, which did not present a risk of collapse but did reveal the potential for falling hazards; 3) the precise locations of damage to the pyramidion during future strong earthquakes cannot be identified by analysis, and 4) although the shaft of the Monument will experience much larger stresses and deformations under the MCE ground motions compared to the Mineral event, the magnitude of the stresses and predicted deformations will result only in relatively minor nonlinearities, not in a life safety hazard.

CONCLUSIONS AND RECOMMENDATIONS

This section of the report summarizes our conclusions about the vulnerability of the Monument to critical seismic damage that might result from an MCE, an earthquake with a return period of 2,475 years. Specifically, this vulnerability assessment sought to identify the potential risk of structural damage that might cause local collapse or shedding of large blocks of stone, thus endangering visitors. In addition to conclusions, this section sets forth recommendations and brief justification for the recommendations made. The following factors provide important context for understanding the conclusions and recommendations made herein:

1. As was discussed earlier in this assessment report, an earthquake event with a return period of 2,475 years --- the MCE --- is considered to be a “rare” event, not an earthquake with a high probability of recurrence. Until relatively recently, seismic assessment and design for structures throughout the United States was based on an earthquake with a return period of 475 years. For the Monument, such an earthquake would produce shaking on the National Mall with a much lesser intensity than that considered in this assessment. The recommendations from this assessment ought to be understood in the context of the rarity of an MCE event by definition.
2. This seismic assessment was conducted for the full, unreduced MCE rather than two-thirds of the MCE as is normal practice today for seismic assessment of most structures in the United States. The use of the full MCE rather than two-thirds of the MCE was an engineering choice made to account for the high visibility and importance of the Monument, among other things. There is no requirement, and little precedent for using the full, unreduced MCE on a historic structure. On net, this choice resulted in the seismic input used for this assessment being effectively 50 percent greater than would have been used for assessment of typical structures. The predictions relating to damage that might arise during a future MCE considered this greatly amplified seismic input.
3. The MCE ground motions that were considered for this assessment are not only rare but are spectral-matched and therefore have characteristics that impart short-, intermediate- and long-period dynamic input at the same time. This type of ground motion suite is therefore considering many different earthquakes occurring simultaneously, rather than representing the energy of any single earthquake. For most structures this has little effect, but structural characteristics of the pyramidion make spectral-matched ground motions conservative for predicting damage.
4. The Mineral event caused --- particularly with respect to the pyramidion --- as strong or stronger shaking to the Monument than would the postulated MCE. The effects of the Mineral event on the pyramidion might therefore be reasonably considered to be as bad, or worse than, that which might be caused by an MCE.
5. Most potential categories of damage to the Monument are best characterized as resulting from brittle mechanisms. Brittle failure mechanisms are generally considered to be undesirable, but in actuality, the degree of undesirability is indelibly linked to the consequence of failure and the likelihood of that consequence. Fracturing of teeth is an undesirable mode of failure because it might cause a pyramidion panel to fall, but none of the teeth that fractured during the Mineral event resulted in a falling panel. This knowledge should temper to some degree, concern about

damage to teeth in future earthquakes. Similarly, shifting rib stones might be considered a brittle failure mechanism that could lead to a catastrophic failure if the shifting is enough to cause instability of a rib, but very substantial shifting of rib stones can occur prior to the onset of instability. This knowledge should temper to some degree, concern about shifting rib stones.

6. It is not possible to accurately characterize the potential risk from falling mortar or stone chips or spalls since the potential for these events is related closely to the condition of the stone and mortar immediately preceding the earthquake and an analysis mesh cannot reasonably isolate very localized stress concentrations that can cause mortar or stone to break free and fall. The Monument should be expected to shed minor amounts of mortar and stone in any strong earthquake, in addition to the types of damage caused by the Mineral event.
7. Despite the uncertainties inherent in analyzing a structure like the Monument during future earthquakes with unknown characteristics, the structural analyses conducted during this assessment are a reasonable basis for judging the seismic adequacy of the Monument and for developing recommendations about the need to selectively strengthen it or the acceptability of leaving it as-is. The analytical predictions clearly identify the primary categories of damage noted in the pyramidion after the August 23 Mineral event, including the shifting of rib stones, cracking of stone panels and the fracturing of the “teeth” that support the panels. The analyses moreover predict “spreading” of the uppermost portion of the shaft and the concomitant damage to the vertical joints in the upper 30 feet. At the same time, the analyses explain the minor damage to the bulk of the Monument’s height.

This seismic assessment supports the conclusion that there is negligible risk of significant structural damage to the Monument from an earthquake that might lead to global loss of stability or large-scale collapse, especially as it pertains to the foundations and shaft. The soils that support the Monument do not appear to be at all at risk during a 2,475-year event and only minor tensile stresses that would at worst result in bed joint cracking in the mid-height of the Monument are predicted in the Monument’s shaft below the 450-foot elevation. The regions where tensile cracking might occur are at an elevation where header courses extend the full width of the shaft walls, thus the walls are quite dimensionally stable and not prone to disintegration. Thus the bulk of the Monument’s structure appears to be sufficiently resistant to the postulated 2,475-year earthquake motions that no seismic interventions below 450-feet can be justified.

Above the 450-foot elevation, the subject of potential earthquake damage and risk become somewhat more nuanced; essentially though, this assessment has concluded that the risk of significant structural damage above the 450-foot elevation that can jeopardize the safety of visitors is low. This conclusion is at least partially related to the seismological finding that the Monument has by some measures already experienced an earthquake event whose intensity substantially exceeds a 2,475-year event, particularly with respect to the specific components of the ground shaking that excite the pyramidion. As presented in the AMEC report, the August 23 Mineral event caused unusually intense shaking in a relatively narrow range of periods, shaking with an intensity equivalent to an earthquake with a return period of between 2,000 and 3,000 years. At the same time, the structural analyses indicate that this period range essentially coincides with the periods of shaking to which the pyramidion is most vulnerable. Despite the intensity of the pyramidion’s response during the Mineral event, no collapse actually occurred although certain conditions documented after the earthquake were considered to present potential falling hazards. Therefore, the question of whether the risks from a 2,475 year event are substantial enough to warrant selective strengthening to the upper portion of the Monument is a subject that is a very appropriate for discussion, as it is in the following paragraphs.

Upper Shaft

The “spreading” related damage to the upper shaft walls is a predicted outcome of both the Mineral and MCE motions and the predicted stresses from the two events, analyzed separately, are similar. The primary question controlling whether the upper shaft walls require remediation is whether the condition of the upper portion of the shaft will materially worsen in an MCE event given the spreading that already occurred during the Mineral event. As described in the analysis results section of this report, the modeling of this portion of the shaft was linear and did not explicitly account for the behavior of the walls after the onset of cracking in the vertical joints, so although we have conducted analysis of the Mineral and MCE earthquakes “in series”, the “in-series” analyses do not address this question directly.

The cracking to the vertical joints in the upper portion of the shaft is understood to cause an immediate enhancement to the in-plane flexibility of the masonry (i.e. a reduction in stiffness); resistance to spreading subsequent to cracking is provided largely by the iron cramps that are more flexible than mortar. This sudden reduction in stiffness was not explicitly modeled, although analytical bounding techniques were used to account for some softening of the uppermost portion of the shaft walls.

The cramps provide substantial post-cracking strength to the masonry and it is likely that they were installed for the specific purpose of resisting spreading. Our assessment is that these cramps appear to be sufficient to limit further spreading of the walls and do not require supplementing.

Ribs

The ribs of the pyramidion exhibited damage from the Mineral event. The general categories of known damage to the ribs consisted of shifting of some rib stones relative to adjacent rib stones, spalling of rib stone corners, and damage to “teeth” The subject of the damaged “teeth” will be addressed separately.

The shifting and spalling of the rib stones is largely the result of deformation of the ribs in frame action and the rocking of individual rib stones relative to adjacent rib stones. Rocking necessarily destroyed the bed joint-to-stone bond and shifting could have damaged mortise and tenon joints. The primary potential concern with respect to shifting rib stones is loss of stability. If the rib stones shift too much, they will become unstable. The shifting of the rib stones during the Mineral event was of minor proportion and the spalls are not large. The damage is not judged to compromise the strength or stability of the pyramidion. Damaged to mortise and tenon joints, if any occurred, would not directly affect stability of the ribs. As was the case for the “spreading” of the shaft walls, the germane question is whether the effects of an MCE event superimposed on the current condition of the ribs suggests that remedial measures should be taken prior to the occurrence of an MCE. Via the “in series” analyses conducted during this assessment, i.e. the Monument subjected analytically to the MCE motions subsequent to the Mineral motions, this question was directly addressed.

As described in the post-earthquake damage assessment report, the maximum shifting of the rib stones documented after the Mineral event was on the order of 0.75 inches. Because the mortise and tenon joints were not explicitly modeled, the pre-Mineral model did not explicitly rely on the resistance to shifting provided by the mortise and tenon joints, but did so implicitly by calibrating the nonlinear friction-pendulum links between rib stones such that the residual displacements predicted by the Mineral event analysis were in the same range as the documented residual displacements.

Because of the potential concerns regarding stability should shifting of rib stones become very large, we conducted a more detailed analysis of the analysis output with respect to this issue, including detailed

evaluation of the predicted shifting for the individual synthetic Mineral and MCE motions, as well as detailed evaluation of “in series” analyses in which all MCE motions were re-start analyses from the endpoint of the Mineral (Whittier2) runs. In all cases, the analysis predictions from the individual synthetic Mineral and MCE motions revealed that all “average maximum” and all “maximum maximum” rib stone residual and instantaneous displacements are well within the range where rib stability would not be a potential issue.

In addition, the “in series” analyses conducted during this assessment predict that the MCE will also cause shifting of some rib stones and that in some cases this shifting will be additive to that which occurred on August 23. These “in series” analyses also indicate that the total shifting after the two events will not bring any rib stones to the point of instability, although the analyses indicate that at the elevation just below the tie beams, the residual and instantaneous offsets are substantially larger than anywhere else. Some of this may be an artifact of the modeling idealizations for the very complex joinery in this area, but there appears to be conceptual justification for concluding that this elevation is in general more prone to offsets than any other due to the configuration of the pyramidion elements and the presence of the tie-beams.

When the “maximum maximum” of all the unreduced MCE motions superimposed on the Mineral motions are evaluated, there is a single pair of unreduced MCE motions for which centroidal displacement of the rib stones just below the tie-beams is predicted to be approximately 2.7 inches. This is a large displacement, yet there are strong reasons to conclude that these over-estimate what might really happen during an MCE, among them that the MCE motions on which the analyses are based are “envelope” spectral matched time histories. As such, the MCE motions over-estimate demand on the pyramidion because they excite all modes that potentially affect the pyramidion at the same time. No single MCE event could actually do that. While we do not find interventions to restrict further potential movement of the rib stones to be necessary to provide stability, this specific condition could be studied in more detail. From one perspective, restraining future movement of the rib stones might appear to be advisable because the consequences of excessive shifting are severe, but there are multiple reasons to not contemplate such restraints if they are not necessary to ensure safety. Modifying historic fabric unnecessarily is one such reason. Moreover, restraints have the potential to alter the means by which the pyramidion successfully resisted the Mineral event and could have unintended detrimental consequences during future earthquakes.

Future spalling of the edges and corners of rib stones is another category of damage that might be considered for potential remediation. We conclude that spalling is a consequence primarily of rocking of individual rib stones, and rocking is mode of response that we believe is beneficial to the response of the pyramidion in part because it introduces needed flexibility. Restraint systems designed to lessen rocking are therefore not endorsed.

Teeth

Damage to teeth during the Mineral event occurred with some frequency and is considered to be a precursor to possible shedding of panels. Although no panels were shed during the Mineral event, the earthquake exposed this mode of behavior as a vulnerability of the pyramidion. The distribution of broken teeth is roughly predicted by the analyses in that the teeth with the higher predicted forces generally coincide with the locations of actual tooth damage, but the correlation is too rough to explain specific locations of damage. This is believed to result in part from the imprecise manner in which masonry is constructed (essentially, the mating of each panel on each tooth is different); in part from the imprecision

that results from the sensitivity of any model developed to simulate the nonlinear response of rocking systems; and in part from the fact that the nonlinear time history inputs developed by AMEC do not represent the exact dynamic motion experienced at the site during the Mineral event. These uncertainties are inherent in seismic analysis in general, particularly for analyses that are at the boundaries of current technology, as these are.

Despite the uncertainties, the analyses and damage documentation survey reveal trends that can be used to generate an understanding about the behavior of the teeth during the Mineral event and their likely behavior during the MCE, and to inform recommendations about the appropriateness of remedial steps to strengthen undamaged the panel-to-rib connections. Key relevant points for consideration include:

- a. the forces predicted at any given tooth are nearly always predicted to be smaller during the MCE than during the Mineral event;
- b. the strengths of the teeth appear to be highly variable in that there are a number of instances in which teeth that were damaged are predicted to have been subjected to lower forces during the Mineral event than teeth that did not break;
- c. there is no clear pattern that would indicate the teeth at certain elevations or on certain ribs are more vulnerable to damage than others;
- d. there is a clear pattern revealed by the field survey that the teeth that are located at vertical joints between panels, i.e. that support the corners of two panels, are more vulnerable to damage than teeth that support individual panels.

Due to the uncertainties described, it may be tempting to simply strengthen all the teeth while repair work takes place. At the same time, however, there is compelling evidence -- as follows -- that strengthening of all the teeth with brackets would not be a worthwhile effort.

About half of the teeth at which new steel brackets are being installed were actually damaged during the Mineral event to the point that repairs were recommended. The balance of the bracket installation is to address presumed load re-distribution issues arising from the compromised support at damaged locations or to address cracked panels. By this measure, approximately 20 percent of the primary rib stone teeth were damaged during the Mineral event to the point where repair was recommended. Nearly all of these were at locations where a vertical joint between panels aligns with the tooth, which demonstrates that these double panel locations are substantially more vulnerable than the single panel locations. The majority of the additional brackets specified for installation during the repair phase to address load-redistribution issues and other issues were also added, as it turns out, at double panel locations. Therefore, most of the more vulnerable teeth at double panel locations have already been strengthened with brackets and there is little justification for adding brackets to teeth at single panel locations since they have been proven to be much less vulnerable. In accordance with the above vulnerability analysis, it is our recommendation to add brackets to the teeth supporting double panels that are not currently scheduled for repair. These include eight locations in the field of the facets below the tie-beams. Although no panels actually fell during the Mineral event, the addition of brackets to these locations will further limit the potential for a panel or portion of a panel creating a falling hazard during a future very strong earthquake. These brackets are not intended to mitigate a current falling hazard.

Both the numerical and conceptual analyses of the pyramidion indicate that the largest residual and instantaneous displacements are likely to occur between rib-stone courses D and E just below the tie-beam. (See Figure 10 for identification of courses.) While we believe that some component of the

numerical analysis prediction for this displacement is an artifact of the modeling idealizations for the tie-beams and complex joinery in this portion of the pyramidion, it is reasonable to expect that behavior of the pyramidion at this elevation is uniquely vulnerable. We therefore also recommend that if additional brackets are to be added at currently undamaged locations, brackets be added to select teeth located at course E just below the tie-beam elevation. There are six teeth at course E that are not currently planned to have brackets installed during the repair phase at which the installation of brackets is judged to be an appropriate intervention.

Panels

A few panels were cracked during the Mineral event; certain other cracked panels appeared to have occurred for non-earthquake related reasons prior to August 2011. Of the cracked panels, one experienced an offset across the crack significant enough to warrant external stabilization, all are being repaired by filling the cracks with epoxy repair materials, and one other is being stabilized.

The analyses appear to generate predictions of damage for the Mineral event that correlate quite well with actual locations of earthquake-related panel cracking. Within the constraints of any seismic assessment, the models are therefore judged to be sufficiently reliable to predict future panel damage and to be employed as a basis for recommendations about the panels. Comparison of the analysis results for the MCE with the results for the Mineral event indicates that the predicted magnitude of out-of-plane bending stresses in the panels is similar for the two earthquakes. In addition, there is consistency between the predicted locations of the panels with the greatest bending stress. Based on these analysis findings, it appears most likely that the MCE may cause currently cracked panels, scheduled for repair, to re-crack but is less likely to cause cracking in other panels dissimilar. As discussed earlier, there is some risk that cracked panels can work themselves free. Though none have done so either in the 1886 earthquake or during the Mineral event, one large panel fragment moved inward about two inches and might have fallen into the interior had the earthquake duration been longer. Due to the inclination of the panels as installed, there appears to be less likelihood that a large panel fragment could fall outward.

Uncracked panels in locations corresponding to those that cracked during the Mineral event are candidates for cracking in future MCE level events. Consideration could be given to pre-emptive measures for these panels.

Cruciform

The cruciform experienced minor spalling during the Mineral event, but caused a large spall to a supporting rib stone. The geometry of the rib stones and the surfaces that mate with the cruciform are designed to provide gravity support to the cruciform. The cruciform is very much a keystone for the four center ribs and in elevation exhibits the hallmark characteristics and shape of a traditional keystone. Absent severe spreading of the center ribs and the pyramidion as a whole, it appears very unlikely that the cruciform would lose gravity support completely. As such, no measures are recommended for the keystone for the purpose of protecting life safety. However, because significant movement of the keystone can be a precursor to larger scale geometric changes to the ribs and can lead to loss of function of the center arched-frame ribs, consideration of preventative measures to maintain the position of the keystone without altering the manner in which the structure wants to behave could be given.

Tie Beams

One of eight tie beams experienced a crack near a connection with a center rib. This crack compromised the gravity support for the tie beam. While the coarsely discretized and linear-elastic model does not explain why the tie beam cracked, the tie beams appear to be important elements for the lateral support of the pyramidion and the cracking to the tie beam did pose a potential falling hazard to occupants. The tie beam repairs that are currently scheduled appear to address the potential falling hazard caused by damage to these elements. As for the cruciform, loss of a tie beam can be a precursor to larger scale geometric changes to the pyramidion. Consideration of preventative measures to maintain the position of the tie beams without altering the manner in which the structure wants to behave could be given.

REFERENCES

- American Society for Civil Engineers. *Seismic Rehabilitation of Existing Buildings, ASCE/SEI 41-06*. Reston, VA: American Society of Civil Engineers, 2006, 428 pp.
- American Society for Civil Engineers. *Minimum Design Loads for Buildings and Other Structures*. ASCE/SEI 7-10. Reston, VA: American Society of Civil Engineers, 2010, 608 pp.
- Army Corps of Engineers. *Crushing of 36 2-inch cubes*, letter dated December 18, 1878.
- Army Corps of Engineers. *Crushing of six 2-inch cubes of marble from Beaver Dam Quarry*, letter dated December 19, 1878.
- Army Corps of Engineers. *On the comprehensive strength of marble cubes*, letter dated January 24, 1879.
- Berry, Paul. *Reduced Copies of Measured Drawings*. HAER No. DC-5. Washington, DC: Historic American Engineering Record, 1986.
- Brewer, Mark. "Marble Joinery in the Washington Monument." *National Archives*, 8 pp.
- Computers and Structures. *CSI Analysis Reference Manual for SAP2000, ETABS, SAFE, and CSiBridge*. Berkeley, CA: Computers and Structures, Inc., August 2010, 494 pp.
- Cummings, Uriah. *American Cements*. Boston, MA: Rogers & Manson, 1989.
- Guidelines for Performance-Based Seismic Design of Tall Buildings*. PEER Report No. 2010/05. Prepared by the TBI Guidelines Working Group. Berkeley, CA: Pacific Earthquake Engineering Research Center, University of California, November 2010, 104 pp.
- John Milner Associates, Inc. *Washington Monument and Associated Structures. Volume I - Washington Monument. Historic Structure Report*. Prepared for the National Park Service Denver Service Center and National Park Service National Capital Region, June 2004, 486 pp.
- Maryland Geological Survey, Vol. 2*. Boston, MA: The Johns Hopkins Press, 1989.
- Oehrlein & Associates Architects. *Evaluation of the Washington Monument Washington, DC*. Prepared for the National Park Service Denver Service Center-Eastern Team, December 1993, 301 pp.
- TMS-ACI-ASCE Committee 530. *Building Code Requirements and Specification for Masonry Structures (TMS 402-11/ACI 530-11/ASCE 5-11)*. Detroit, Mich: American Concrete Institute, 2011.

Final Report
August 29, 2012
WJE No. 2012.0346

National Park Service, Denver Service Center
NAMA 184461 WAMO Seismic
NPS Contract: C2000080100
NPS Task Order: P12PD20437